SERVICE REVENUE EVALUATION METHODOLOGIES TO MAXIMIZE THE BENEFITS OF ENERGY STORAGE

A Dissertation
Presented to
The Academic Faculty

by

SeyyedMohammadSadegh Vejdan

In Partial Fulfillment
of the Requirements for the Degree
Doctor of Philosophy in the
School of Electrical and Computer Engineering

Georgia Institute of Technology
May 2020

SERVICE REVENUE EVALUATION METHODOLOGIES TO MAXIMIZE THE BENEFITS OF ENERGY STORAGE

Approved by:

Dr. Santiago Grijalva, Advisor
School of Electrical and Computer Engineering
Georgia Institute of Technology

Dr. Richard Simmons
Strategic Energy Institute
Georgia Institute of Technology

Dr. Maryam Saeedifard
School of Electrical and Computer Engineering
Georgia Institute of Technology

Dr. Muhammad Marwali
Department of Operations
New York Independent System Operator

Dr. Daniel Molzahn
School of Electrical and Computer Engineering
Georgia Institute of Technology

Date Approved: November 13, 2019

To make the world a better place

ACKNOWLEDGEMENTS

I would like to acknowledge everyone who helped me achieve my goals and dreams. Specifically, I would like to express my sincerest gratitude to my advisor, mentor and role model, Professor Santiago Grijalva for his continuous support, vision and guidance throughout this journey. I would like to thank my committee members Dr. Maryam Saeedifard, Dr. Richard Simmons, Dr. Daniel Molzahn and Dr. Mumammad Marwali for their valuable time and helpful feedback. I would like to thank the other professors whom I had a chance to work with and learn from them: Dr. Meliopoulos, Dr. Harley, Dr. Sanaye-Pasand and Dr. Feizollahi.

I would like to thank my research sponsors for providing great opportunities for me to grow personally and academically; Specifically, National Electric Energy Testing, Research and Applications Center (NEETRAC) and Mr. Frank Lambert, and Strategic Energy Institute, Energy Policy and Innovation Center and Dr. Richard Simmons.

I had amazing internship experiences at New York Independent System Operator (NYISO) and Prosumer Grid Inc. I would like to thank my managers and colleagues including Dr. Marwali, Mr. Ganesan, Mr. Swider from NYISO, and Mr. Higley, Dr. Sandoval, Dr. Hernandez and Dr. Tariq (Prosumer Grid Inc.). I am grateful of having worked with them.

I would like to thank my amazing friends and colleagues whose presence and support made my life more enjoyable.

Finally, I would like to express my appreciation to my dear family, Dr. Morteza Vejdan, Sedigheh Eshraghi and my lovely sister Fatemeh Vejdan, for their unconditional love and support who sacrificed everything they could for my personal and career development. I would also like to thank my uncle and aunt Dr. Reza and Terry Fassihi for their support as my close family in the U.S.

TABLE OF CONTENTS

LIST OF TABLES

LIST OF FIGURES

LIST OF SYMBOLS AND ABBREVIATIONS

AGC	Area Generation Control
BTM	Behind-the-meter
CAISO	California Independent System Operator
DSO	Distribution System Operator
ESS	Energy Storage System
IPP	Independent Power Producer
ISO	Independent System Operator
LMP	Locational Marginal Prices
LP	Linear Program
MILP	Mixed Integer Linear Program
NPV	Net Present Value
NYISO	New York Independent System Operator
O&M	Operation and Maintenance
PJM	Pennsylvania-New Jersey-Maryland
PV	Photovoltaic System
RPS	Renewable Portfolio Standard

SUMMARY

The objective of this research is to develop novel methodologies and tools for service revenue evaluation of electrical energy storage systems. Energy storage systems can provide a wide range of services and benefits to the entire value chain of the electricity industry and, therefore, are becoming a favorable technology among stakeholders. The U.S. Government and various states have set initiatives and mandated energy storage deployment as part of their grid modernization roadmap. The key to an increased deployment of energy storage projects is their economic viability. Because of the significant potential value of energy storage as well as the complexity of the decision-making problem, sophisticated service evaluation methodologies and service optimization tools are highly needed.

The maximum potential value of energy storage cannot be captured with the evaluation methodologies that have been developed for conventional generators or other distributed energy resources. Previous research studies mostly operational strategies for energy storage coupled with renewable energy sources and the benefits and business models of privately-owned energy storage systems are not well understood. Most of the existing literature focuses on evaluating energy storage systems providing a single service while multiservice operation and evaluation is often not considered. The few available methods for multiservice evaluation study a limited number of services and cannot be readily implemented into a computational tool due to complexity and scalability issues. Accordingly, this research proposes novel service evaluation methodologies with two main objectives:

a. Discover the maximum value of energy storage systems for single and multiservice applications,
b. Provide flexibility, scalability and tractability of implementation.

In order to meet these objectives, various methodologies based on statistical analysis, dynamic control, mixed integer linear programming, convex optimization and decomposition have been proposed. The challenges, complexities, and the benefits of modeling energy services using a scalable approach are analyzed, solutions are proposed and simulated with realistic data in three main chapters of this research: a) energy storage in wholesale energy markets, b) generic multiservice revenue analysis of energy storage, and c) temporal complexities of energy storage optimization models: value and decomposition. Simulation results show the feasibility of the proposed approaches, and significant added values to the economic viability of energy storage projects using the proposed methodologies. Energy storage decision makers including public utility commissioners, transmission/distribution system operators, aggregators, private energy storage owners/investors, and end-use customers (residential and commercial loads) can benefit from the proposed methodologies and simulation results. A software tool has been developed for multiservice benefit cost analysis of energy storage projects. It is hoped that with the significant unlocked value of energy storage systems using the proposed tools and methodologies, more of these technologies be deployed in the future grids to help communities with their sustainability and environmental goals.

CHAPTER 1. INTRODUCTION

1.1 Grid Modernization and Challenges

The electrical power grid is a strategically important infrastructure of every nation. A modern power grid plays a crucial role in the nation's prosperity and economic growth. Therefore, many nations worldwide are conducting grid modernization projects including the integration of new physical and information technologies to transform the traditional power grid making it smart, resilient, and sustainable. The U.S. Department of Energy's Grid Modernization Multi-Year Program [1] defines six key attributes of a modernized grid [2]:

- Resilient: Quick recovery from any situation or power outage
- Reliable: Improves power quality and fewer power outages
- Secure: Increases protection to our critical infrastructure
- Affordable: Maintains reasonable costs to consumers
- Flexible: Responds to the variability and uncertainty of conditions at one or more timescales, including a range of energy futures
- Sustainable: Facilitates broader deployment of clean generation and efficient end use technologies

Many new technologies can provide some of these attributes while imposing challenges on others. For example, renewable energy sources provide clean energy. However, they challenge the reliable delivery of electricity due to the uncertain and intermittent nature of solar irradiance and wind speed. Therefore, the reliable integration of these new technologies requires a great amount of operational flexibility.

1.2 Energy Storage Solutions

Energy storage systems (ESSs) can provide the operational flexibility for reliable operation of renewable energies. ESSs are available in multiple sizes and technologies ranging from large pumped hydroelectric systems to small-scale electrochemical battery cells [3]. Some technologies such as pumped hydro have been operating for more than a century [4] while many of them are in their nascent stage e.g., Vanadium-Redox battery and gravity energy storage (GES) [5]. An extensive list of energy storage technologies and their characteristics are available in [6]. Figure 1 compares ESS technologies based on their range of power and energy ratings and regarding their main use in the electricity industry [7].

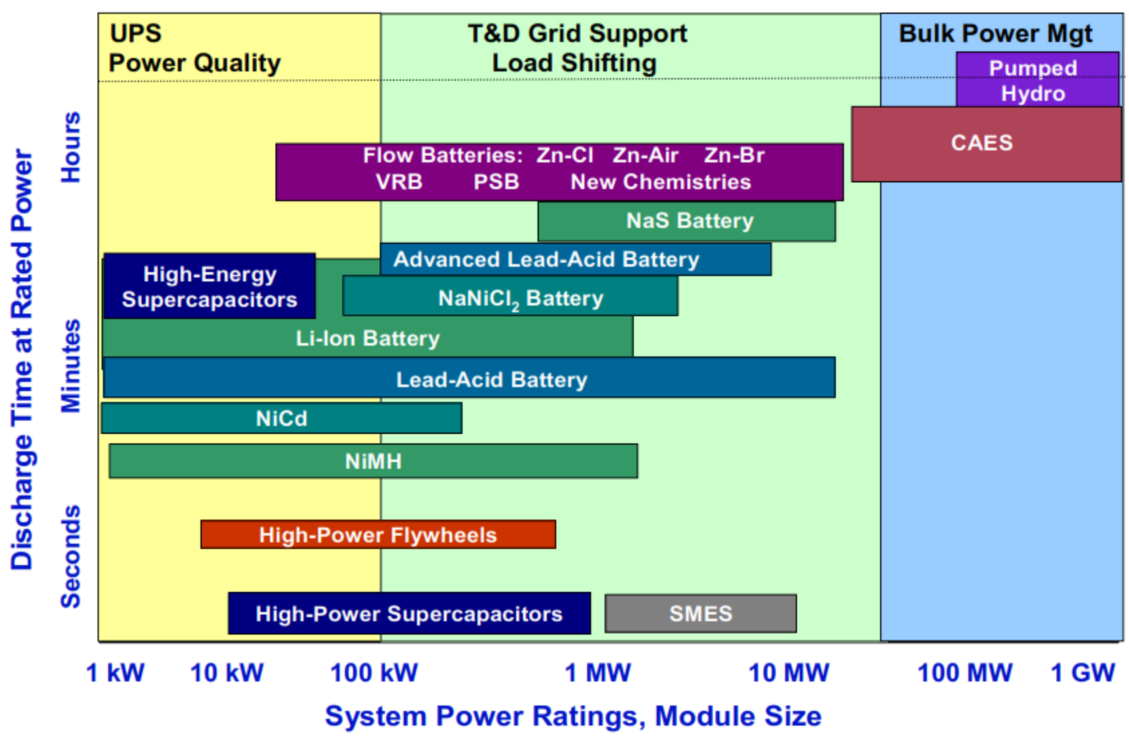

Figure 1 – Energy storage technology ratings

Each energy storage technology has physical characteristics that make it more suitable for different types of applications. For example, the large capacity[1] of pumped hydro storage is favorable for bulk energy management. On the other hand, flywheels can store less energy relative to their maximum output power, but their extremely fast response is favored for regulation and power quality applications. Because of these unique characteristics, several applications of energy storage have been identified [8]. Figure 2 presents applications based on EES physical characteristics i.e. power and energy requirements [9].

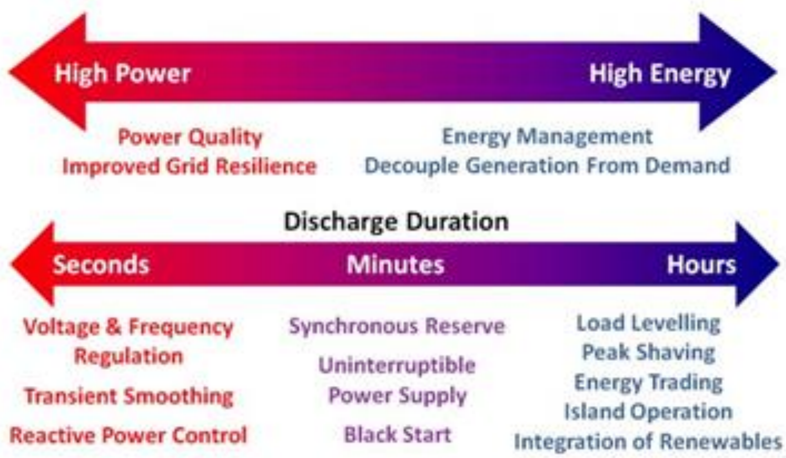

Figure 2 – Grid-scale energy storage applications [9]

ESS applications can contribute to improving the grid modernization attributes. They improve resiliency by securing backup power. Also, power system operators can call ESS owners to provide rapid responses to better compensate for the variability of renewable energy sources. Thus, ESSs improve power system reliability. They can also provide clean and affordable energy by shifting the time of energy use. Excess clean energy produced at a lower cost during off-peak hours is stored and time-shifted to the peak hours when the

[1] The number of continuous hours that energy storage can be discharged at its maximum output power

energy price is high. Due to their numerous benefits, ESSs are favored by various stakeholders from generation and transmission level to distribution and behind-the-meter customers. Figure 3 shows the stakeholders and beneficiaries of energy storage technologies.

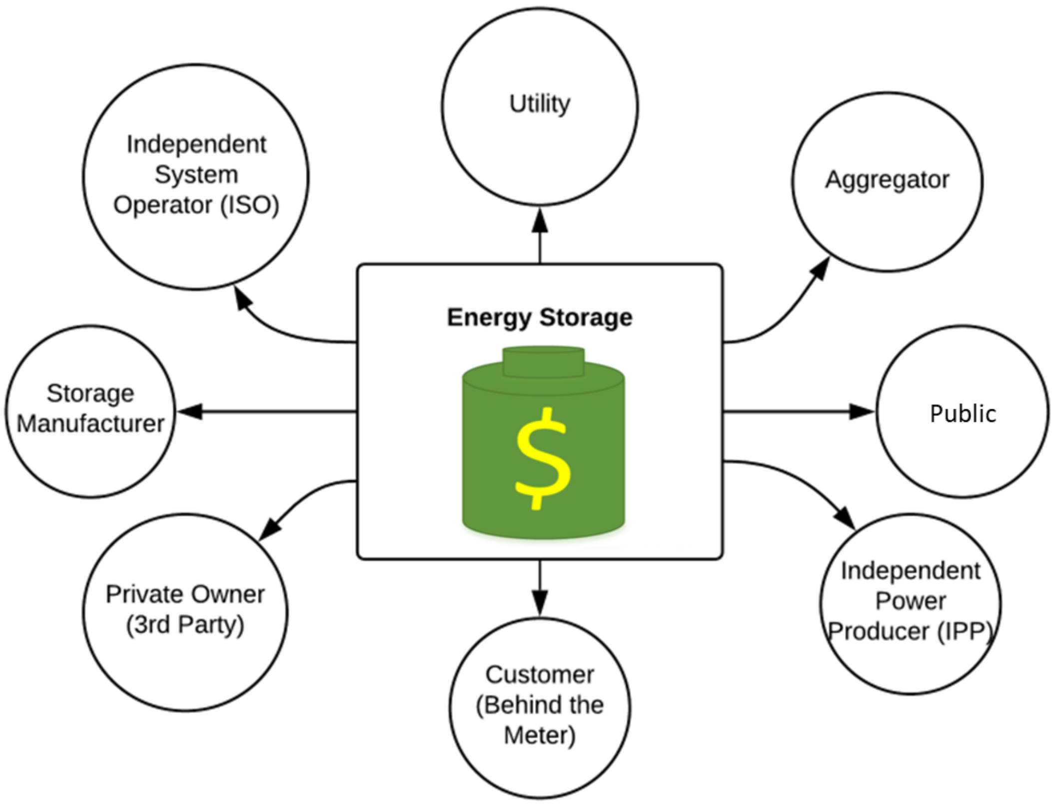

Figure 3 – Energy storage stakeholders and beneficiaries

Because of the variety of storage technologies, applications, and stakeholders, several business models are being proposed for ESSs. Economic viability analysis is the key to assess a business model. Such analyses try to answer questions including but not limited to:

- Ownership: Who owns and who operates the ESS?
- Planning:

- What are the main requirements for ESS operator/owner? For example, a system operator may require more flexibility in terms of faster response times, or the market operator wants to incentivize more reserved backup power to improve resiliency. A private ESS owner requires higher revenues from participating in the electricity markets.
- What are the best applications and services of ESS that can meet emerging requirements? And given the applications, what are the best storage technologies that should be deployed?
- Where is the ESS located? Generation, transmission or distribution level or at the customer's site? What are the environmental regulations and market rules? Where is the optimal site to place the ESS? What is the optimal size of ESS?
- How to perform a cost-benefit analysis of ESS? How to monetize all the benefits of ESS? What are the revenue streams and associated costs? What are the risks associated with the cash flows? Who else will benefit from the ESS?

- Operations: How to optimally operate to ensure maximum profit?

Such questions are not trivial to answer since they depend on numerous factors. Meanwhile, analysis of ESS service benefits and revenues can directly help answering many of these questions. Also, since most of the energy storage technologies are relatively new in the electricity industry, less research has been done in developing new methodologies and tools for ESS service benefits evaluation. A better understanding of ESS benefits and revenue streams leads to an increased deployment of these technologies which further facilitates the integration of renewable energies and paves the way for grid modernization goals.

1.3 Research Need

Several publications and reports by the U.S. Department of Energy and the National Laboratories have identified energy storage applications and benefits [6]–[8], [10]. Reference [10] differentiates between applications and benefits and defines application as a *use* while a benefit is a *source of a value*. It further defines the *internalizable benefits* as those that can be readily captured and monetized by a stakeholder. With all the various potential benefits identified for ESSs, their profitable deployments in large-scale systems are still hindered. The U.S. Energy Storage Association (ESA) has set the goal of “35 by 25” where by 2025, the installed capacity of energy storage in the U.S. should reach 35 GW [11]. As of June 2018, there needs to be an additional deployment of 9 GW to reach that goal [12]. However, the annual deployment was 0.3 GW in 2018 and estimated to be less than 0.5 GW in 2019 [13]. With the current rate of deployment, the goal cannot be reached unless profitable ESS is viable. The profitability of most of the current ESS projects is impacted by the high capital costs and low estimated revenues.

It is expected that as the new ESS technologies become more mature, their capital costs decrease in the next few years [14]–[17]. On the other hand, low estimated revenues are due to the lack of understanding of how ESS benefits can be monetized and evaluated as revenue streams that can be collected by a stakeholder [8], [18]. Figure 4 illustrates the proposed concept of *the lost revenues of ESS* on the way from applications as potential benefits to internalizable service revenues. Shortcomings in the ESS modeling [8], regulatory barriers [18], and implementation challenges are the main sources of ESS revenue loss.

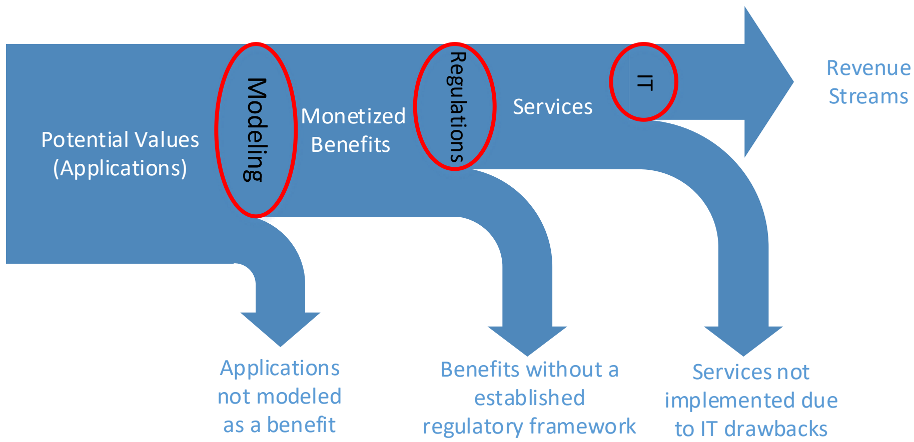

Figure 4 – The lost revenues of ESS

The focus of this dissertation is on the first component of lost revenues, i.e. values that are not captured due to the lack of proper modeling. A better modeling of ESS would reveal higher values of ESS that can help regulators and policy makers to better remove the regulatory barriers. The tools and methodologies used by industry for evaluation and revenue analysis of new technologies, e.g. distributed generation, are not specifically designed for ESS and thus, cannot capture the maximum benefits that can be provided by ESS flexibility and unique characteristics. Four of the salient differences of ESS with other energy resources are as follows [7]:

- ESSs are "net-zero energy" resources within a horizon, ignoring roundtrip efficiency, and their operation do not follow a standard pattern as, for example, in solar energy. ESS operation can change the dispatch of the system in each time period rather than net generation within a horizon.

- ESSs are “limited-generating-energy” resources due to their limited stored energy capacity.

- ESSs are “state-dependent” and their operation highly depends on their previous state. They impose intertemporal constraints that should be considered in the model.

- ESSs can provide multiple services simultaneously. However, the optimal operation cannot be determined based on a rule-based or priority dispatch approach requiring sophisticated optimization methods.

Potential service revenues need to be better understood with optimal methodologies and operating strategies to ensure maximum profitability of ESS projects while capturing the above key considerations.

Most of the literature on ESS analyzes its value for integration of renewable energy resources while the privately-owned ESS benefits and business models are not well-understood, which deter private third-party from investments. As the capital cost of energy storage continues to decrease, especially in the case of battery systems with up to 49% in the next five years [14], more private investments are expected in these systems. Thus, benefit analyses of privately-owned storage systems are timely and crucial. Also, many ESS projects depend on either a single or a just a few services as their revenue streams. In both cases, ESS operation is mostly determined by heuristic rules that are not optimal and therefore underestimate the maximum potential value of ESS. With more than 25 applications identified for ESS [6], [8], and the complexity of modeling due to service synergies and interdependencies, it is virtually impossible to model all the combination of services without a structured information model. Also, ESS evaluation studies are mainly dependent on local input parameters such as market prices at the specific location or the local network capacity. Thus, it is quite challenging that for each location, a separate analysis be conducted and the ESS operation be modeled differently. A systematic approach and advanced methodologies to address these challenges are, therefore, timely and highly important to many stakeholders.

1.4 Research Contributions

In this dissertation, novel methodologies for evaluation of energy storage services have been proposed and developed to:

- Maximize the revenues of ESS from providing services, and
- Improve the computational analysis of ESS.

The main contributions of this dissertation are:

- Developing a straightforward method for analyzing the ESS revenues in the day-ahead energy market: Day-ahead energy market service revenues are analyzed by using realistic data, and novel methods for estimating the expected revenue are developed based on classification, regression, and optimization algorithms. The results provide a straightforward method for analyzing the ESS revenues in the day-ahead energy market. Private investors and market operators can directly benefit from these results to determine the best location in the grid with the maximum energy arbitrage revenue.
- Developing an optimal market participation strategy for ESS to capture the significant value of real-time energy time shift using a dynamic optimization

model: The proposed method is shown to be quite robust against price forecast uncertainty and can capture the high value of energy time shift in the real-time market. Results disclose that the value of energy time shift in the real-time market is almost twice of that in the day-ahead market.

- Developing a risk-averse market participation strategy for ESS for day-ahead and real-time energy arbitrage: These participation strategies are also modeled with optimization problems and analyzed using realistic market data. The proposed approach hedges the owner's revenue against the uncertainty of the real-time prices.
- Designing a systematic approach for the optimal analysis of ESS multiservice operation: besides energy markets, ESS participation in other markets and local services are also studied. Due to the complexity of the problem, a systematic approach is designed to analyze the multiservice operation of ESS. A generic optimization approach is proposed that can analyze multiple service operations and revenues and can be scalable to analyze any combination of services.
- Implementing an interactive software tool for the optimal revenue analysis of ESS: An optimization-based software tool is also designed for multiservice revenue analysis of ESS. Test cases have been analyzed based on realistic data from CAISO market and Georgia Power tariff rates to quantify the benefits of multiservice ESS.
- Developing a stochastic optimization model for multiservice participation of ESS: The proposed model jointly optimizes the scheduling and real-time dispatch decisions. The value of the added complexity of the problem is quantified with realistic data.

- Developing decomposition techniques to efficiently solve large-scale ESS optimization problems: Simulation results show that intractable ESS problems can be solved efficiently with the proposed techniques and parallel computing.

1.5 Organization

The rest of this dissertation is organized as follows. Chapter 2 reviews the literature on energy storage service modeling methodologies. Chapter 3 presents the proposed methodologies on estimating the ESS revenues from participating in the wholesale energy markets. Chapter 4 proposes the generic multiservice revenue analysis framework, introduces the developed software tool, and provides test cases results. Chapter 5 addresses the temporal complexities of ESS optimization models. It quantifies the value of the complexities and proposes decomposition techniques accordingly. Chapter 6 concludes this dissertation and discusses future work. An overview of the developed software tool is provided in Appendix A.

CHAPTER 2. LITERATURE REVIEW

This chapter reviews literature on ESS applications and their benefits as well as methodologies for ESS revenue evaluation, service modeling, electricity market participation and optimal dispatch. The organization of this chapter is as follows. Section 2.1 presents a comprehensive set of energy storage benefits and applications identified in the literature. Section 2.2 reviews the ESS service modeling and revenue evaluation methodologies based on key modeling considerations. Sections 2.3, 2.4, and 2.5, respectively review the literature on

- Energy storage participation in wholesale energy markets,
- Multiservice revenue analysis of energy storage, and
- Temporal complexities of energy storage optimization problems,

Each of these sections describes the problem, reviews the literature and identifies the research gap.

2.1 Energy Storage Applications, Services, and Benefits

Energy storage technologies can bring significant value to the entire value chain of the electricity industry. Several publications and reports have identified energy storage applications and benefits including the Grid Energy Storage report by the Department of Energy [8], a whitepaper by Electric Power Research Institute (EPRI) [7], and two reports by SANDIA National Laboratories [6], [10]. Reference [10] differentiated between applications and benefits, and defined application as a use while a benefit is a source of a value. It further defined the internalizable benefits as those that can be readily captured and monetized by a stakeholder.

Energy storage applications are grouped into six main categories while some may belong to multiple categories:

1. Bulk energy services:
    a. Energy time-shift/arbitrage (in day-ahead and real-time markets),
    b. Supply capacity (long term forward contracts in the capacity market)
    c. Reduced fossil fuel generation and air emissions
2. Ancillary services:
    a. Frequency regulation
    b. Spinning (synchronous), non-spinning, and supplemental reserves
    c. Voltage support
    d. Black start
    e. Flexible ramping product
3. Transmission infrastructure support services:
    a. Transmission upgrade deferral
    b. Transmission congestion relief
    c. Transmission stability and sub-synchronous resonance damping
    d. Under/Over- frequency load shedding reduction
    e. Transient voltage dip improvement
4. Distribution infrastructure support services:
    a. Distribution upgrade deferral
    b. Volt/VAR support

c. Loss reduction

d. EV load support

e. Solar back-feeding elimination

f. Reducing tap regulator actions

g. Improving asset utilization

5. Renewable integration services:

a. Renewable energy time-shift/arbitrage

b. Renewable capacity firming

6. Customer energy management services:

a. Power quality

b. Power reliability/resiliency

c. Retail electric energy time-shift/arbitrage

d. Demand charge management

e. Demand response participation

With all these identified applications, the main question is how to model them in order to evaluate their potential benefits. The following sections review the existing literature on modeling methodologies.

2.2 Energy Storage Service Modeling and Revenue Evaluation Methodologies

The literature on energy storage service modeling can be studied from multiple criteria including modeled services, ownership assumptions (utility, third-party, etc.), modeling approach (rule-based or optimization), market impact, uncertainty modeling. In this section, we review the literature considering each criterion.

In order to quantify the benefits of ESS services, different models are proposed ranging from rule-based algorithms [7], [10], [19], [20] to more advanced optimization methods such as linear programming (LP) [21]–[27], mixed-integer linear programming (MILP) [28]–[33] and non-linear programming (NLP) [34]–[36]. In rule-based algorithms, the ESS operates based on a heuristic rule that is supposed to result in a high benefit. Although not optimal, these methods are easily implementable on the storage dispatch controllers with limited computational capability. An example of these methods is charging during morning hours and discharging in the afternoon hours. Optimization methods, on the other hand, result in the optimal operation of ESS during a time horizon. In linear programming models, the objective function and the constraints are linear. Although more accurate and reliable than rule-based models, LP does not capture all the dynamic characteristics of ESS. More detailed modeling is done with MILP and NLP at the expense of extra computational burden.

Regardless of the model, the economic analysis of the ESS market services is based on the market prices. Models vary in terms of taking the prices as fixed or variable with respect to the storage output. If the ESS output does not impact the market prices, the storage is a price-taker, and if it does, it is a price-maker. Price-taker ESS is studied in [19], [20], [23], [25]–[29], [32]–[35], [37] while [21], [22], [24], [30], [31], [36] consider price-maker ESS. The former is valid for small-scale ESS that does not have a market power. In the case of large-scale ESS, the latter approach is more realistic and the owner must submit strategic bids to optimally take advantage of price difference and at the same time not depressing this price difference [22].

The uncertainty of input parameters such as price and renewable output power data can be modeled in a deterministic [19]–[22], [24]–[29], [32]–[35], [37] or stochastic/robust fashion [23], [30], [31], [36]. In deterministic models, “perfect foresight” and “back-casting” approaches are mainly used while stochastic models utilize sampling from a discretized scenario set or dynamic programs such as Markovian process [23].

Other relevant issues and considerations such as the ESS optimal sizing as well as degradation and life cycle analyses are also explored the impact of storage capacity and efficiency on its revenue evaluation and profitability [19], [31], [34], [36]. Furthermore, a number of studies considered a physical network in their models to simulate the network constraints and to determine locational marginal prices (LMPs) in the market clearing process [24], [30] or for the optimal placement of the ESS [35].

2.3 Literature on Energy Storage Participation in Wholesale Energy Markets

ESS owners can participate in wholesale electricity markets, provide services, and collect revenues. Wholesale markets can have various services different under each regulatory. However, they usually include energy, capacity and ancillary services. In this section, we focus on the ESS energy market participation. Literature on the other services are reviewed in the next sections.

ESS participate in the wholesale energy markets to perform energy time-shift or energy arbitrage (EA). This is the most well-known application of energy storage also known as the “buy low, sell high” approach. Taking advantage of the energy price variation, the ESS owner benefits from the EA service by buying cheap energy to charge the ESS during off-peak periods and discharging it to sell expensive energy during peak periods of the day.

The economic evaluation of ESS models the EA service as the only revenue stream in [19], [21]–[26], [29]–[31], [34] and as one of the revenue streams stacked with other service revenues in [20], [27], [28], [32], [33], [35]–[37].

The EA service evaluation is studied in the literature using various methodologies. One of the main assumptions is related to the market power of energy storage. In price-maker models, the storage bids into the market, and the cleared price becomes a function of all the power suppliers' bids. Strategic bidding approaches are proposed to find the optimal scheduling of energy storage maximizing the revenue from EA and other market-based services [38]–[43]. These approaches are based on bi-level optimization problems where the upper problem is the ESS revenue maximization problem. The process of clearing the market is the lower level problem, and it requires the bidding information of the other market actors. Since the bids are not publicly available data in all market regions, the actual applicability of these analyses for realistic storage service evaluation is limited. Moreover, these models are computationally involved, and their scalability and computational time are other limiting factors. Other price-maker approaches have used the price-load sensitivity to model the impact of the ESS operation on the market price [22], [26].

The EA service evaluation under a price-taker model is analyzed in [44]–[52]. The service revenue is optimized separately [44]–[46], or co-optimized with other market products, such as frequency regulation [47]–[52]. Linear and mixed integer optimization are used to determine the maximum revenue with historical market data as inputs to the optimization models. While the market prices contain valuable information about the potential revenue from energy arbitrage, no analysis is yet conducted on the price data statistics for the evaluation of energy arbitrage service. This research gap is covered in sections 3.2 and 3.3.

Energy markets are usually settled in at least two auctions: one held on the day before energy delivery time known as the day-ahead (DA) market and the other one held a few minutes before the delivery time known as the and real-time (RT) or balancing market [53]. These markets are described in sections 3.2 and 3.3, respectively. Previous studies have explored the value of storage systems providing the EA service in either the DA or the RT energy market [21], [26], [29], [44], [46], [50], [54]–[57]. Linear optimization models are proposed and simulated with historical DA market prices of PJM [26], [49], CAISO [50], ISONE [48], and ERCOT [51] to evaluate the maximum potential revenue of the EA in the U.S. electricity markets. Studies of the EA value in the Australian and European markets are presented in [54], [55]. In these analyses, the ESS is assumed to be a price-taker without any market power.

The ownership of a storage as an EA service provider is shown to have a great impact on the value of this service [21], [26], [56]. It is very likely that with the trend in the deployment of new intermittent renewable generations, the RT price variation will continue to increase. As a result, more RT arbitrage opportunities are expected, which will increase the profitability of energy storage projects. The energy storage participation and dispatch strategies in the RT market are developed in [29], [44], [56], [57]. Almost all the studies underline the significance of the forecasting accuracy on the maximum value of the EA service. Thus, a robust dispatch can compensate for the low forecast accuracy. Furthermore, none of the previous studies has investigated or compared both market values for the EA service. Solutions for these research gaps are proposed in section 3.3.

While the RT market can have a higher EA value compared to the DA market [58], higher price volatility with greater forecast errors in the RT market, can limit the profitability of the RT EA if the ESS participates only in this market. This is not desirable for a risk-averse ESS operator or owner. Thus, RT market participation should be considered as an extra revenue stream for the ESS that is added to the less risky revenue from the DA market. A few research has been done on optimizing both DA and RT EA revenues including [59]–[61]. These works incorporate price uncertainties in the optimal bidding problem via stochastic and robust optimization. However, they do not consider ESS degradation which is an important modeling consideration especially for electrochemical ESS [62]. They also do not provide enough insights on the impact of model parameters on the EA revenues and the ESS economics and profitability. These research gaps are studied in section 3.4. where optimization-based solutions are proposed and simulated with realistic data.

2.4 Literature on Multiservice Revenue Analysis of Energy Storage

Besides the EA service, ESS can provide many other services to increase its utilization and profitability. From the various application and potential services listed in section 2.1, only a subset of the services is feasible for each ESS project. Feasible services depend on the ESS location (transmission, distribution, and behind-the-meter) and its operating stakeholder (ESS owner, ISO, utility, customer, etc.) [21]. The benefits of ESS offered by these services must be clearly defined for different ESS stakeholders in order to facilitate further investment and deployment of ESS. The growing body of research on ESS services focuses mostly on the benefits that ESS can offer to the system operator in terms of reduced costs [60], [61], [63], [64]. However, due to the decreasing capital costs ESS, merchant ESS, i.e. privately-owned and operated ESS as a single entity, can become profitable by maximizing their revenue from providing multiple service simultaneously [65]. Thus, analysis of their benefits and revenue streams is valuable and requires significant research and advanced methods [38], [43], [65].

The optimization of ESS operation for multiple services is discussed in the literature [28]–[50], and [65]–[70]. These works define the ESS location, operator and a few test cases based on a subset of feasible services. Accordingly, they proposed models and methodologies specifically tuned for the few selected services. In other words, the proposed methodologies are application/service-specific. These services include participation in wholesale market products, distribution-level services, and behind-the-meter (BTM) services.

ESS evaluation methodologies for multiservice wholesale market participation is studied in the literature where the authors of [50], [69], [70] investigated the ESS value for performing energy arbitrage and frequency regulation. The combined energy and reserve services are evaluated in [33], [42], [71]. Optimization models for application of ESS in providing wholesale market services as well as local distribution services are proposed in [66], [72], [73] with the objective function of maximizing the market service revenues subject to constraints modeling the local distribution service requirements. These approaches do not necessarily maximize the ESS owner's revenue since some services are modeled as hard constraints. Therefore, the ESS must provide those at any expense unless infeasible. While this can be done to ensure the availability of critical services, it is not a revenue maximizing approach. Hence a more comprehensive analysis for these services is needed from the ESS owner's perspective. In chapter 4, we propose a generic optimization framework for modeling multiservice ESS that covers these research gaps.

Customer-sited (BTM) ESS benefits and services are analyzed in the literature for optimal sizing, scheduling and real-time dispatch. BTM ESSs have often been used as a complement to photovoltaic systems (PV), in order to maximize the benefits derived from the solar panels [74]. However, current studies have shown that various optimization techniques can utilize standalone ESS to generate reliable revenue streams for BTM customers under both time-of-use (TOU) and demand charge (DC) tariffs [10], [74]–[84]. Customer bill management and opportunities for EA have been the primary drivers for standalone BTM research. Depending on the cost of the ESS, these revenue streams can result in reasonable payback periods that demonstrate the economic viability of ESS systems in certain conditions [10], [74], [77], [78]. Under a TOU tariff, EA is the primary source of revenue, however [10], [78], [79] demonstrate that when the tariff includes a DC, then peak shaving is significantly more profitable than EA.

When optimizing for battery capacity and power under a DC tariff, the quickest pay back periods are seen with smaller batteries, because generally the revenue from DC cost reduction grows linearly while the cost of energy necessary for peak shaving experiences exponential growth [78], [80], [81]. Another benefit of utilizing ESS for peak shaving applications is that since the DC is calculated monthly, with proper optimization only the peak loads for the month need to be shifted, which can allow operators to avoid daily cycling and can extend the operational lifespan of their ESS [81]. Specific use cases of ESS can also decrease net emissions. The authors in [80] determined that in specific regions the composition of the generation fleet results in a net increase in overall emissions when incorporating ESS, which means that tariff redesign may be necessary to reduce overall emissions.

All these benefits and services can contribute to the economic viability of BTM ESS in a variety of use cases. However, in order to generate revenue, the system must be optimally operated considering uncertainties and forecast errors. Optimal operation and real-time control strategies for BTM ESS are proposed using noncooperative game theoretic analysis [85], [86], mixed integer quadratic programming [87] and stochastic dynamic programming [88]–[90] that can consider forecast uncertainties. It is shown that even when forecasting errors are present in the model, there is a minimal impact on the overall revenue of the system and resulting payback period [77].

While the existing literature and previous work on BTM ESS analysis provide valuable methodologies, they are specifically designed for certain tariff rates and cannot be readily used and implemented in a tool to model various rate structures currently used in many utilities. For example, Georgia Power has more than 60 tariff rate schedules [91]. A flexible tool for BTM ESS analysis must cover a wide range tariff rate structures to aid BTM ESS owner/operators in making informed decisions on the procurement and operation of ESS. Using our proposed generic optimization modeling approach in chapter 4, we provide a flexible model for BTM ESS analysis in section 4.6.2.

2.5 Literature on Temporal Complexities of Energy Storage Optimization Problems

Optimizing ESS operation for multiple services improves the financial viability of ESS projects and helps stakeholders understand the maximum value of these technologies. However, different timescales of services and the temporal dependency of ESS operation drastically increase the computational complexity of these optimization problems. Some services have monthly resolution, e.g. capacity auctions in market areas such as NYISO, while some other services may vary in a few seconds with significant uncertainty, e.g. frequency regulation. Joint optimization of these services, one with a high-resolution stochastic behavior and other one with long time horizons, is numerically challenging, but can provide significant value as shown in section 5.4.

The current practice is to compromise between the value of the model complexity and the computational capabilities in building and solving that model. A typical approach used by many researchers and industry actors for long-time horizons in energy storage optimization problems is to break the long-time horizon into smaller horizons and then optimize for smaller ones [92]. For example, instead of solving the optimal operation for one year, the operation is optimized in 365 days separately with the constraint that ESS state-of-charge at the beginning and end of each day should be equal. This approach is not globally optimal and underestimates the ESS benefits. Moreover, some services have temporal resolution of longer than a day. For example, the capacity market in many areas, such as NYISO and ISONE, is a monthly service and capacity bids are unique within each month [93]. Thus, daily optimization does not yield optimal solution. High resolution temporal complexity is usually simplified in the literature where real-time operation models with the high resolution (e.g. in seconds) are decoupled from the lower resolution (e.g. hourly) scheduling problems. Some models use sequential approaches that first solve the scheduling problem and the optimal decisions are passed to the high-resolution operation problem for real-time control purposes [94]. Although the numerical tractability is improved by these simplifications, the value of jointly optimized scheduling and real-time operation is still compromised. Therefore, these complicating temporal aspects is another factor that hinders current optimization models to capture the maximum ESS value.

Decomposition techniques and variations of distributed optimization methods are proposed in the literature for tractable solutions of large-scale optimization problems in power and energy systems [70], [95]–[100]. An early work on solving large-scale energy storage optimization problems proposes an aggregation-decomposition method for multi-reservoir systems [101]. This method deals with the spatial aspect of ESS optimization and does not study the temporal aspect. An improved decomposition-coordination and discrete differential dynamic programming method is proposed in [102] to effectively solve a large-scale hydropower system. The objective function is to maximize the generated power, which is not the case for market participation. Another method is to exploit periodicity in system properties, e.g. diurnal patterns of parameters, using time discretization [103]. The method improves the computational time and the objective function compared to daily optimization, but it provides conservative results. Although the results of these works reduce the solution time of a large-scale system operation optimization problem, none of these works studied multiple ESS services and their respective complexities. Also, most of them face implementation challenges on the existing solvers and cannot be readily used in an ESS simulation software. These research gaps are covered in chapter 5.

CHAPTER 3. ENERGY STORAGE IN WHOLESALE ENERGY MARKETS

3.1 Introduction

This chapter presents novel methodologies for evaluating energy storage revenues from participating in wholesale energy markets. The focus is on energy market services and their revenues since they can be readily internalized and captured in terms of monetary values by the ESS owner. Day-ahead (DA) energy market is analyzed first. A new method based on the statistics of realistic energy market data is developed. EA revenue analysis in the real-time market (RT) is presented next. Its significant value is captured by the proposed shrinking horizon optimization approach. A risk-averse decoupled method maximizing the revenues from both day-ahead and real-time markets is also developed and discussed in the final section of this chapter. The sections of this chapters were published in [58], [92], and [104], respectively.

3.2 Day-Ahead Energy Arbitrage Revenue Analysis

This section focuses on the revenue of the EA service in the DA energy market. This service is defined as charging the storage by buying energy during periods with low market prices and discharging it by selling the stored energy during periods when the market price is high. The objective is to understand the expected revenue from this service given a daily price data, and to gain insight on the correlation of the optimal revenue with respect to price data statistics. While it is known that the price changes would increase the revenue from energy arbitrage, no measure of “favorable” volatility is provided that can be used to determine the expected revenue. The proposed method can substitute the complex and computationally cumbersome calculations for this analysis, especially in the case of long time-horizon market data for multiple pricing nodes. The rest of this section introduces the day-ahead energy arbitrage service and the energy storage market participation model. Next, the optimization and proposed approaches are discussed.

3.2.1 Day-Ahead Energy Market

Day-ahead energy markets are developed in restructured power systems so that market actors (power producers, consumers, and traders) buy/sell their consumed/produced energy for the next day. It is assumed that the DA market of day *d* closes at noon of day *d-1*. Market participants submit their bids by then. The independent system operator (ISO) receives the buyers' bids and sellers' offers and operates the market by solving an optimization problem with the objective of maximizing the social welfare, i.e. producers' surplus and consumers' benefits, subject to the network constraints, i.e. line ratings and voltage limits. The ISO clears the market and sets the electricity price for every hour of the next day [53]. Both the demand and the cost of generation change during the day, and the resulting daily electricity price spread creates a unique business model for energy storage owners. They can buy low-cost energy during off-peak hours and sell it back at higher costs during peak hours.

3.2.2 Energy Storage Participation the Day-Ahead Energy Market

Energy storage owners can participate in the day-ahead market to perform energy arbitrage and earn revenues. Since energy storage can operate both as generation and load, owners submit both bids and offers to the day-ahead market. Specifically, for the energy arbitrage, they submit bids for off-peak hours when they are expected to be charging, and submit offers for peak hours when they expect to be discharging. In order to maximize the energy arbitrage service revenue, storage owners forecast day-ahead prices, and optimize the dispatch using optimization models. To guarantee that the bids and offers will be cleared, they can submit zero prices for both. In this way, all the quantities are cleared in the market and will be paid or charged based on the market price of that hour.

3.2.3 Optimization Approach

To capture the maximum revenue of the ESS owner from the EA service, mixed integer linear programming (MILP) models are proposed in the literature and a common one is given in Equations (1)–(7). Equation (1) is the objective of this optimization problem which is the energy storage owner's revenue from the energy arbitrage service given the day-ahead prices π_t as input parameters. The decision variables are output charging and discharging powers, $P_t^{chg,DA}$ and $P_t^{dis,DA}$ (continuous variables) as well as u_t^{chg} and u_t^{dis} (binary variables) showing whether storage is being charged or discharged or idle at time step *t*. Equation (2) enforces the constraint that energy storage cannot be charged and discharged at the same time step. Equations (3) and (4) limit the output powers by their minimum $P_{\min}^{chg}, P_{\min}^{dis}$ and maximum values $P_{\max}^{chg}, P_{\max}^{dis}$. The energy level defined in (5) and is also constrained within its limits $E_{\min}, E_{\max}$ in (6) to ensure a reliable operation. The net exchanged energy is zero during the time horizon, modeled by (7) where the final energy level E_T equals the initial one E_0. The charging and discharging efficiencies are denoted by η_{chg} and η_{dis}, respectively. The storage energy loss over time is modeled by the self-discharging efficiency denoted by η_s.

$$\max \sum_{t=1}^{T} \pi_t \left(P_t^{dis,DA} - P_t^{chg,DA} \right) \Delta t \qquad (1)$$

subject to

$$0 \le u_t^{dis} + u_t^{chg} \le 1 \qquad \forall t \in \mathcal{T} \qquad (2)$$

$$P_{\min}^{dis}.u_t^{dis} \le P_t^{dis,DA} \le P_{\max}^{dis}.u_t^{dis} \qquad \forall t \in \mathcal{T} \qquad (3)$$

$$P_{\min}^{chg}.u_t^{chg} \le P_t^{chg,DA} \le P_{\max}^{chg}.u_t^{chg} \qquad \forall t \in \mathcal{T} \qquad (4)$$

$$E_t = \eta_s E_{t-1} + \left(\eta_{chg} P_t^{chg,DA} - P_t^{dis,DA} / \eta_{dis} \right) \Delta t \qquad \forall t \in \mathcal{T} \qquad (5)$$

$$E_{\min} \le E_t \le E_{\max} \qquad \forall t \in \mathcal{T} \qquad (6)$$

$$E_T = E_0 \qquad \forall t \in \mathcal{T} \qquad (7)$$

In this model, the storage is assumed to be price-taker, and its operation does not impact market prices. It also assumed that all future prices are known for the entire time horizon and they require a complete forecast of future prices to provide acceptable accuracy. Since storage revenue analysis is conducted for the life span of the project, which is in years, knowing all future prices with acceptable accuracy to be used in an optimization model is not a realistic assumption and forecasting them is also quite challenging. Therefore, the lower accuracy of forecast prices especially for a long time-horizon directly impacts and degrades the revenue analysis results and make investment decisions less reliable. Moreover, such optimization models and calculation processes are computationally demanding for not only long time-horizon price data but also multiple pricing nodes. Electricity markets have more than a thousand of pricing nodes and investors would like to know the best one to install energy storage that can provide maximum revenues. This requires solving giant optimization problems for every single pricing node which is extremely time consuming and highly dependent on the accuracy of the price forecast for every time step of the entire analysis time horizon. Another drawback of such optimization models is that they provide little insight on the expected revenue with respect to the input price data. In other words, it is valuable to know a feature of the input price data, so that we can estimate the energy arbitrage service revenue with a good accuracy. Since estimating a feature is much easier than knowing all the price data points, it facilitates the EA revenue analysis. The proposed methodology is described next and it overcomes these difficulties and drawbacks.

3.2.4 Proposed Approach

By the definition of the EA service, the price volatility is favorable in terms of the EA service revenue but there has been no research on quantifying that feature. Thus, the objective of is to find the best statistics of the price data that correlates with the EA service revenue. Analyzing DA energy market data from U.S. electricity markets, we observe that seasonal prices have different patterns and statistics. This is because the energy demand varies continuously creating temporal price spreads. One of the key factors is the seasonal weather change resulting energy demand and price variations. Figure 5(a) and (b) respectively show a 3D plot and a heat map of annual prices of 2016 in the Pennsylvania-New Jersey-Maryland (PJM) market at the aggregate node [105]. Besides the daily changes, different price shapes are also seen for summer and winter seasons where the former has one peak in the evening, and the latter has two daily peaks: one in the morning and the other one in the evening.

Price data for other years in the PJM and also other U.S. electricity markets show similar seasonal patterns. Therefore, the price data needs to be classified based on the seasonal pattern before finding favorable statistics.

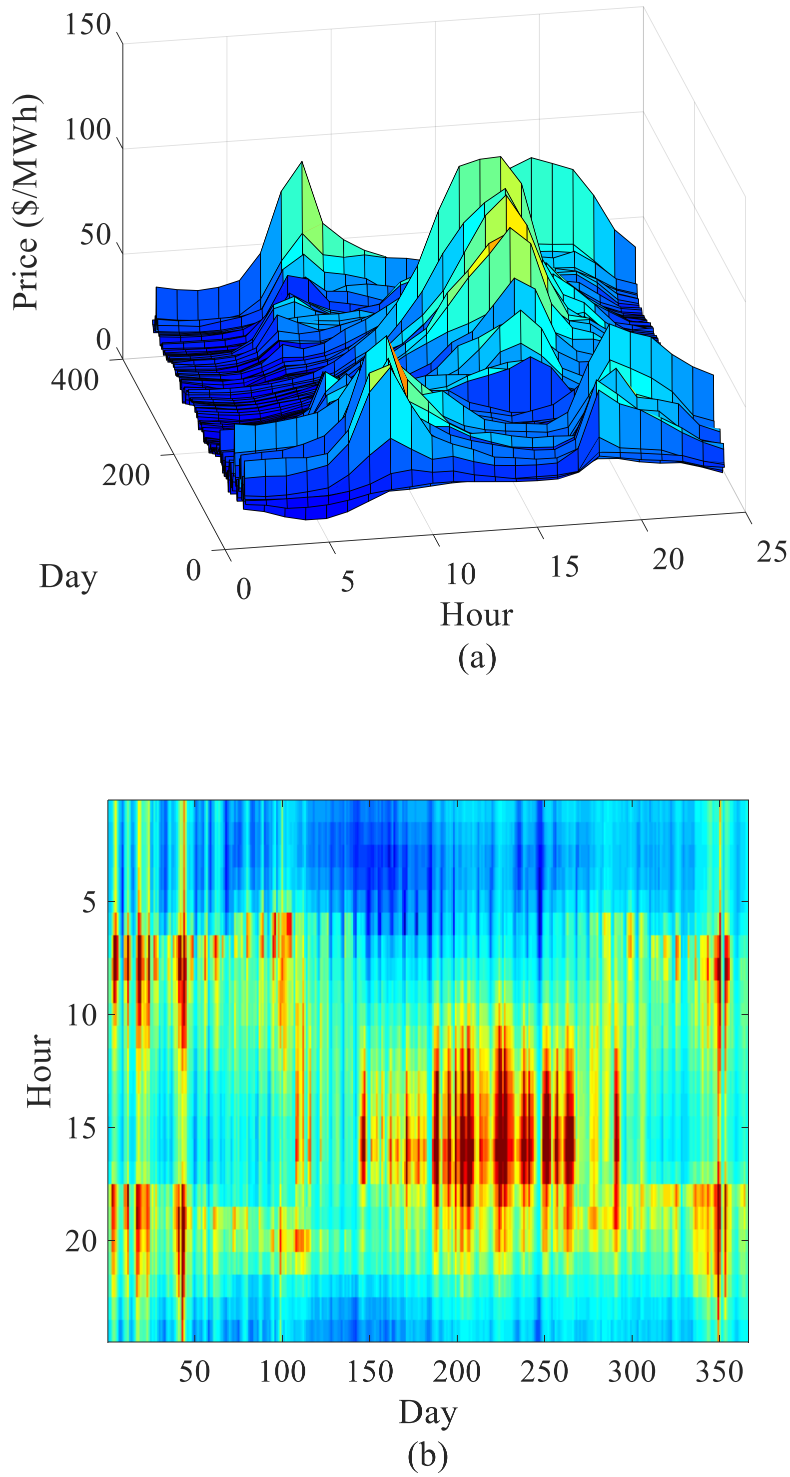

Figure 5 – Temporal price variations in the PJM market during 2016 a) 3D plot and b) heat map

3.2.4.1 Price Clustering

A novel clustering algorithm that classifies the realistic price data is proposed and developed here. This step is necessary since seasonal prices are different in shape and their statistics. The proposed algorithm determines when summer and winter start and when they end in terms of electricity prices.

The optimization problem in (1)–(7) is expressed as a linear function of electricity prices. In other words, if the price is doubled while maintaining the same shape, so does the revenue while the charging/discharging pattern does not change. Leveraging on this fact, any set of daily price data with high linear correlation (i.e., similar shapes) would result in identical dispatch, and the revenues would be proportional to the correlation coefficient. Accordingly, based on the price pattern observation, the prices are classified into summer and winter prices using a novel clustering method to determine when each season starts (in terms of electricity prices) and how long it lasts. Thus, we developed a clustering algorithm inspired by the *k*-means algorithm used in machine learning [106]. In this algorithm, we used the Pearson correlation coefficient (PCC) to measure the linear correlation of two daily price data. Generally, for two data samples x and y with respective means of $\bar{x}$ and $\bar{y}$, the PCC is expressed as:

$$PCC = \frac{\sum_{i=1}^{n}\left(x_i - \bar{x}\right)\left(y_i - \bar{y}\right)}{\sqrt{\sum_{i=1}^{n}\left(x_i - \bar{x}\right)^2}\sqrt{\sum_{i=1}^{n}\left(y_i - \bar{y}\right)^2}} \tag{8}$$

The flowchart of the proposed clustering algorithm is illustrated in Figure 6. The algorithm starts by choosing two initial base prices for the two seasons. Here, we chose Jan. 15th and July 15th for winter and summer initial base prices, respectively. This choice is arbitrary,

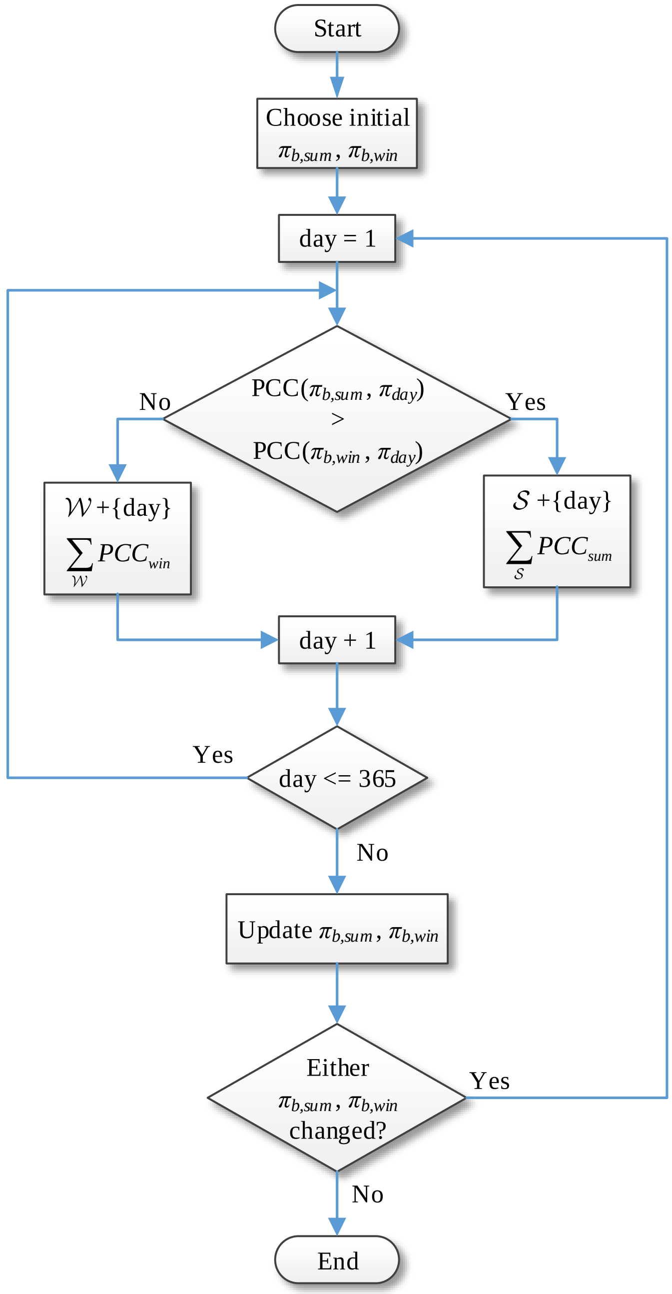

Figure 6 – The flowchart of the proposed clustering algorithm

however, in order to reduce the number of iterations, we chose distinct summer and winter prices rather than boundary prices in April and October. Then, the algorithm rolls on a daily basis, and for each day, it calculates the PCC of the price with the two base prices. The day is then added to the set with greater PCC (set $\mathcal{S}$ for summer and set $\mathcal{W}$ for winter).

The total sum of PCCs in each cluster is updated afterwards. This process iterates until all the days are clustered. After this process, all the two by two PCCs within each cluster are calculated and the daily price with the greatest sum of PCCs is chosen as the new base price. If either of the new base prices is different from the old ones, the algorithm reiterates from day 1, otherwise terminates. The final results are two clusters including summer and winter daily prices, as well as two base prices for each cluster.

3.2.4.2 The Linear Regression Model

In order to quantify the value of energy arbitrage with respect to price statistics, a first order polynomial (straight line) is fitted to the price data statistics of each cluster using the linear regression model:

$$y = X\beta + \varepsilon \tag{9}$$

where y is the vector of daily energy arbitrage revenues, X is the matrix of regressors with the first column of all ones and the second column of daily price statistics, β is a two-element parameter vector (intercept and slope), and ε is the error term. The best estimate of the β parameters that minimizes the squared errors is given by least-squares as in (10).

$$\hat{\beta} = \left(X^T X\right)^{-1} X^T y \tag{10}$$

Using these parameters, we can find the linear relationship between the daily price statistics (X) and the estimated daily revenues ($\hat{y}$).

$$\hat{y} = X\left(X^T X\right)^{-1} X^T y \tag{11}$$

The estimation error is given by:

$$e = y - \hat{y} = \left(I - X\left(X^T X\right)^{-1} X^T\right) y \tag{12}$$

where I is the identity matrix. The goodness of linear fitting models can be expressed by several measures. Here, the R-squared value (also known as coefficient of determination) is used. The R-squared value is calculated as:

$$R^2 = 1 - \frac{SS_{res}}{SS_{tot}} \tag{13}$$

where

$$SS_{res} = \sum_i e_i^2 = \sum_i \left(y_i - \hat{y}_i \right)^2 \tag{14}$$

$$SS_{tot} = \sum_i \left(y_i - \bar{y} \right)^2 \tag{15}$$

3.2.5 Simulation Results and Discussion

This section provides the results of the proposed methodology. First, the storage owner's maximum revenue is calculated using Equations (1)–(7). The clustering algorithm results are then provided. Prices statistics of dispersion are introduced next, and the results of the linear regression model are presented lastly.

3.2.5.1 Optimization Results

Using the optimization model (1)–(7) and the PJM historical prices, the owner's revenue from the EA service is computed for the day-ahead market of the last five years. Hourly day-ahead market prices at the aggregate node were analyzed from 2013 to 2017 [105]. Data was cleaned, and the missing days without the price data were removed from the dataset. The missing hours are linearly interpolated using the adjacent hours. The simulation parameters corresponding to the energy storage device are

$P_{\max}^{dis} = P_{\max}^{chg} = 100MW$, $E_{\max} = 100\,MWh$, $E_0 = 0.5E_{\max}$, $E_{\min} = 0$, $\eta_{chg} = \eta_{dis} = 0.95$, $\eta_s = 1$, $\Delta t = 1hr$.

As an example, the day-ahead prices and the optimal dispatch for two sample days (1/9/2017 and 9/21/2017) are shown in Figure 7. These two days result in maximum winter and minimum summer revenues in the year 2017. The price shapes are different such that the winter day has two peaks, one in the morning and the other in the evening with the price range of $72 during the day. However, the price shape of the summer day has only one peak during the evening with the price range of $8. The charging and discharging patterns are different due to different price shapes. The revenue in the winter day is $7,785 while the summer day provides only $490.5, which is 6.3% of that for the winter day.

3.2.5.2 Clustering Results

The proposed clustering algorithm is run on the five-year historical price data of PJM and converged within 3, 2, 3, 3, and 4 iterations for 2013 to 2017, respectively. The results are shown in Figure 8. It can be clearly seen that the proposed algorithm is capable of clustering seasonal prices based on their shapes. Figure 8(a) and (b) show the sets of summer and winter prices. Final base prices in Figure 8(c) show that the peak prices of the two clusters are almost equal while the minimum price of summer is lower than that of winter. Each of these prices has a favorable feature for energy arbitrage service. While the daily price spread is greater in summer, the winter prices have two peaks providing opportunities for two charging and discharging cycles in a day. The analysis of results provided later shows that the two-peak feature of winter prices is more favorable for energy arbitrage resulting in higher revenues in winter days.

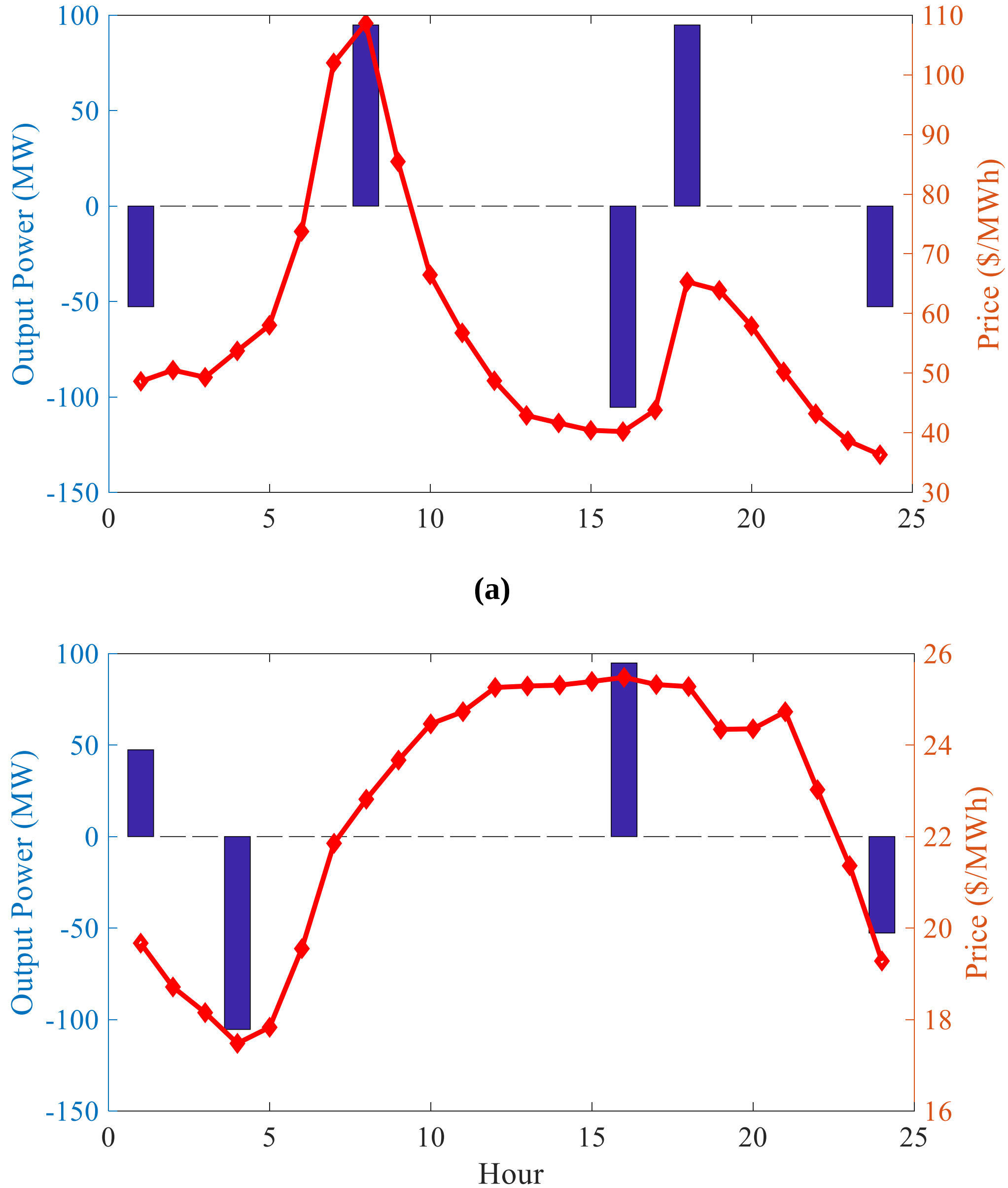

(a)

(b)

Figure 7 – Daily price and optimal dispatch for a) Jan. 9th and b) Sept. 21st 2017

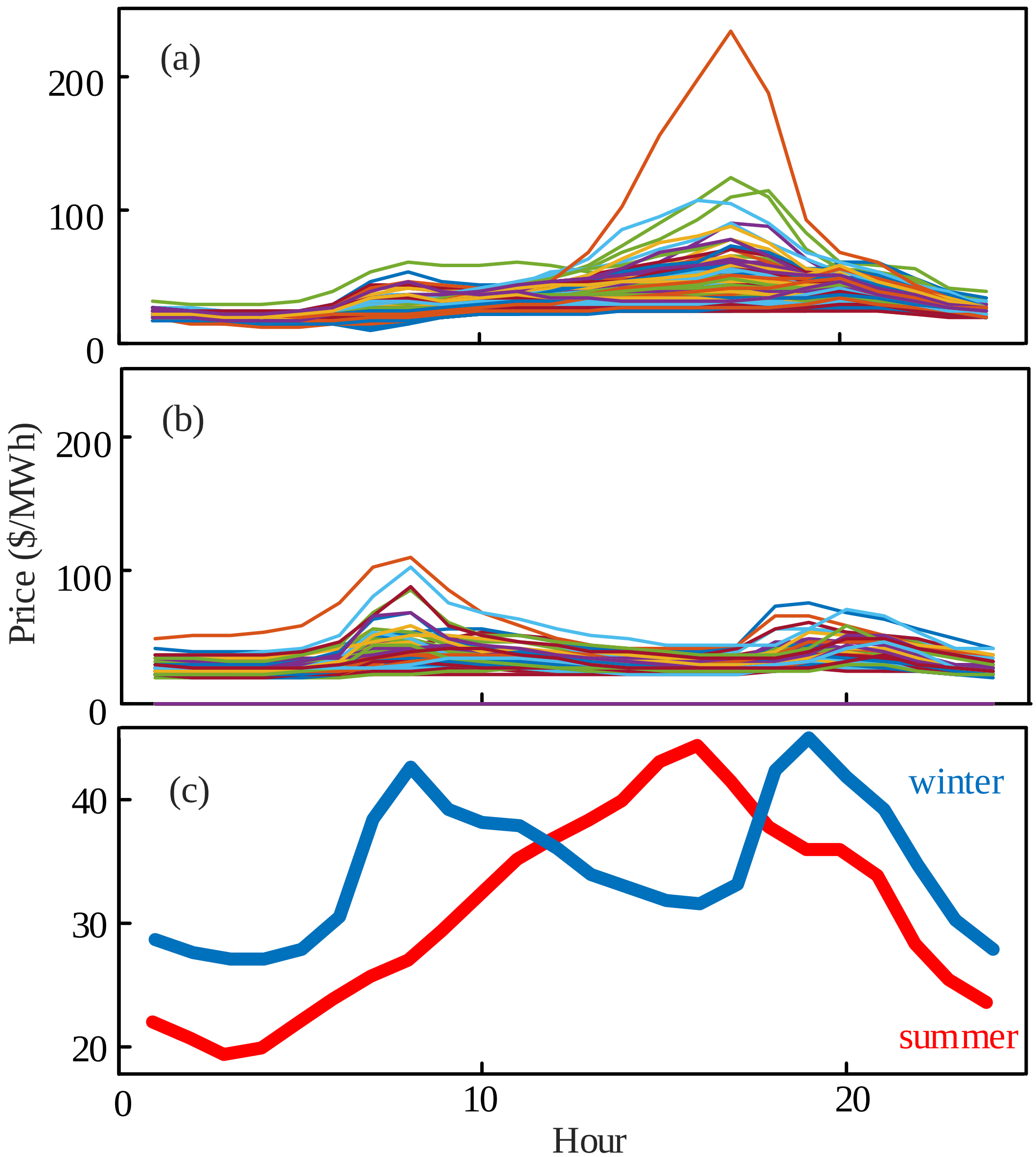

Figure 8 – Results of the proposed clustering algorithm: a) summer, and b) winter daily price clusters, and c) base prices of clusters

Clustering results for each year are shown in Figure 9. The range of the boxplots shows the middle 95% of the clustered summer days in each year. There are few days in summer and winter months with the price of the other shape. These days are considered outliers, and are not considered in determining the set of summer and winter days. Apart from 2017, the summer days for each year overlaps greatly. Using these results, we consider the set of summer days to include days 101 to 282. The set of winter days include the rest of the days in a year.

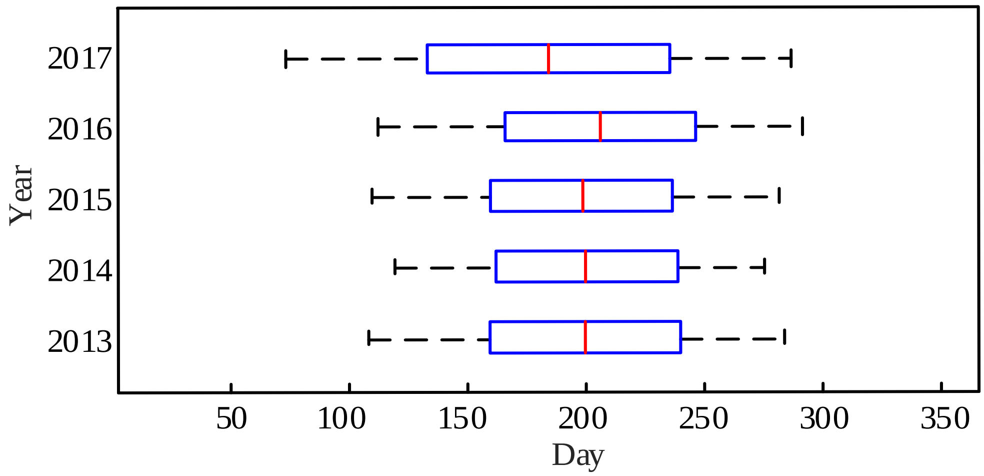

Figure 9 – Boxplot of summer days in each year clustered by the proposed algorithm

Once daily prices are clustered, we use each cluster's statistics to find a linear relationship with the maximum daily revenue calculated from Equations (1)–(7). Therefore, the following daily price statistics of dispersion are tested:

- range: $\pi^{\max} - \pi^{\min}$,
- standard deviation: $\sigma = \sqrt{\frac{1}{N_T}\sum_{t=1}^{N_T}\left(\pi_t - \overline{\pi}\right)^2}$,
- mean absolute deviation (MAD): $MAD = \frac{1}{N_T}\sum_{t=1}^{N_T}\left|\pi_t - \overline{\pi}\right|$, where $\overline{\pi} = \frac{1}{N_T}\sum_{t=1}^{N_T}\pi_t$. i.e. the average of absolute difference from the mean price.

3.2.5.3 Linear Regression Results

The linear regression model is applied to both summer and winter clusters for different price statistics. The tuples of revenue and statistics for each cluster are plotted in Figure 10, as well as the fitted lines. In these plots, red crosses are for summer and blue circles are for winter. The estimated parameters of the fitted lines, and the R-squared values are reported in Table 1 for different clusters and price statistics.

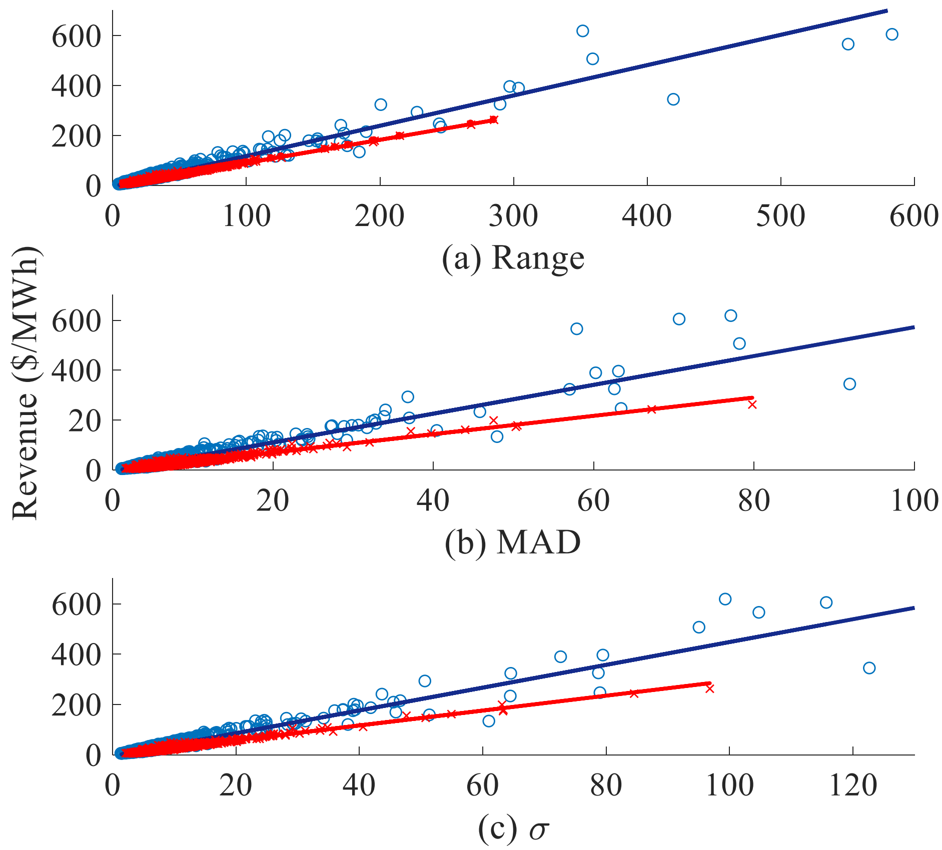

Figure 10 – Linear regression results: revenue vs. price a) range, b) MAD, and c) standard deviation

Table 1 – Linear Regression Model Results

Parameter	Season	Range	MAD	σ
β0	summer winter	-2.55 -4.16	-2.98 -5.01	-1.77 -5.08
β1	summer winter	0.92 1.21	3.67 5.77	2.96 4.53
R-squared	summer winter	0.9868 0.9486	0.9415 0.9253	0.9619 0.9484

The results show that winter revenues are in general higher than summer revenues. The sensitivity of winter revenues with respect to price data statistics is always larger than those of summer. This is justified by the general price shape of winter daily prices. Because winter prices have two daily peaks, there is more opportunity for energy arbitrage in those days. Furthermore, the results reveal that the energy arbitrage revenue is linearly correlated with the electricity price data statistics of dispersion. Among the tested statistics, the revenue shows the best linear relationship with the price range. Therefore, given the electricity price data of a node, its expected revenue from the energy arbitrage can be easily expressed as a linear function of the price range. This simplifies the service benefit analysis for the utilities and investors. In addition, with the prices of different pricing nodes in a region, the problem of the optimal placement of energy storage in terms of the highest energy arbitrage value is simplified to finding the node with the highest sum of daily price ranges.

The results provided are for fixed energy storage parameters, such as efficiency and capacity. Sensitivity analysis can be performed within the same framework. While linear sensitivities change by varying energy storage parameters, the greater winter revenues and their sensitivities remain unchanged. Also, if the capacity of the energy storage is high enough to impact the energy market price (price-maker energy storage), the optimization model in [22] can again be used in our proposed framework to determine the service value. It is expected that higher extreme prices will emerge in the future energy markets with more renewables integrated into the grid. This adds to the value of energy arbitrage service from energy storage projects promising a unique business opportunity for the future grid.

3.3 Revenue Analysis of Energy Storage Participating in the Real-time Energy Market

This section presents a methodology for the revenue analysis of the EA service in the real-time (RT) electricity market. It is very likely that with the trend in the deployment of new intermittent renewable generations, the RT price variation will continue to increase. As a result, more RT arbitrage opportunities are expected, which will increase the profitability of energy storage projects. Previous studies underline the significance of the forecasting accuracy on the maximum value of the EA service. Thus, a robust dispatch can compensate for the low forecast accuracy. Furthermore, none of the previous studies has investigated or compared the DA and RT market values for the EA service.

We show the significant value of the EA service in the RT compared to the DA market using historical market prices and propose a dynamic optimization approach based on the shrinking horizon algorithm to capture the maximum EA revenue. With this objective, we first introduce the RT electricity market and provide statistical analysis results based on PJM historical market data. Next, we use the optimization model described in Equations (1)–(7) to compare the maximum value of the EA service in the RT market with respect to the DA market. This model assumes a perfect foresight of the future prices. However, the uncertainty of the RT prices limits the applicability of that model and yield to undesirable results. Therefore, a more realistic participation model of the storage in the RT market is proposed using a shrinking horizon optimized dispatch algorithm to increase the EA revenue in the RT market. The simulation results show that the new methodology is a robust tool to capture the high value of the RT market even under high levels of uncertainty.

3.3.1 Real-Time Energy Market

Since operating the electricity grid deals with numerous uncertainties, delivering and dispatching the required energy cannot be planned with great certainty one day before the actual delivery time as it is planned in the DA market. Therefore, almost all the restructured power systems have at least another market established for energy trading nearer to the actual time of delivery. The DA market is introduced in section 3.2.1 where all the prices are known the day before after the DA market is cleared. In the RT market, however, prices are updated in RT (e.g., every five minutes), hence they are not known in advance. The operator balances the RT generation and load, and based on the amount of energy needed for these balancing actions, the RT price is set [53]. Accordingly, the higher variability of RT prices is evident with the higher penetration of intermittent renewable generation. To illustrate this, a statistical analysis is performed on the PJM historical price data. PJM is selected since it serves the greatest number of customers in the U.S. Other market data is also observed, and similar results are found.

3.3.2 Statistical Analysis of the PJM DA and RT price data

Aggregate hourly DA and RT market prices from 2013 to 2017 were analyzed. Although RT market prices are 5-minute data, hourly-averaged RT prices are used to make DA and RT sample sets statistically comparable. It should be noted that five-minute prices have more variations that can increase the profitability of EA. Data was cleaned, and the missing days without the price data were removed from the dataset. The missing hours are linearly interpolated using the adjacent hours.

Table 2 – Statistical Analysis of PJM Energy Prices in DA and RT Markets ($/MWh)

Year	2013	2014	2015	2016	2017
Mean DA	37.15	49.16	35.61	30.01	30.21
Mean RT	36.57	48.40	33.43	27.27	28.97
Median DA	34.62	38.10	30.58	27.48	27.46
Median RT	32.25	34.48	26.62	24.03	25.28
IQR DA	11.94	18.64	13.55	11.75	11.66
IQR RT	11.69	18.67	11.18	8.62	9.68
Std DA	15.46	51.87	22.63	11.58	12.02
Std RT	20.69	65.43	27.91	14.64	17.75

Table 2 shows the relevant statistics of five-year prices in both markets: mean, median, interquartile range, and standard deviation of each market. Although the mean price of DA is higher than that of RT in all years, the standard deviation of RT prices is much higher than that of DA. The analysis shows the higher price variations in the RT market that can provide more EA values if exploited properly.

3.3.3 Energy Storage Participation the Real-Time Energy Market

The energy storage can participate the RT market to perform EA. Energy storage participation in the DA market is described and modeled in section 3.2.2. Storage participation in the RT market is based on the RT prices, and the storage owner dispatches in RT, and buys and sells at the RT price for charging and discharging, respectively. In order to quantify the owner's revenue from each of these markets, and for a clear comparison between them, optimization models are used.

3.3.4 Maximum Revenue with Perfect Foresight

The maximum revenue from the EA service is possible when all future prices are known with certainty. To find this maximum in both markets, the optimization model presented in (1)–(7) is used. This modeling approach renders a benchmark for the EA service evaluation, and it is important for economic decision-making strategies of private storage projects. Using the optimization model and the PJM historical prices, the owner's revenue from the EA service is computed for DA and RT markets of the last five years. The simulation parameters are set to identical to those in section 3.3.4 The optimization model is run for all days with the available price and the revenue is averaged over each year and normalized by the storage output power. The results are shown in Figure 11.

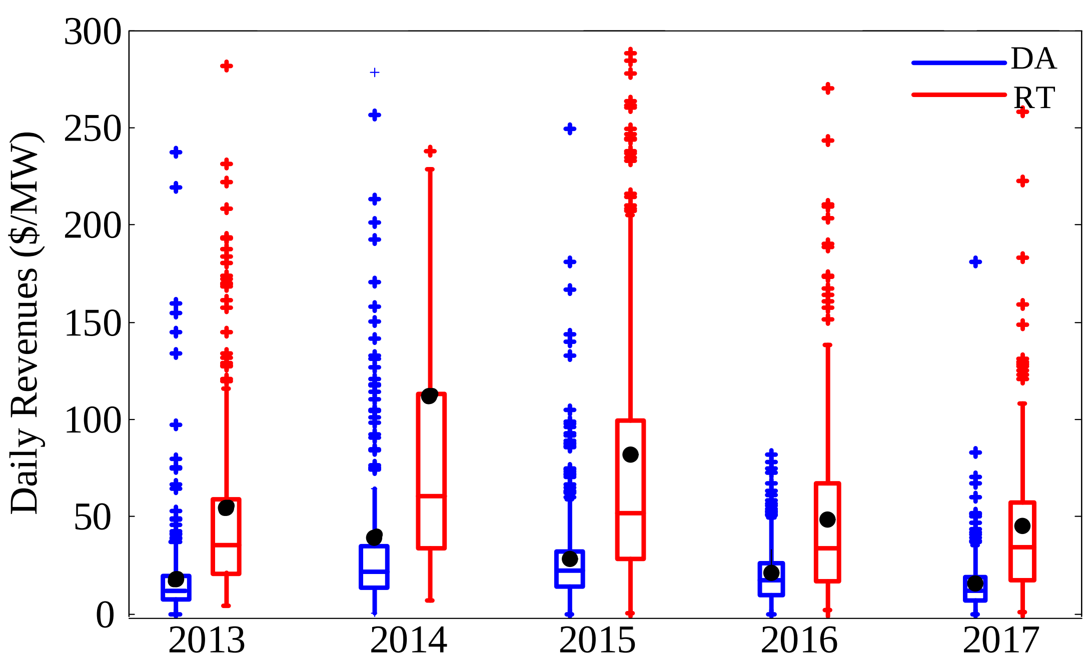

Figure 11 – Daily revenues from the EA in DA and RT markets

The value of the EA service is quantified by the results where the mean revenue is in the range of 15–40 $/MW for the DA and 45–112 $/MW for the RT market. The correlation between the price variations and the revenues from each market is evident comparing Table 2 with Figure 11. The results confirm higher revenues (about twice as much) from EA in the RT market than in the DA. The above results are for a fixed efficiency and energy capacity. Therefore, A sensitivity analysis is conducted to investigate the sensitivity of the EA service revenue with respect to the roundtrip efficiency ($\eta_{chg} \times \eta_{dis}$) and storage capacity, defined here as the number of hours that the storage can operate discharge at maximum power, that is equal to $E_{\max} / P_{\max}^{dis}$. Two simulations are run separately where in the first one, the roundtrip efficiency is swept from 50% to 100% while the capacity is set to one hour, and in the second one, the capacity is swept from one hour to 24 hours and the roundtrip efficiency is set to 90%. The EA daily revenue is computed and averaged over all the days of the five-year data. The results are illustrated in Figure 12.

The results reveal that the EA revenue from the RT market is greater than that of the DA market regardless of the storage parameters. The difference in these market revenues grows slowly with the roundtrip efficiency, and it is almost constant with respect to the storage capacity. Also, in both markets, the average revenue increases with the roundtrip efficiency and the storage capacity. However, it reaches saturation for high storage capacities. This is reasonable since after a certain capacity, the storage has collected most of the energy needed for the EA. More revenues are achieved only if the output power limit increases. Moreover, the marginal revenue is higher for lower capacities and higher efficiencies meaning that a low capacity but highly efficient storage can capture most of the maximum revenue. The marginal revenues for an ideal storage with one-hour capacity are $1.75 per efficiency percentage and $31.69 per an hour. These values can be used to evaluate the EA revenues in PJM based on the storage parameters.

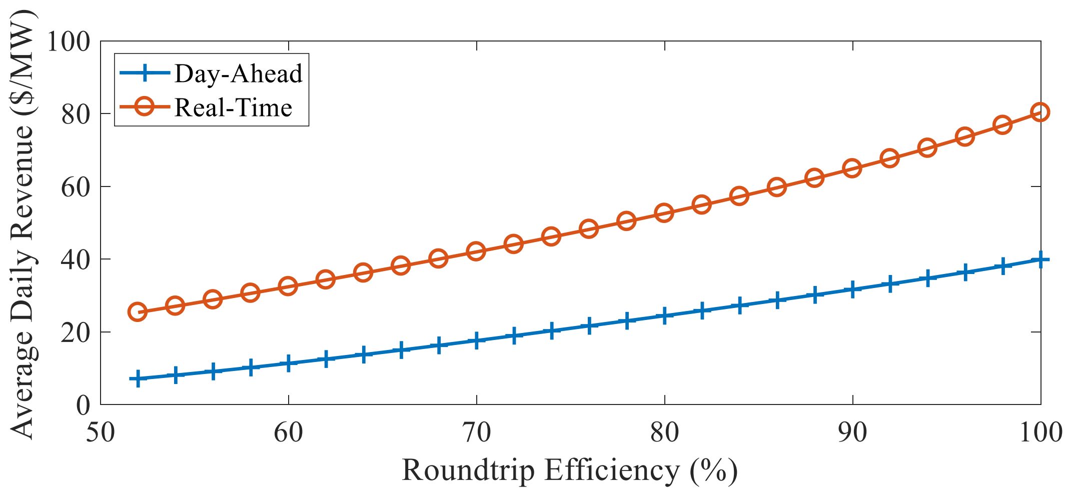

(a)

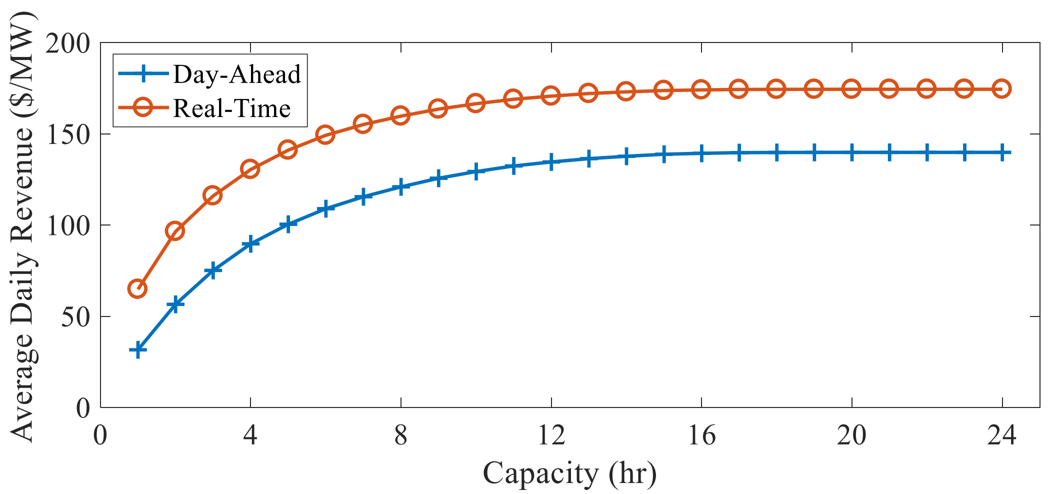

(b)

Figure 12 – Average daily revenue from EA in DA and RT markets with respect to: a) roundtrip efficiency, and b) storage capacity

While the RT market is more profitable than the DA for the EA service assuming a perfect foresight, its application should consider the larger errors of price forecasts in the RT market due to the higher price variability. Thus, the more realistic case of the EA service evaluation with forecast errors is discussed next.

3.3.5 *Impact of Uncertainties and Forecast Errors*

The effect of uncertainty in price forecasts is investigated in this section. Uncertainty is modeled with two approaches: back casting and random normal error. The back-casting approach considers the realized prices of the day *d* for the dispatch of the day *d+1*. In the second approach, the assumption of the perfect foresight of future prices (π^{PF}) is altered by adding a random noise that models the uncertainty in the forecast. The altered price $\left(\pi^{err}\right)$ is:

$$\pi_t^{err} = \pi_t^{PF}\left(1+e\right) \qquad \forall t \in \mathcal{T} \qquad (16)$$

where *e* is a random variable sampled from a normal distribution ($e \in \mathcal{N}(0,\sigma)$) and σ is the error standard deviation. The model accounts for larger forecast errors ($\left|\pi_t^{err} - \pi_t^{PF}\right|$) when the actual price is high as in the case of price spikes that are predicted with greater errors. The altered price in both DA and RT markets is used for the storage dispatch.

3.3.5.1 Proposed Algorithm

The RT forecast errors are larger due to the higher RT price variability. However, the RT dispatch can be optimized at the beginning of each time period as soon as the RT price is realized. For example, at the beginning of hour *t*, the RT price for that hour (π_t) is set by the ISO. Knowing this price, the RT dispatch is optimized for period *t* up to *T*, as described in the Algorithm 1 where $\hat{\pi}_i$ is the forecast price for period *i*, which is known by either back-casting or random normal error. It is assumed that the updated dispatch is calculated right at the beginning of the period *t*, without any delay. The method is not highly dependent on the forecast accuracy compared to the linear optimization since it updates the dispatch for the remaining time of the horizon at the beginning of each time period when a new price data is realized. This method is known as the shrinking horizon dynamic programing [107].

Algorithm 1 Shrinking horizon dispatch

1: $t = 1$
2: **while** $t < T$ **do**
3: Solve:

$$\max\left[\pi_t\left(P_t^{dis,RT} - P_t^{chg,RT}\right) + \sum_{i=t+1}^{T}\hat{\pi}_i\left(P_i^{dis,RT} - P_i^{chg,RT}\right)\right]\Delta t$$

Subject to Equation (2),

$$P_{\min}^{dis}.u_t^{dis} \le P_t^{dis,RT} \le P_{\max}^{dis}.u_t^{dis},$$

$$P_{\min}^{chg}.u_t^{chg} \le P_t^{chg,RT} \le P_{\max}^{chg}.u_t^{chg},$$

$$E_t = \eta_s E_{t-1} + \left(\eta_{chg} P_t^{chg,RT} - P_t^{dis,RT} / \eta_{dis}\right)\Delta t,$$

Equations (6), (7).

4: $t = t + 1$
5: **end while**

3.3.5.2 Simulation Results

The EA revenue from both markets using the back-casting approach are calculated for various efficiencies and capacities. The storage parameters are as in section 3.2.5.1. The optimized dispatch based on the price data of the previous day is multiplied by the actual price data of the running day to find the actual revenue. Results are then divided by those calculated with perfect foresight in section 3.3.53.3.4 to show the ratio of actual collectible revenues with forecast uncertainties to the ideal maximum revenues. Figure 13(a) and (b) present the percentage of the revenue for DA and RT markets, respectively, using back-casting as the forecast approach.

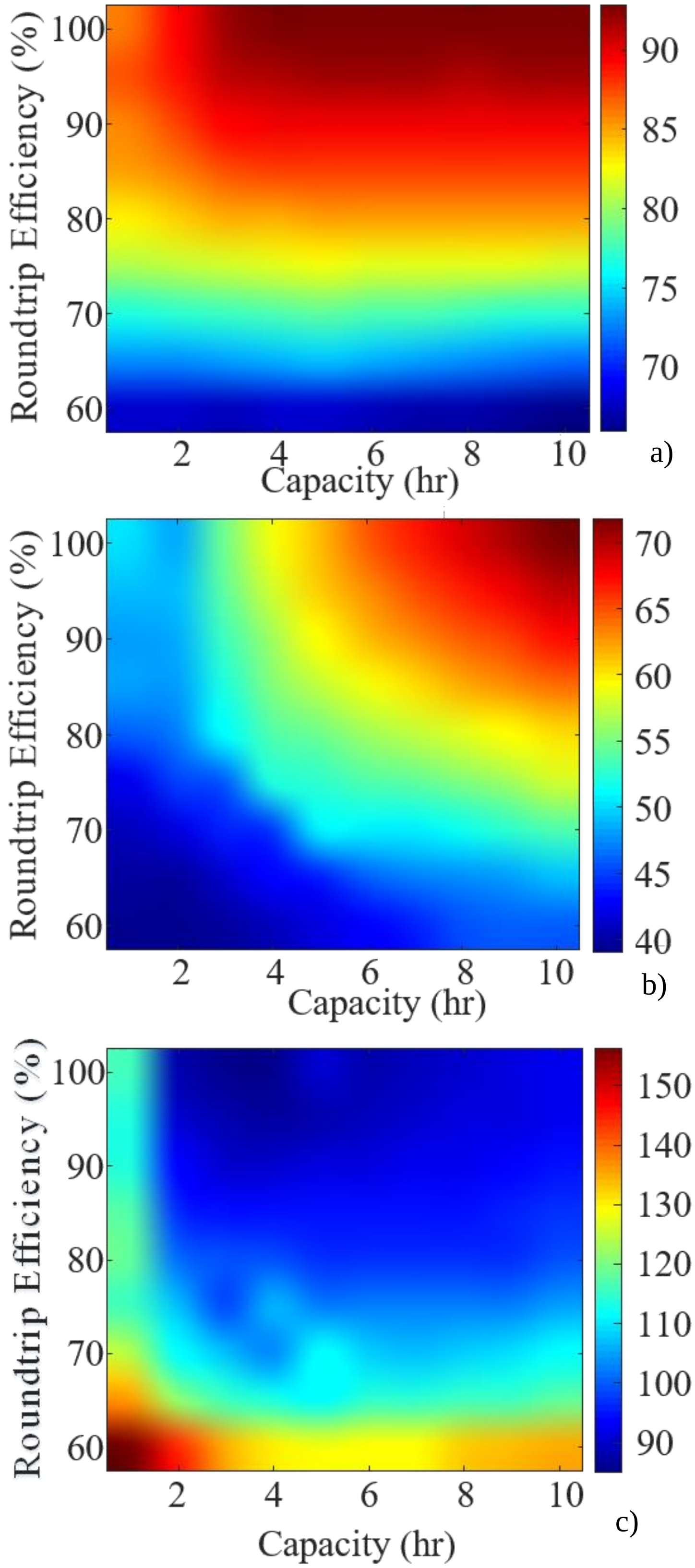

Figure 13 – Collectible percentage of revenues using back-casting for price forecast (a) DA and (b) RT markets, and (c) RT over DA

The back-casting method can collect higher percentage of perfect foresight revenues in the DA market than in the RT market. This is because DA prices show higher correlations within two consecutive days than the RT prices. Thus, the DA prices of the previous day is a fair estimate of those of the running day and the optimized dispatch would result in higher percentage of the maximum revenue. Across the simulated range of efficiencies and capacities, the percentage is between 66%–93% for DA and 39%–72% for the RT market. Higher ratios are seen for more efficient storages. Note that even the 39% of the maximum potential revenue for the RT market, with twice the DA market value, is still comparable to 93% of that in the DA one. The actual collected revenue from the RT market relative to that from the DA one is illustrated in Figure 13(c). This ratio ranges between 85%–156%.

The collectible revenues from both markets under uncertainties modeled with random normal errors are also calculated for various efficiencies and error standard deviations and compared to the ideal maximum revenues. Capacity is set to be 100 MWh (1hr). The parameter σ is taken from the interval 0.02 to 0.1 to model the error of short-term price forecasts. Considering that the relative error is within 10% of the nominal value [108] for 95% of the time, the maximum error with 2σ standard deviation must be less than 10% error. As a result, a $\sigma \leq 0.05$ is sufficient. The selection of this parameter considers an extra margin for extreme cases such as price spikes. Accordingly, the forecast error is expressed as

$$\%\, forecast\_error = 200\sigma \tag{17}$$

The altered price in Equation (16) is input to the optimization models for a range of forecast errors between 4%–20% [109]. Using forecast prices, the dispatch is optimized, and the revenues are calculated using actual prices. Average daily revenues from both DA and RT markets are calculated and normalized based on the revenue in the perfect foresight case. Results are shown in Figure 14(a) and (b) for DA and RT markets, respectively. Modeling the forecast uncertainties with random normal errors results in the higher percentage of the collectible revenue from the RT market than the DA one. Even in the extreme case of 20% error, the RT dispatch captures more than 85% of the maximum potential revenue while the DA dispatch cannot capture more than 75% in this case. The higher ratio of the collectible revenue in the RT market is due to the dynamic optimization dispatch strategy, the proposed shrinking horizon algorithm, which updates the dispatch at the beginning of each period just as the price is realized. The inclusion of the most recent price in the dispatch enables it to better capture the price spikes resulting in higher revenues.

In both DA and RT markets, the percentage of revenue decreases with the increase in forecast errors, as expected. However, the rate of this decrease is lower for the RT market. This is also explained by the less sensitive dynamic dispatch strategy. Moreover, the RT revenue with the price forecasts is shown to be more than 15% higher than the back-casting approach. For instance, if the error of the RT price forecast is known to be the extreme value of 20%, for a 1MW/1MWh storage system with 80% efficiency, higher revenues are expected if the RT price forecasts are used to find the optimal dispatch. This strategy can collect more than 91% of the maximum potential revenue while the back-casting approach cannot collect more than 47%.

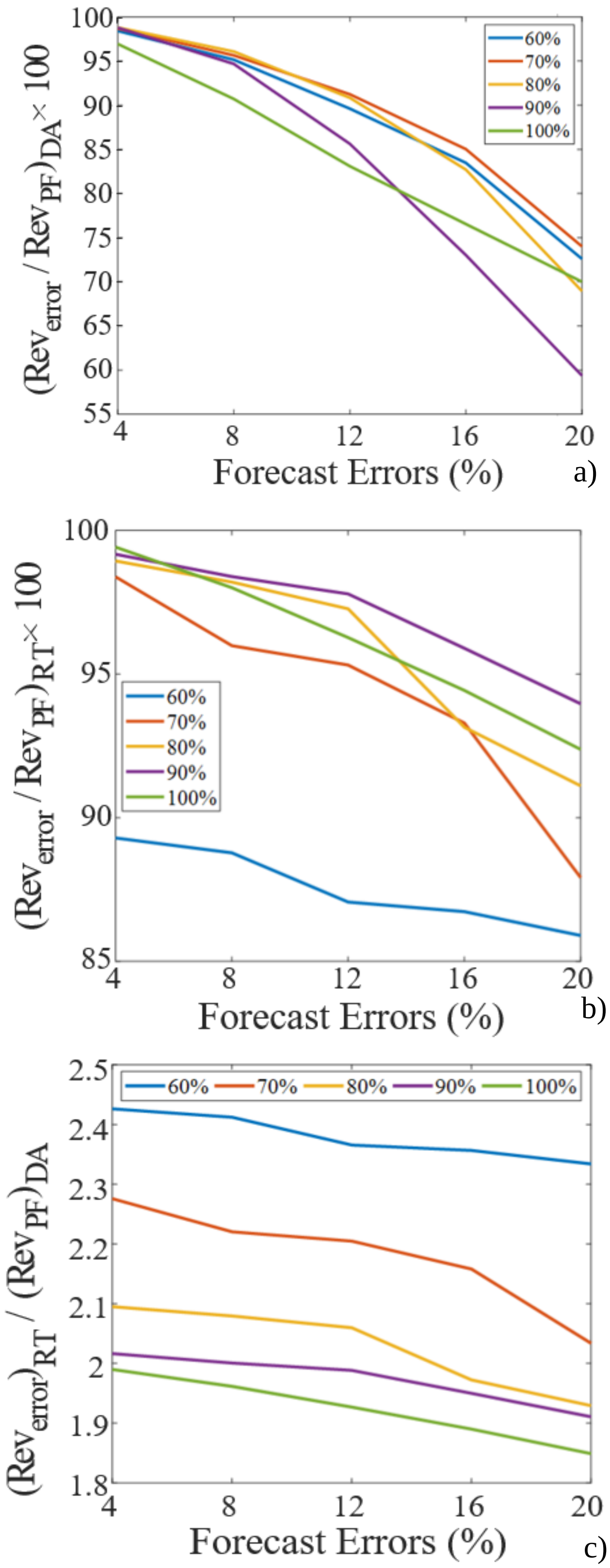

Figure 14 – Collectible percentage of revenues using random errors for price forecast (a) DA and (b) RT markets, and (c) RT over DA

The analysis also shows that if the storage participates only in the DA market for the EA, the back-casting approach results in relatively higher revenues in case of large forecast errors. Generally, the results can help storage owners decide on the optimal dispatch based on the accuracy of the DA price forecasts for a wide range of efficiencies and capacities. For example, if the error of the DA price forecast is known to be 10%, for a 1MW/1MWh storage system with 80% efficiency, higher revenues are expected if the DA price forecasts are used to find the optimal dispatch. This strategy can collect almost 95% of the maximum potential revenue while the back-casting approach cannot collect more than 82%.

The value of the RT market with uncertainties relative to the DA with perfect foresight is described in Figure 14(c) for a 1MW/1MWh storage system across a wide range of efficiencies. Even in the worst-case scenario where the RT price forecast error is 20%, the RT market revenue from the EA service is more than 1.8 times the revenue from the DA market considering a perfect foresight. Results for larger storage capacities up to 10 hours, still show a 10% surplus in the RT market with large errors compared to the DA market with perfect foresight. Furthermore, storage units with lower capacities and efficiencies show higher relative revenues from the RT compared to the DA. With the high EA value of RT market shown with realistic market data, ESS owners can rely on the RT market as an additional revenue stream to utilize their assets financially more attractive.

3.4 Revenue Analysis of Energy Storage Participating in both Day-Ahead and Real-time Energy Markets

The participation of ESS in DA and RT energy markets is studied so far. Here, we propose an optimal operating strategy to maximize the revenue of energy storage systems (ESS) that participate in both DA and RT energy markets. While we showed that the RT market can have more than twice the arbitrage value compared to the DA market higher price volatility with greater forecast errors in the RT market, can limit the profitability of the ESS energy arbitrage if the ESS participates only in this market. This is not desirable for a risk-averse ESS operator or owner. Thus, in this section, RT market participation is proposed as an extra revenue stream for the ESS that is added to the less risky revenue from the DA market. We seek to optimally stack the arbitrage service values of DA and RT energy markets. Moreover, the optimization models are modified in this section to account for ESS market power and degradation. The rest of this section is organized as follows. First, we describe the proposed decision framework for ESS market participation. The mathematical formulation is presented next. We further provide simulation results and conclude this section.

3.4.1 Market Participation Models

It is proposed that the ESS operator can participate in and collect revenues from both the DA and RT energy markets. In this setting, the operator decides the optimal values of the ESS output power that maximize the revenue in both markets and submits the corresponding bids for each market. The timeline for this decision process is illustrated in Figure 15. Two consecutive days are shown and denoted by *d-1* and *d*.

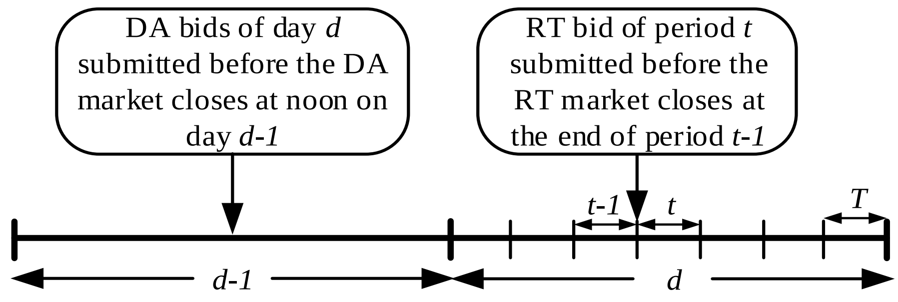

Figure 15 – DA and RT market participation timeline

3.4.1.1 Day-ahead operation

It is assumed that the DA market of day *d* closes at noon of day *d-1*. Market participants submit their bids by then. Next, the market operator computes the DA market prices based on the received bids. Market results (cleared prices and bids) are released a few hours later. The ESS operator estimates the DA energy prices, solves the proposed quadratic optimization program that maximizes the DA net revenue, finds the optimal DA dispatch, and submits the charging and discharging bids accordingly to the market. Since ESS has no fuel cost for generation, the operator bids at zero price for discharge bids. Charging bid prices are assumed to be at the maximum price. Thus, both bids are always cleared at the market price with the submitted quantity. However, the ESS operation is assumed to affect the market price. The DA price is assumed to be an affine function of the ESS net output power [110]:

$$\pi_t^{DA} = \pi_t^{DA0} + \gamma\left(P_t^{dis,DA} - P_t^{chg,DA}\right) \qquad \forall t \in \mathcal{T} \quad (18)$$

where the intercept π_t^{DA0} is the DA forecast price with no ESS operation determined by a back-casting method. The slope γ is calculated from linear interpolation of the price versus demand curve in the given market [26]. This assumption is based on the realistic market data. For example, Figure 16 shows the DA price versus the system load in the PJM market during December 2018 [105]. The price is increasing with more demand. Since the storage output $\left(P_t^{dis,DA} - P_t^{chg,DA}\right)$ can be regarded as a negative demand, the value of γ is the negative of the slope of the interpolated line on the price-demand curve. When the DA market closes, the ESS operator receives revenues based on the DA cleared prices multiplied by the operation of ESS. Obviously, prices can be different from the forecast ones.

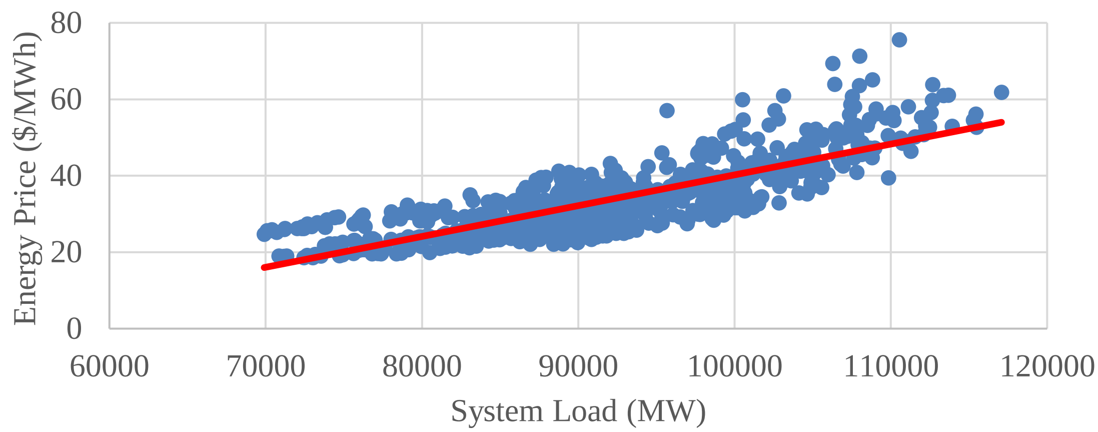

Figure 16 – DA price versus load data in PJM during December 2018

3.4.1.2 <u>Real-time operation</u>

When day *d* starts, the ESS operator can participate in the RT market by deviating from its DA dispatch. It is assumed that the RT market for each hour is run and cleared on an hourly basis, and that the RT market for period *t* is closed and cleared right before it starts. The shrinking horizon algorithm [107] is used to optimally exploit this hourly rolling framework. Specifically, before period t starts, the ESS operator estimates the RT prices for the rest of the day [t, T], solves an optimization problem that maximizes its net revenue, and submits the optimal bid only for period t. This process is repeated for every period. The submitted bid represents the ESS output deviation from the DA value. Any deviation is transacted at the RT price. It is also assumed that the RT operation of the ESS does not affect the RT prices since it operates after the price is cleared. Similar to the DA market, price forecasts are used to find the optimal dispatch while the revenue is calculated based on actual price data.

3.4.1.3 Uncertainty

Uncertainties in price forecasts of DA and RT markets are modeled as follows. For the DA market, the ESS operator uses the price data of day *d-1* to find the optimal dispatch of day *d*. This is the back-casting method [26]. In section 3.3.5.2, we showed that for ESS with efficiencies higher than 70%, the obtained revenue using this method is more than 80% of the case with perfect foresight. Thus, the method provides a considerable ratio of maximum revenue. For the RT market, the forecast price is determined by a normal relative error described by Equation (16). Assuming a constant standard deviation for forecast errors up to 20%, the obtained revenue is more than 86% of the case with perfect foresight verifying the robustness of the shrinking horizon optimization method. Moreover, a more realistic model is proposed here. Since the probability of larger forecast errors increases for later time periods, the standard deviation of the normal relative error depends not only on the forecast error, but also on the time difference between the forecast period t and the current optimization period τ as in (19).

$$\sigma_t = (t-\tau)\sigma^{\max} \qquad \forall t,\tau \in \mathcal{T}; t > \tau \tag{19}$$

The maximum standard deviation $\sigma^{\max}$ is determined by the error of the forecast method (17). Several samples of the relative error e must be taken to capture a wide range of price scenarios. As an example, price forecast errors for 10 sampled scenarios are shown in Figure 17. For each hour t, the standard deviation of the relative error (σ_t) is determined by (17) and (19). Then, a sample is taken from a normal distribution. This sampling is process for all the hours is repeated 10 times to generated 10 sampled scenarios shown in Figure 17. As can be seen, using the model in (19), the variability of the relative error increases for later time periods. Note that this linear model can be improved by statistical analysis of historical prices and their forecasts. For example, a model with higher variabilities during certain hours of the day can also be developed which is out of the scope of this work.

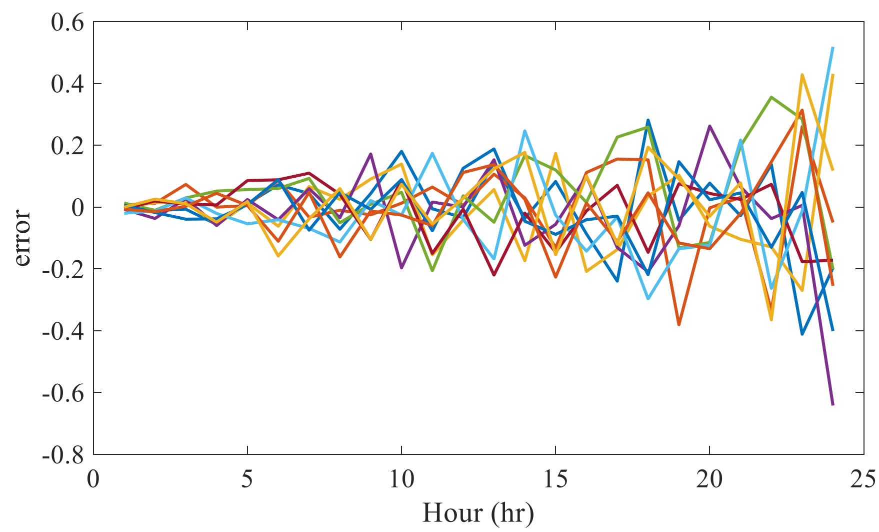

Figure 17 – RT price forecast errors

3.4.1.4 <u>Degradation</u>

In formulating the optimization problems for both DA and RT markets, the ESS degradation is modeled with a cost term in the objective functions. The cost term represents the loss of ESS useful life due to charging and discharging cycles and is modeled by a cost parameter multiplied by the output energy, i.e. the sum of ESS charged and discharged energies. The parameter is determined by the total capital cost of ESS divided by the total number of life cycles and further divided by total charged and discharged energies in a full cycle that is approximated by (20).

$$C = \frac{capital\_cost}{life\_cycles \times Capacity \times 2} \tag{20}$$

Including this cost term prevents the ESS from frequent charging and discharging cycles that adversely affect its useful life. Therefore, it provides a more realistic optimal operation. Moreover, the cost term prevents the simultaneous charging and discharging and therefore binary variables in Equations (2)–(4) can be relaxed.

3.4.2 Mathematical Formulation

Here we provide the mathematical modeling and formulation of the proposed optimal dispatch in DA and RT markets.

3.4.2.1 Quadratic Program for DA Optimization

The optimal operation of a price-maker ESS in the DA market is found by plugging the price and degradation models, Equation (18) and (20), respectively, in the objective function of Equation (1) as

$$\max \sum_{t=1}^{T} \left[\pi_t^{DA} \left(P_t^{dis,DA} - P_t^{chg,DA} \right) - C \left(P_t^{dis,DA} + P_t^{chg,DA} \right) \right] \Delta t \tag{21}$$

subject to Equations (3)–(7), (18), (20).

The first term in the objective function, Equation (21), is the DA market revenue, and the second one is the cost of degradation due to cycling. The decision variables are $P_t^{dis,DA}$ and $P_t^{chg,DA}$. Since the DA market price is a linear function of ESS output powers as in Equation (18), the proposed optimization problem is a quadratic program. The formulation is convex due to the negative coefficients (γ) of the quadratic terms. Thus, any local optimum is global. The operational constraints of ESS are similar to Equations (3)–(7). Note that the binary variables can be relaxed; Because the structure of the problem with positive prices for all periods, does not require integer variables [66], and no optimal solution exists with both $P_t^{dis,DA}$ and $P_t^{chg,DA}$ being non-zero.

3.4.2.2 Mixed Integer Linear Program for RT Optimization

The optimal operation of ESS in the RT market is found by solving the following optimization problem on an hourly basis for each period τ in the time horizon.

$$\max \sum_{t=\tau}^{T} \left[\pi_t^{RT} \left(P_t^{dis,RT} - P_t^{chg,RT} \right) - C\left(P_t^{dis,RT} + P_t^{chg,RT} \right) \right] \Delta t \tag{22}$$

subject to (2)–(7), and the following constraints

$$0 \le P_t^{dis,RT} \le \left(P_{\max}^{dis} - P_t^{dis,DA} \right) u_t^{dis} \tag{23}$$

$$0 \le P_t^{chg,RT} \le \left(P_{\max}^{chg} - P_t^{chg,DA} \right) u_t^{chg} \tag{24}$$

$$E_t = \eta_s E_{t-1} + \left(\eta_{chg} \left(P_t^{chg,DA} + P_t^{chg,RT} \right) - \left(P_t^{dis,DA} + P_t^{dis,RT} \right) / \eta_{dis} \right) \Delta t \tag{25}$$

Note that the binary variables are present in the RT formulation since RT prices can become negative and therefore, these variables are needed to avoid simultaneous charging and discharging operation. Also, DA dispatch decisions are treated as parameters in the RT formulation. The proposed optimization problem is a MILP that can be solved efficiently with current available solvers. The optimization problem is solved several times for each period to efficiently cover the set of uncertain RT prices. Assuming equiprobable scenarios realizations for uncertain prices, the expected value of the revenues is considered for further calculations.

3.4.3 Simulation Results

The proposed methodology is tested on a 1MW/2MWh energy storage system with 90% roundtrip efficiency ($\eta_{chg}\eta_{dis} = 0.9$), and no self-discharge ($\eta_s = 1$). The chosen power and energy ratings are the most common ratings based on the DOE energy storage database [111]. Charging and discharging efficiencies are assumed to be equal ($\eta_{chg} = \eta_{dis} = \sqrt{0.9}$). The initial energy level is assumed one half of the full capacity (E_0 = 1 MWh). Hourly aggregated load and price data of the PJM market from 2013 to 2017 was used [105]. Data was cleaned before any calculations and the missing points were interpolated. The price-load sensitivity is calculated as 0.00066 $/MWh/MW [22]. The optimization models are convex if $P_{\min}^{chg} = P_{\min}^{dis} = 0$, and the global optima are guaranteed in finite time. The models are implemented and solved in MATLAB 2017a [112] using *quadprog* and *intlinprog* functions for DA and RT optimization, respectively.

Several test cases were simulated to derive the optimal revenue of the ESS operator for various conditions and for a wide range of parameters. In the first case, both DA and RT prices were assumed to be known with perfect foresight and no degradation cost is included ($C=0$). This case is necessary and helpful to understand the maximum potential revenue from energy arbitrage in both markets. Figure 18 demonstrates the annual revenues from DA and RT markets in this case for 5 years. The total revenues are $108,700 and $36,162 for DA and RT markets, respectively. The RT market participation increases the revenue obtained in the DA market by more than 50% on average. This participation is a considerable revenue stream for the ESS operator and thus can increase the profitability of the ESS projects and incentivize ESS investors.

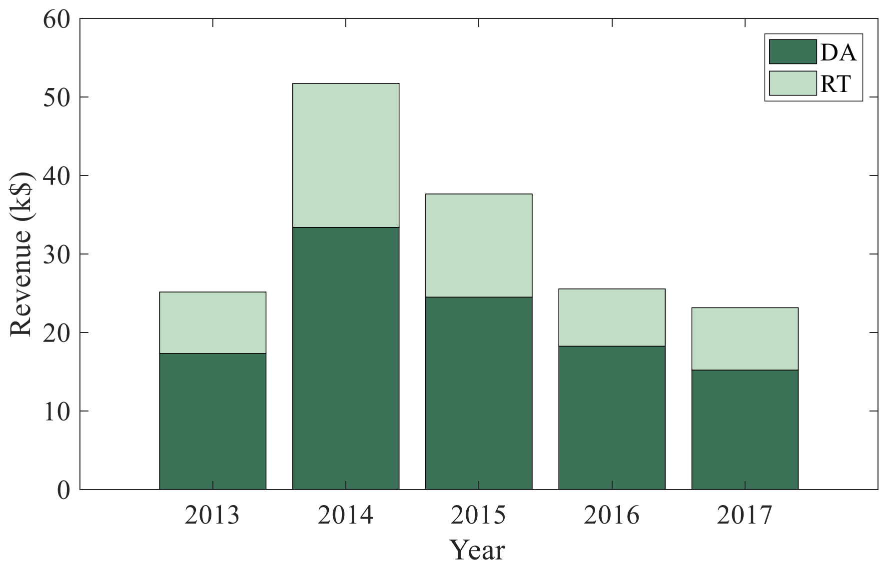

Figure 18 – DA and RT annual revenues in the base case

3.4.3.1 <u>Market power</u>

The impact of ESS market power on the revenue is investigated by running the simulation for various values of the price-load sensitivity γ. All the other parameters are the same as in the first case. DA and RT revenues are shown in Figure 19. From (18), it is obvious that increasing the absolute value of γ translates into the increased market power of ESS. However, DA and RT revenues do not change for values of γ up to 6.6 \$/MWh/MW meaning that the simulated ESS has a negligible market power. Nevertheless, the proposed quadratic formulation can be applied to any ESS with its specific ratings, and accounts for its impact on the market price. It is worth noting that for γ = 6.6 \$/MWh/MW, the DA revenue decreases due to the price depreciation resulted by the ESS output. Accounting for the effect of price depreciation on the DA revenue, the ESS operator avoids unprofitable operations. This leaves more capacity for the RT operation and as shown in Figure 19, the RT revenue increases. The total revenue, however, remains the same. For the case of greater market power with higher values of γ, the DA revenue further decreases, and RT revenue increases as well as the total revenue. Increasing γ, finally decreases the DA revenue to zero and all the revenue is obtained from the RT market that is greater than the first case revenue. However, this is not an attractive option for the risk-averse ESS operator due to higher price variability of the RT market. Participation in the DA market is necessary for such ESS operators to secure a considerable revenue with lower risk levels.

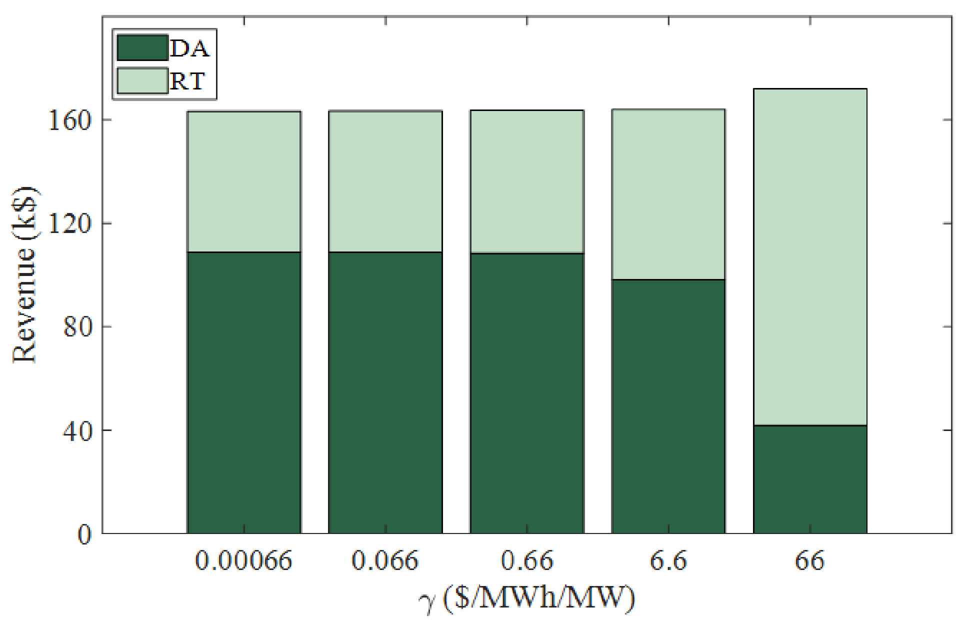

Figure 19 – DA and RT total revenues versus price-load sensitivity

3.4.3.2 Price uncertainty

Uncertainties in price forecasts were considered and modeled as described while the degradation cost is still zero. This case determines the impact of forecast errors on market revenues. Various cases are tested with different levels of price forecast error. The price uncertainty of the DA market is modeled by the back-casting method in all the cases with nonzero forecast error. The RT market price uncertainty is modeled by averaging the revenue over 100 scenarios generated from sampling normal relative errors. For example, in the case of 50% error, $\sigma^{max} = 0.25$, then standard deviation for each period is determined by (19). Next, 100 random scenarios are generated by sampling from a normal distribution of e in (16). For each scenario, the RT optimization problem in section 3.4.2.2 is run and the maximum revenue is averaged over all 100 scenarios to find an estimate of the maximum revenue. Figure 20 shows the revenues of the two markets for 5 forecast errors. The DA revenue decreases as the price forecast error increases from 0% to 25%. Again, this decrease provides more opportunity for RT market participation and higher revenues as shown in Figure 20. Since all the cases with non-zero forecast error use the same error model, no change in DA revenues is expected. Furthermore, the RT revenue decreases negligibly even when the forecast error is 100%. The total revenue in this case is more than 94% of that in the case of no error. These results attest the robustness of the dynamic optimization model proposed for the RT market participation.

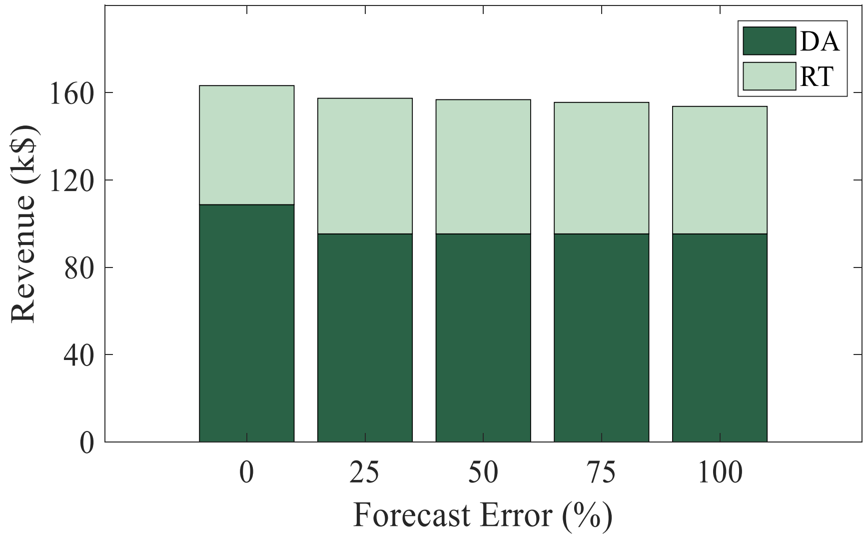

Figure 20 – DA and RT total revenues versus forecast errors

3.4.3.3 ESS degradation

The impact of various degradation costs is studied in two cases: a) without price forecast error, and b) with 50% forecast error. The respective revenues are illustrated in Figure 21(a) and (b). In both cases, the DA revenue decreases as the degradation cost increases. This is an expected trend since inclusion of the degradation cost in the objective function, reduces the maximum revenue by eliminating less profitable arbitrage opportunities. The RT revenue, however, has a different trend with increasing the degradation cost. Although less profitable arbitrage opportunities are still avoided, more capacity is available for the RT market as the DA market becomes less profitable with fewer charging and discharging cycles due to degradation cost. As shown in Figure 21, in both cases, the RT revenue first increases and then decreases for higher values of the degradation cost. Interestingly, the total revenue in the case of 50% forecast error is greater than that of the case without forecast error for any non-zero degradation cost. This is again because of less DA operations that provides more RT arbitrage opportunities. A highly important result of this analysis is that the inclusion of the ESS degradation model for the optimal operation can avoid unnecessary operations that adversely impact the ESS useful life. Therefore, although the optimal revenue is decreased, the useful life of the ESS increases and considerable replacement costs can be saved using the proposed model.

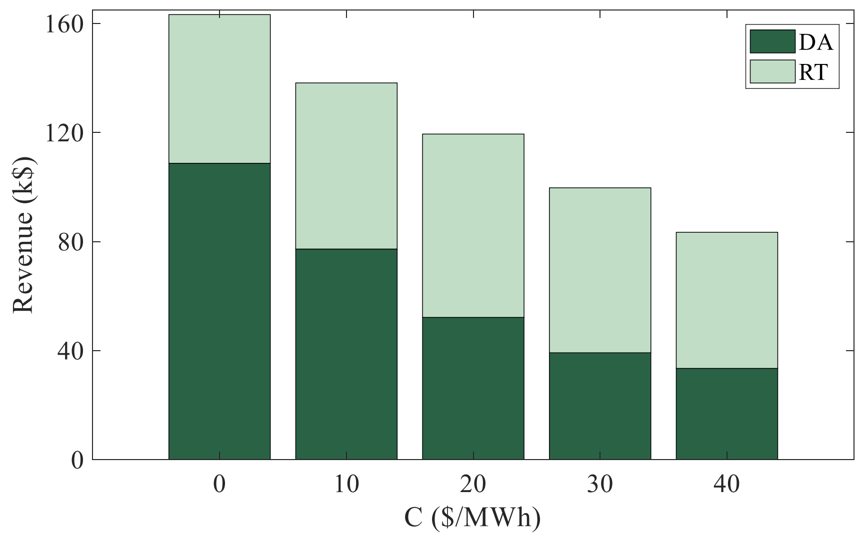

(a)

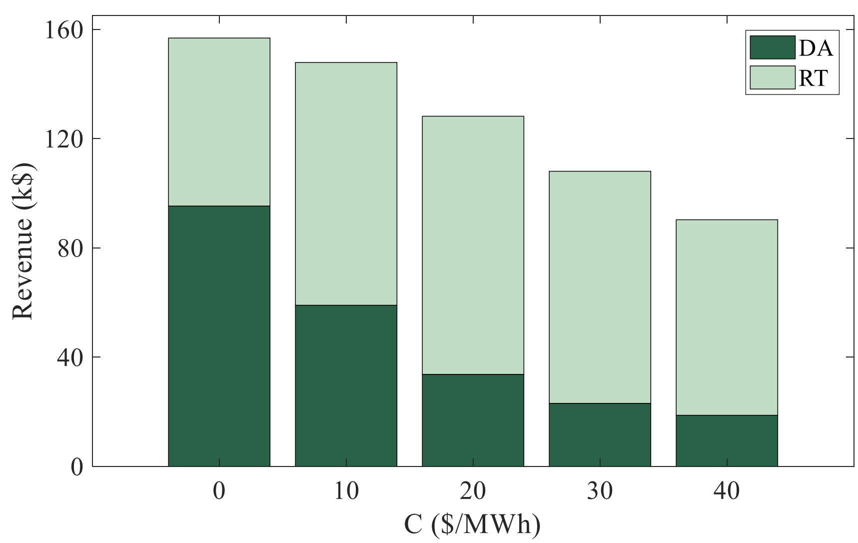

(b)

Figure 21 – DA and RT total revenues versus degradation cost with a) perfect foresight and b) 50% forecast error

3.4.4 Economic Viability

The economic viability of four ESS technologies is assessed using the proposed optimization model. Among various ESS technologies, only those with long enough duration (more than two hours) are chosen that are more suitable for energy arbitrage service. Similar ESS parameters and price data is used as in section 3.4.3. as well as realistic technology-specific data [14], [113] provided in Table 3.

Table 3 – ESS Technology Data and Financial Results

Technology	Pumped Hydro	Compressed Air	Sodium Sulfur	Lithium Ion
Useful Life (years)	50	40	10	15
Life Cycles	15,000	12,000	2,500	4,500
Capital Cost ($)	440,000	260,000	900,000	840,000
C ($/MWh)	7.33	5.42	90	46.67
5-year Revenue ($)	153,600	154,500	46,400	72,000
NPV (M$)	1.09	1.22	-4.04	-2.08

The degradation cost C is calculated using (20). Optimization results include the total revenue obtained by the four ESS technologies in 5 years considering 50% forecast error, and the net present value (NPV) of each technology. Results show that pumped-hydro and compressed air are economically viable ESS technologies with the energy arbitrage revenue stream. Moreover, Sodium Sulfur and Lithium Ion technologies are not currently economically competitive with others in the case of energy arbitrage service. This is because of two factors: a) higher capital cost of batteries and b) lower revenue because of high degradation cost due to lower number of life cycles. Thus, extensive research is needed on battery energy storage technology to lower the capital costs and increase the number of life cycles. Furthermore, market and business models need to be developed to capture multiple revenue streams.

3.5 Summary

This chapter presented novel methodologies for evaluating energy storage revenues from participating wholesale energy markets. The methodologies are presented in three folds:

- Day-ahead energy arbitrage revenue:

A straightforward method is proposed to accurately estimate the expected arbitrage revenue based on the statistics of market price data. A machine-learning-based clustering algorithm is proposed to classify the seasonal prices. The revenue in each cluster is fitted to the daily price statistics using a linear regression model. The proposed method was tested on the five-year PJM historical day-ahead energy market prices. It is observed that the service revenue is mainly determined by the price data shape. The results of the linear regression model show that the clusters revenue is linearly dependent on the dispersion statistics of the price data, mostly the range. The results can benefit utilities and investors to analyze the energy arbitrage revenue in a straightforward manner using simple statistics of the energy market prices. The proposed clustering method is also a useful tool for other applications, such as an offline suboptimal dispatch.

- Real-time energy arbitrage revenue:

The higher value of the real-time (RT) energy arbitrage compared to the day-head (DA) is achieved by the proposed optimization model. The actual participation models in both markets are discussed and appropriate optimization models are deployed to quantify the value of each market. While a linear program is found suitable for the DA market, higher revenues are captured by the proposed dynamic optimization model known as the shrinking horizon control algorithm. Results disclose the outstanding performance of the proposed dispatch in application to the RT market participation for the EA service. The uncertainty of the market price forecasts is also modeled in optimization models. Sensitivity analysis with respect to forecast errors and storage roundtrip efficiencies in their currently available ranges reveal that the value of RT market for the EA service is always greater than that of the DA market.

- Day-ahead and real-time energy arbitrage revenue:

An optimization approach is proposed that models the participation of ESS in both day-ahead and real-time energy markets to determine the maximum revenue of an energy storage operator from the energy arbitrage service. Quadratic and dynamic mixed integer optimization models are developed for day-ahead and real-time markets, respectively. Price sensitivities to ESS operation, price forecast errors, and ESS degradation model are considered in this study to estimate the arbitrage revenues more realistically. The model is tested on the PJM historical data as well as technology-specific parameters. The results show that the energy arbitrage revenue is highly dependent on these parameters and can vary significantly depending on the technology. Moreover, including the energy storage degradation model in the optimization problem can reduce less profitable arbitrage operations and increases its useful life. Finally, new ESS technologies need to provide multiple services to be economically viable. Therefore, advanced optimization models are needed for multiservice ESS operation and evaluation.

CHAPTER 4. GENERIC MULTISERVICE REVENUE ANALYSIS OF ENERGY STORAGE

4.1 Introduction

Although energy storage is well-known for its energy arbitrage service, our findings on day-ahead and real-time energy arbitrage and a few other studies in [24]–[26] reveal that energy markets cannot guarantee sufficient revenues for the financial viability of many new storage technologies such as batteries. Therefore, ESS owners need to rely on multiple revenue streams to cover the currently high capital costs of ESS. With almost 30 identified applications and benefits [3], [8], the *potential* value of energy storage is expected to be significant. However, *monetizing* that significant value requires advanced modeling methodologies that can capture all the synergies and conflicts between these applications and be flexible and scalable for different combination of applications. Modeling multiservice operation of ESS will increase the *bankable* value of ESS which is paramount for their benefit-cost analysis and deployment. Accordingly, it helps stakeholders (regulators, ESS owners, system operators, end-use customers, etc.) understand the maximum value of ESS facilitating the deployment of these technologies as well as renewable energies.

Most of the research in this area has focused on wholesale market service revenues. However, ESS applications are not limited to wholesale market services which have a defined participation model. Therefore, these "non-market" applications are not well-understood and analyzed for ESS although they can provide significant additional revenue streams for ESS owners. Analyzing all these benefits is very complicated and project specific. A systematic approach is needed to facilitate such analyses while ensuring the maximum profitability. Automating this process using new software tools can provide significant value. Designing a scalable information model is key to develop a software for ESS project analysis. The model should capture all the details of the analysis and uses optimization models to maximize the benefits. The service benefit modeling and analysis is the crux of this information model. Since ESS services can be valued differently by stakeholders we propose a generic optimization model for co-optimizing the revenues from multiple services. The generality and flexibility of the model enables its application by many stakeholders in various grid levels with different regulations and policies.

4.2 Objective and Contributions

The objective of this chapter is to propose a systematic methodology for multiservice analysis of energy storage operation based on a generic optimization framework that can co-optimize the ESS revenues from multiple services. The main question to be answered is how to *optimally operate* energy storage systems to obtain the *maximum value* from providing *any combination of services*. The focus is on *scalability* and *modularity* of the analysis which requires a sophisticated system design. The generic optimization formulation is the center of this design which is also the main contribution of this chapter. A software tool is also developed based on the designed system architecture. The tool is tested on real-world applications and is already being tested by utility industry partners for their energy storage studies and projects.

The contributions of this work include:

1. Developing an information model for energy storage techno-economic studies, e.g. optimal operation, scheduling services, benefit-cost analysis, etc.
2. Proposing a generic optimization model for co-optimizing the revenues from multiple services
3. Developing an optimization-based software tool for ESS cost-benefit analysis
4. Simulating the optimization model in realistic test cases and scenarios

The rest of this chapter is organized as follows. Section 4.3. presents the information system design and data model. The generic optimization framework is described in section 4.4. The developed software is introduced in section 4.5. Finally, section 4.6. provides the applications of the proposed methodology in two realistic test cases of energy storage revenue analysis. These two test cases are published in [104] and [114].

4.3 System Design and Data Model

The system design for energy storage analysis tool is illustrated in Figure 22. Three main modules are designed:

- Data Integration: This module handles the input data required for the optimization and post optimization analyses. It has an object-oriented data structure to efficiently handle large amounts of data.
- Optimization: This module builds an optimization program based on the input data and solves it. This module is discussed more in detail in section 4.4.
- Output Processing: This module calculates the outputs of the study based on the optimization results.

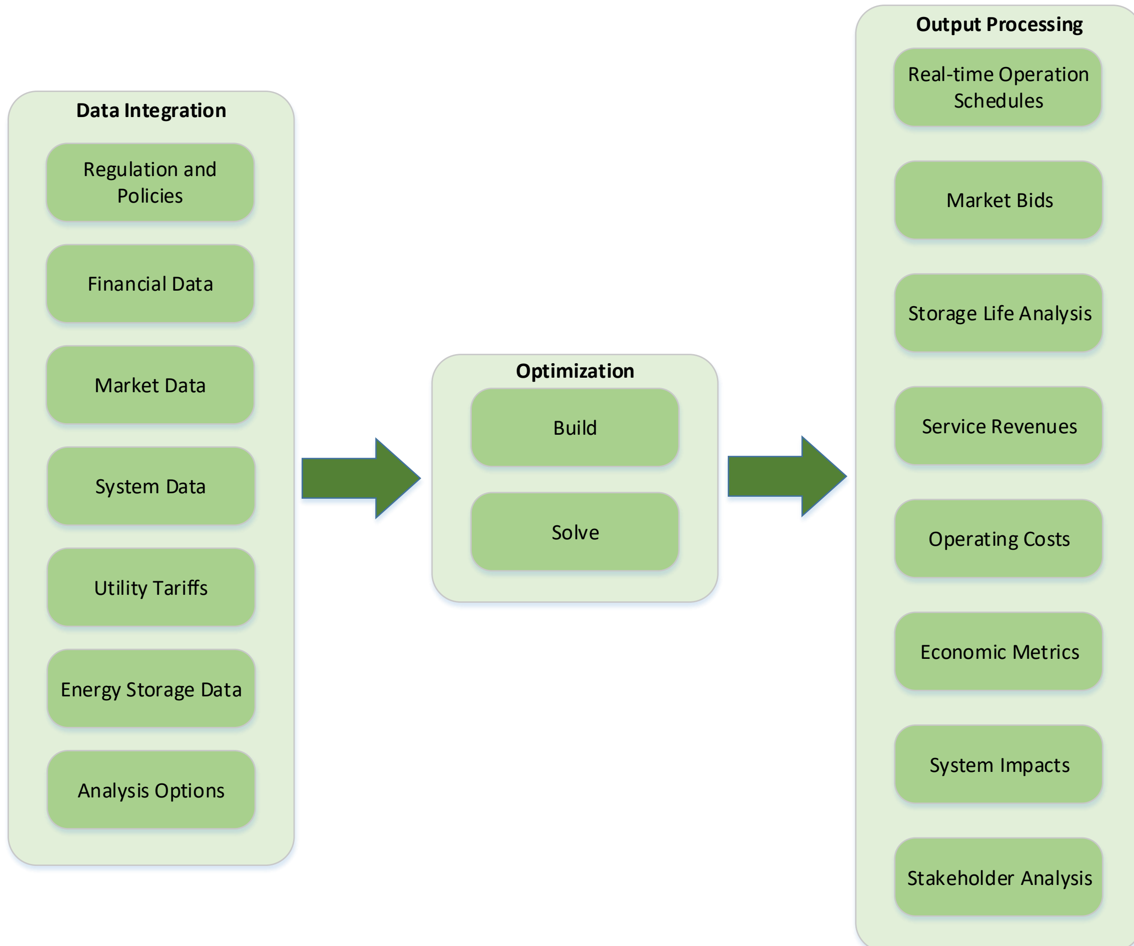

Figure 22 – System design for energy storage analysis tool

For the flexibility and scalability of the data integration module, an object-oriented programming approach is used. An overview of the class diagram developed for the data integration module is illustrated in Figure 23. The diagram is in the standard Unified Modeling Language (UML) format and it describes the static structure of data, including classes, their attributes and relationship between the entities and objects in the module. Note that although the current work is developed for energy storage resources, it can be generalized to many other distributed energy resources, e.g. PV, flexible demand, etc., and even conventional resources, e.g. gas turbines, considering resource specific parameters and constraints.

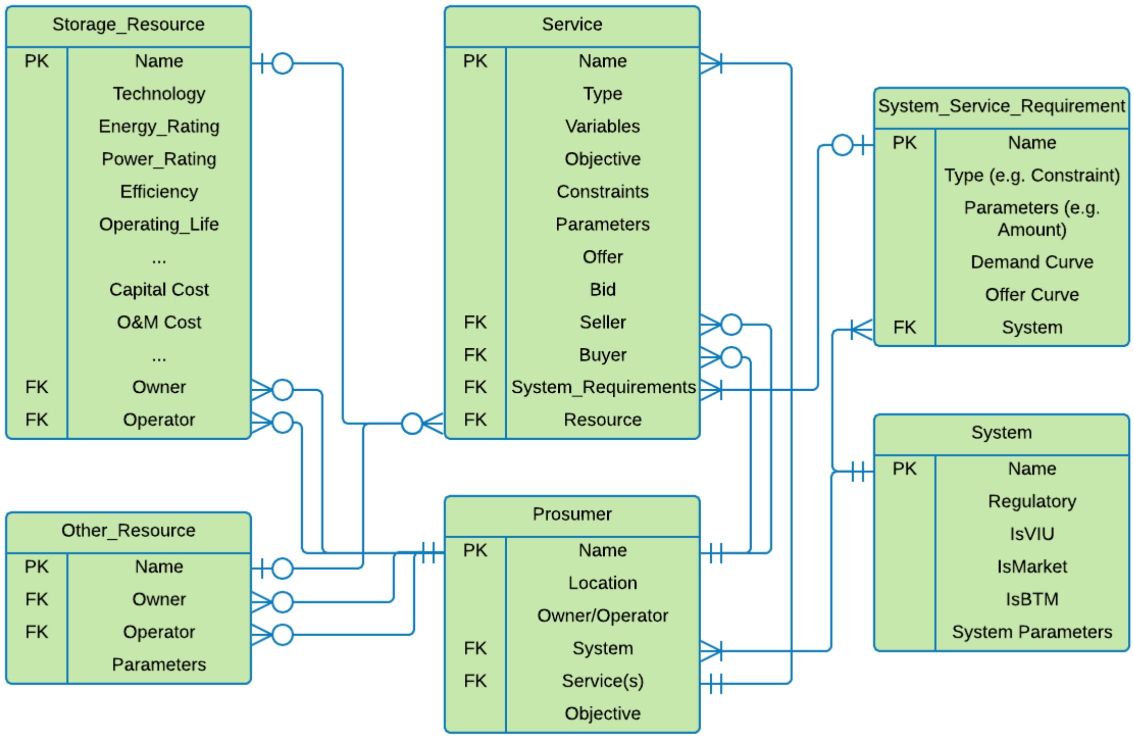

Figure 23 – UML diagram of the data integration module

The relationship between services and prosumers as stakeholders is defined based on Table 4. A marked cell means that the stakeholder can operate the energy storage resource to benefit from that service by increasing its utility function or minimizing its operating cost. Note that since ISOs are non-profit market administrators, they cannot benefit from owning resources and obtaining revenues from market products and services. However, they can operate ESS owned by market participants to minimize the total cost of acquiring and providing market services. Using Table 4, the optimization model can be formulated that maximizes the operator's utility function from providing an application/service, subject to a set of constraints. After the optimization model is solved and the optimal ESS dispatch is found all the other stakeholders' utility functions for the selected services can be evaluated.

Table 4 – ESS Services Versus Stakeholders

	Stakeholder					
Application/Service	ISO	IPP	Utility/ DSO	Aggregator	Customer (BTM)	3rd-party owner
Energy Arbitrage (DA/RT)	×	×	×	×	×	×
Frequency Regulation	×	×	×	×		×
Reserve Market	×	×	×	×		×
Capacity Market	×	×	×	×		×
Flexible Ramping	×	×	×	×		×
Investment Deferral	×	×	×			
Volt/VAR Support	×		×			
Black Start	×	×	×			
Reliability (Back-tie) Services	×		×			
Outage Avoidance/Islanding	×	×	×			
Demand Response	×		×	×	×	
Congestion Management	×		×			
Reduced Generation Fossil Fuel Use and Air Emissions	×	×	×		×	
Renewable Integration and Capacity Firming	×	×	×		×	
Loss Reduction	×		×			
Improve Asset Utilization	×	×	×			
Transmission Stability Damping	×	×				
Sub-synchronous Resonance Damping	×					
U/O-frequency Load Shedding Reduction	×	×				
Transient Voltage Dip Improvement	×					
Backup Power		×	×		×	
EV Load Support			×	×	×	
Solar Back-feeding Elimination		×	×		×	
Equipment Life Extension (e.g. Reducing Tap Regulator Action)			×			

4.4 Generic Optimization Framework

The generic optimization framework models energy storage applications as services in a flexible and scalable manner. The proposed model is operator- and service-agnostic meaning that the structure of the model does not change for each service or depending on the operator. All the service- and operator- specific modeling details are captured as parameters to the generic optimization model. The modular design of the optimization model enables to simulate any combination of services without having a separate model for each combination. The generic optimization model includes:

a. The energy storage optimization model without any services that includes:

- Storage decision variables (set X_{ESS}):
    - Storage dispatch variables, e.g. output power and energy $P_{ESS}^{+/-}, E_{ESS}$
    - Storage product offers $p_{ESS} \in \{E^+, E^-, P^+, P^-, R^+, R^-\}$ for the total energy, power and ramp rate offers.

    These two set of variables are distinct since the offered products may not be dispatched at the same quantity as offered.

- Storage objective function (J_{ESS}): without any services, the objective function is defined as zero.
- Storage parameters:
    - Decision variables upper and lower bounds ($b_{ESS}^{\min/\max}$), e.g. energy and power ratings,

- Efficiency parameters $\eta_l, \eta_{chg}, \eta_{dis}$ for leakage, charging and discharging efficiencies,
- Cost parameters (C), e.g. cost of degradation,
- Boundary values, e.g. Stored energy at the beginning and end of the optimization horizon.

- Storage constraints (feasible set $\mathcal{X}_{ESS}$):
  - Constraints on decision variables:

$$b_{x,ESS}^{\min} \le x_{ESS} \le b_{x,ESS}^{\max} \quad \forall x_{ESS} \in X_{ESS} \tag{26}$$

  - Intertemporal constraints, e.g. $E_{ESS,t} = \eta_s E_{ESS,t-1} + \eta_{chg} P_{ESS,t}^{+} \Delta t - P_{ESS,t}^{-} \Delta t / \eta_{dis}$
  - Charging/discharging constraints: where simultaneous charging and discharging operation is avoided.
  - Degradation constraints, e.g. limited number of life cycles

b. Modular service optimization models that for each service (s) includes similar components including:

- Service decision variables (set X_s):
  - Service status binary variable (u_s) to represent the enable/disable status of that service,
  - Service dispatch variables ($P_s^{(+/-),(\max/\min)}, E_s^{\max/\min}$), e.g. demand,
  - Service product offer variables $p_s \in \{E_s^{+}, E_s^{-}, P_s^{+}, P_s^{-}, R_s^{+}, R_s^{-}\}$: energy, power and ramp rate offered by the service in both charging and discharging directions.
- Service parameters:

- Price (Π_s): the marginal value of each variable in the objective function,
- Upper and lower bounds of service variables ($b_{x(s),s}^{\max/\min}$),
- Product sensitivity $\alpha_{p,s,x_{ESS}}$: the impact of service product variable p on the storage decision variable x_{ESS}. If x_{ESS} is a dispatch variable, $\alpha_{p,s,x_{ESS}}$ is also called the product dispatch-to-contract ratio which is the ratio of the dispatched product to its offered quantity.

- Service objective function (J_s) that defines the operator's utility value from providing that service. This is mathematically expressed as

$$J_s = \Pi_s^T X_s \tag{27}$$

- Service constraints (feasible set $\mathcal{X}_s$):
  - Service variable constraints:
    - Dispatch variable constraints:

$$b_{x(s),s}^{\min} u_s + b_{x_{ESS},s}^{\min}(1-u_s) \le x_s \le b_{x(s),s}^{\max} u_s + b_{x_{ESS},s}^{\max}(1-u_s); \forall x_s \in \left\{P_s^{\max/\min}, E_s^{\max/\min}\right\} \tag{28}$$

    - Product variable constraints:

$$b_{x(s),s}^{\min} u_s \le x_s \le b_{x(s),s}^{\max} u_s ; \forall x_s \in \{E_s^+, E_s^-, P_s^+, P_s^-, R_s^+, R_s^-\} \tag{29}$$

  - Service constraints on energy storage dispatch variables:

$$P_s^{\min}, E_s^{\min} \le P_{ESS}^{+/-}, E_{ESS} \le P_s^{\max}, E_s^{\max} \tag{30}$$

  - Service variable intertemporal constraints:

$$x_{s,t} = x_{s,t+1} \qquad \forall t \in \mathcal{T} \tag{31}$$

where $\mathcal{T}$ denotes any subset of the optimization horizon.

c. Service aggregate model including:

- Aggregation constraints (feasible set $\mathcal{X}_{Agg}$):

$$x_{ESS} = \sum_{s,p} \alpha_{p,s,x_{ESS}} p_s \quad \forall x_{ESS} \in X_{ESS} \tag{32}$$

The process of building the generic optimization model for stacked service analysis is described in the following steps:

1. Create an empty optimization model:
   a. set of variables X={},
   b. objective function $J=0$,
   c. feasible set $\mathcal{X}=\{\}$.
2. Add the energy storage model without any services by updating
   a. X to X_{ESS}
   b. $\mathcal{X}=\mathcal{X}_{ESS}$,
3. For s in the set of services:
   a. Update X to $X \cup X_s$,
   b. Update J to $J+J_s$,
   c. Update $\mathcal{X}$ to $\mathcal{X} \cap \mathcal{X}_s$.
4. Add the service aggregation constraints:
   a. Update $\mathcal{X}$ to $\mathcal{X} \cap \mathcal{X}_{AGG}$.
5. Solve

$$\begin{aligned} &\underset{X}{\text{maximize}} \quad J \\ &s.t. \quad X \in \mathcal{X} \end{aligned} \tag{33}$$

The optimal multiservice operation of energy storage is determined by adding the service objective functions to maximize the total revenues and appending the constraints from the energy storage model, all the services of interest, and the service aggregation model. The structure of the resulting multiservice optimization problem is independent of the selected services. Moreover, the interdependencies between services are captured by the product sensitivity parameters and service aggregation constraints. It is noted that the flexibility of the model can capture additional constraints that are not explicitly mentioned above. For example, if simultaneous participation in regulation and reserve markets is prohibited under a regulatory regime, an additional constraint can be added to model it as

$$u_{reg} + u_{res} \leq 1 \tag{34}$$

4.4.1 Scalability to Additional Dimensions

Another significance of the proposed model is that it is flexible and scalable to many other dimensions besides services including:

a. Time (indexed by t)
b. Space/location/nodes (indexed by n)
c. Storage assets/technologies (indexed by a)
d. Stochastic scenarios (indexed by ω)
e. Blocks (indexed by b)

Including each of these dimensions in the energy storage optimization model updating:

1. The variable space: The cardinality of the new variable space is $|X|\times|Y|$ where $|Y|$ is the cardinality of the new dimension. In other words, all the variables will be indexed by the cartesian product the old dimension and the new one. For example:

$$x_s \quad \forall s \in S \quad \Rightarrow \quad x_{s,t} \quad \forall (s,t) \in S \times T \tag{35}$$

2. The parameter space: This is updated similar to the variable space.
3. The objective function: It is updated by a summation over all the indices in the new dimension. For example,

$$J = \sum_{s\in S} J_s \quad \Rightarrow \quad J = \sum_{t\in T}\sum_{s\in S} J_{s,t} \tag{36}$$

4. The feasibility set: All the existing constraints should hold for each index in the new dimension. Also, additional constraints linking the relationships within each dimension need to be appended to the constraint set. These constraints are defined in Table 5.

4.4.2 Solution Feasibility, Optimality and Tractability

The proposed model is always feasible if the storage parameters (charge/discharge and energy limits and efficiencies) form a non-empty set. All the service constraints are designed with the feasibility guarantee by using either continuous or binary alternatives if their constraints are not met. For example, if a product variable of a service is not in the limits, either that product or the whole service is disabled from the constraints and the objective function and is substituted by energy storage limits.

Table 5 – Dimension-Specific Constraints

Dimension	Constraints	Example
Time (indexed by *t*)	Intertemporal constraints modeling the dynamics and state evolutions in the problem	$E_{ESS,t} = \eta_s E_{ESS,t-1} + \eta_{chg} P^{+}_{ESS,t} \Delta t - P^{-}_{ESS,t} \Delta t / \eta_{dis}$ where the energy at each time step is a function of energy at previous step and the output power at the current step.
Space/ location/ nodes (indexed by *n*)	Grid/network constraints modeling the power flow equations and limited transfer capacity of the network links	$P_{m,n} = B_{m,n}\left(\theta_m - \theta_n\right)$ where $P_{m,n}$ is the power flowing from node *m* to node *n*, $B_{m,n}$ is the susceptance of the link between node *m* to node *n*, and θ_m is the voltage angle at node *m* with respect to the reference node.
Storage assets/ technologies (indexed by *a*)	Storage aggregation constraints modeling the impact of each ESS operation on the others	$\mu_t^{ene} = \mu_t^{ene0} + \alpha^{ene} \sum_{a=1}^{A} \left(P_{t,a}^{chg} - P_{t,a}^{dis}\right)$ where *a* is the index of ESS asset, α^{ene} is the price-load sensitivity, μ_t^{ene} and μ_t^{ene0} are energy prices with and without any energy storage operation, respectively.
Stochastic scenarios (indexed by *ω*)	Non-anticipativity constraints modeling the dependencies between decision variables at different stages	$P_{\omega}^{ene,DA} = P_{\omega+1}^{ene,DA} \quad \forall \omega \in \Omega \setminus \{O\}$ where the day-ahead market bids should be equal in all the real-time stochastic scenarios.
Blocks (indexed by *b*)	Bounds and orders of blocks	$P_t^{ene,DA} = \sum P_{t,b}^{ene,DA} \quad \forall t \in T$ where the total energy bid is the sum of bids in the blocks/segments.

All the terms in the objective function as well as constraints are either linear or convex quadratic with a few binary variables. Thus, the resulted model is either a mixed integer linear program (MILP) or mixed integer quadratic program (MIQP). Both programs can be efficiently solved with the commercially available solvers conditioned on the size and complexity of the model which grows significantly with more dimensions in the model as well as the granularity and size of each dimension. Therefore, the value of a complex model should be compromised with the computational capabilities in building and solving that model. The tractability of ESS optimization problems with several dimensions is analyzed in chapter 5.

4.5 Software

This section introduces the developed software tool for multiservice revenue analysis of ESS. The tool has a graphical user interface that is designed for a straightforward and easy-to-use user experience. The core of the tool is the multiservice optimization model that optimizes the operation of ESS for providing multiple services. Electric utilities, system operators and planners, and private ESS investors can benefit from using this tool. Salient features of the tool are as follows:

- It includes a wide variety of storage technologies with updated technical and cost parameters.
- It includes a comprehensive list of ESS services and service options.
- It co-optimizes all ESS service revenues with advanced optimization methods, and it is not based on heuristics or rule-based methods used in other ESS tools.
- It enables the user to find useful information about ESS projects including:
    - The optimal operation of ESS

- Optimal market bids
- Maximum service revenues
- The “best” ESS technology per case study
- The impact of ESS parameters on dispatch and revenues
- Optimal sizing of ESS
- ESS project cash flows
- Benefit-cost analysis
- System impacts of ESS

Compared to other energy storage evaluation tools, this tool provides more flexibility to the user in modeling multiple services and customizing them based on specific assumptions. Other available tools either do not use optimization or they use optimization with priority tables to dispatch a number of the services based on a user-selected priority. However, this can result in suboptimal solutions where the revenue is underestimated. In the implemented software tool, the optimization solver decides on whether a service is profitable enough to be dispatched or not and, therefore, results in higher total service revenues. An overview of the tool is provided in Appendix A. More information on the tool design, documentation and instructions are reported in [115].

4.6 Application of Multiservice Optimization Model in Realistic Test Cases

The generic multiservice optimization provides flexibility in modeling energy storage optimization problems. The methodology is applied to two realistic test cases described next.

4.6.1 Analysis of Multiple Revenue Streams for Privately-Owned Energy Storage Systems

4.6.1.1 Background

Most of the existing research on ESS services has been for utility-owned ESS and the benefits that ESS can offer to the system operator in terms of reduced costs. On the other hand, privately-owned ESS, an important emerging market, is not well-understood. This test case analyzes four of the most important privately-owned ESS services and applies the optimization models that maximize the owner's revenue for a single service and for multiple combined services. Three market services, namely day-ahead energy, frequency regulation and reserve, as well as a non-market service, investment deferral, are considered as the revenue streams. Non-market services in the previous studies are usually considered as constraints, which do not necessarily increase the owner's revenue. Hence, a more comprehensive analysis for these services is needed from the owner's perspective. A novel revenue estimation model is proposed that captures the benefits of the ESS owner providing investment deferral to the utility. This revenue model also finds the optimal price for the service as the lowest price that the utility pays the ESS owner, who continues to receive benefits from providing the service. The optimal price guarantees the ESS owner's revenue from providing the investment deferral service to the utility. It also minimizes the utility payments for the service while ensuring service provision.

The developed optimization models are simulated with a typical Li-ion battery ESS data as well as the California ISO (CAISO) market prices to provide numerical results. Simulation results show how multiple services are stacked to maximize the owner's revenue. Evaluating stacked service revenues is of great interest to ESS owners and investors since in many cases providing a single service is not sufficient to derive a profit.

4.6.1.2 Service Description and Problem Formulation

In this test case, the ESS services and revenue streams earned by the ESS owner are discussed, and optimization models are proposed. Various combinations of services are modeled to investigate how they can be optimally stacked in order to realize maximum revenue. Note that the flexibility provided by the generic optimization facilitates the implementation of various combinations of services. Each service is described together with the optimization model that maximizes the owner's revenue. In this test case, all models assume that the ESS is a price-taker (i.e., the market price is fixed and does not change based on the ESS bids and offers). Also, the power grid is not included in the models, and hence thermal, voltage, and dynamic constraints are not considered.

a. Energy Arbitrage (EA)

This service is extensively studied in chapter 3. Furthermore, the optimization model described by Equations (1) – (7) is cast into the generic formulation where the decision variables X_s indexed by the service name (s = EA). The price parameters data can be given in the two ways using either of:

1. Energy products where all the price parameters are zero except for energy products:

$$\Pi_{EA} = \left[0, 0, 0, (\pi_{DA}, -\pi_{DA}), 0, 0\right]^T \tag{37}$$

or

2. Power products where all the price parameters are zero except for power products:

$$\Pi_{EA} = \left[0,0,0,0,(\pi_{DA},-\pi_{DA})\times\Delta t,0\right]^{T} \tag{38}$$

where π_{DA} is the day-ahead energy market price and Δt is the optimization time step.

The upper and lower bounds of the energy arbitrage service variables are given as

$$b_{x(EA),EA}^{\max/\min} = \left[\left(1,1\right), P_{ESS}^{\max/\min}, E_{ESS}^{\max/\min}, E_{ESS}^{\max/\min}, P_{ESS}^{\max/\min}, R_{ESS}^{\max/\min}\right]^{T} \tag{39}$$

Note that the upper and lower bounds of the service binary variable are both 1 so that the service is enabled. The rest of the variables do not have any specific bounds other than the ESS variable bounds (energy, power and ramp ratings).

The product sensitivity $\alpha_{p,EA,x_{ESS}}$ are all zero other than

$$\alpha_{E,EA,E_{ESS}} = \alpha_{P,EA,P_{ESS}} = 1 \tag{40}$$

These parameters being equal to one are used in the service aggregation constraints to model that the dispatch-to-contract ratio of energy and power product offers from the energy arbitrage service is one and these products need to be dispatched the same amount as bid and cleared in the energy market.

As mentioned before, the significant benefit of the generic modeling is maintaining the same structure of the optimization problem for all the services. Therefore, the expressions of the service objective functions and constraints are not explicitly provided here.

b. Frequency Regulation (FR)

This service is defined as a change in the active power injection from a resource in response to a frequency deviation in order to help maintain the frequency close to its nominal value [116]. The resource must be dispatchable. The ESS makes a profit from this service by offering its capacity to participate in the frequency regulation market. The revenue is equal to the accepted capacity bid times the price of regulation plus the actual charged or discharged energy times the energy price. The actual energy is determined by the system operator that calls the ESS to provide a certain portion of its offered frequency regulation capacity. Two separate products for regulation up and regulation down are modeled, similar to markets such as the CAISO. It is assumed that all the ESS offered regulation capacities is accepted at the market price. Again, using the generic modeling, only the parameters need to be given as inputs. The price parameters data is given as:

$$\Pi_{FR} = \left[0,0,0,0,(\pi_{RU} + \gamma_{RU}\pi_{DA}, \pi_{RD} - \gamma_{RD}\pi_{DA}),0\right]^T \tag{41}$$

where the only non-zero parameters are those for the power products offered at regulation up and down markets. This price parameter models the frequency regulation revenue as in [50] where the it includes payments for the offered capacities at the market price plus the payments for the energy dispatched at the energy market price. The amount of frequency regulation capacity dispatched by the operator is assumed to be a constant portion of the offered capacity determined by γ_{ru} and γ_{rd} for regulation up and down, respectively. The upper and lower bounds of the frequency regulation service variables are similar to those in the energy arbitrage service in Equation (39). The product sensitivity $\alpha_{p,FR,x_{ESS}}$ are all zero other than

$$\alpha_{P^{+/-},FR,P_{ESS}^{+/-}} = 1 \tag{42}$$

$$\alpha_{P^{+},FR,E_{ESS}} = -\gamma_{RU} \tag{43}$$

$$\alpha_{P^{-},FR,E_{ESS}} = \gamma_{RD} \tag{44}$$

These parameters model how frequency regulation bids impact the aggregated bids as well as the dispatch.

c. Energy Reserves (ER)

This service represents a source of revenue derived from participating in the reserves market. The ESS offers a portion of its capacity to provide extra injection of power to the grid in case of unplanned outages or other events. The service is called by the operator, and the ESS and other resources that participate and are cleared in the market must provide the reserve within 10 minutes. The price parameters data is given as:

$$\Pi_{ER} = \left[0,0,0,0,(\pi_{ER},\pi_{ER}),0\right]^{T} \tag{45}$$

where the only non-zero parameters are those for the power products offered at reserve market. This price parameter models the reserve service revenue as payments only for the offered capacity at the market price π_{ER}. Since the dispatch probability of this service is much lower than that of the frequency regulation, as investigated in [117] and [33], it is assumed that the payments for the dispatch of this service is zero. The upper and lower bounds of the energy reserve service are given as

$$b_{x(ER),ER}^{\max/\min} = \left[(1,1), P_{ESS}^{\max/\min}, E_{ESS}^{\max/\min}, E_{ESS}^{\max/\min}, \left(P_{ESS}^{\max/\min}, 0\right), R_{ESS}^{\max/\min}\right]^{T} \tag{46}$$

This way, it is assumed that this service only has an upward product to be discharged. If this is not the case, the similar bounds for the energy arbitrage service can be used.

The product sensitivity $\alpha_{p,ER,x_{ESS}}$ are all zero other than

$$\alpha_{P^{+/-},ER,P_{ESS}^{+/-}} = 1 \tag{47}$$

These parameters model how reserve bids impact the aggregated bids. Also, again since the dispatch probability is low, the bids impact on the dispatched power and energy level is ignored.

d. Investment deferral (ID)

Utilities can operate their own ESS or use privately-owned ESS to defer the investments in upgrading the T&D assets with additional capacity that is needed to meet load growth. The ESS offers the additional needed capacity during peak load times to mitigate the burden on heavily loaded lines and transformers. In the case of privately-owned ESS, while the utility benefits from the deferred investment cost, the ESS owners must be incentivized to provide this service or let the utility operate the ESS for this service. Therefore, a price-based model is proposed where the owner's revenue is determined as the amount of needed energy offered and dispatched during the peak time multiplied by the service price (π_{ID}). The utility requests the ESS to provide the power P_{ID} at certain times during the day and get remunerated with a fixed price π_{ID}. The price parameters data can be given in the two ways:

1. The service revenue is obtained by the owner only if the full amount of requested power (P_{ID}) is dispatched:

$$\Pi_{ID} = \left[P_{ID}\pi_{ID}, 0, 0, 0, 0, 0 \right]^T \tag{48}$$

where the non-zero parameter is multiplied by the service binary variable. However, the ESS might be able to provide only a portion of that requested power for the investment deferral service:

2. The service revenue is obtained based on the dispatched power:

$$\Pi_{ID} = \left[0, \left(\left(0, \pi_{ID} \right), 0 \right), 0, 0, 0, 0 \right]^T \tag{49}$$

where the minimum discharging power is priced at π_{ID}.

These two definitions of service revenue lead to different simulation results and selection of the proper one should be done based on the service rules under each territory. The second model is used and simulated in the following sections as in [104].

The upper and lower bounds of the investment deferral service variables are given as

$$b_{x(EA),EA}^{\max/\min} = \left[(1,1), \left(\left(P_{ESS}^{+,\max}, \left(0, P_{ID} \right) \right), P_{ESS}^{-,\max/\min} \right), E_{ESS}^{\max/\min}, E_{ESS}^{\max/\min}, P_{ESS}^{\max/\min}, R_{ESS}^{\max/\min} \right]^T \tag{50}$$

where the minimum discharging power is limited between 0 to P_{ID}. Note that if the first service model is used the dispatch power must be greater than the requested power P_{ID}.

The product sensitivity $\alpha_{p,ID,x_{ESS}}$ are all zero since the service does not provide any specific product offers/bids.

Modeling the investment deferral service as a lower bound variable that constraints the ESS minimum discharging variable provides the flexibility in the operation of ESS. For example, if other services are available and the ESS owner can obtain more benefits by providing more power to the other services than the investment deferral, then the model will compromise on the revenue from the investment deferral service. Note that this service is modeled either as a hard constraint or a pre-dispatch service in many ESS studies and tools such as EPRI StorageVET [118]. This approach underestimates the total revenue.

e. Service Stacking

Modeling any combination of services is done via the process described in section 4.4. However, explicit formulation for all the service combinations are provided in [104].

4.6.1.3 Simulation Results

The ESS revenues are assessed for the four services under study and all their combinations. The time dimension is also considered by modeling the intertemporal constraints to capture the temporal value of ESS. ESS parameters and price data are given as inputs to the optimization models as follows. The parameters used for the battery ESS model are presented in Table 6. Price data was taken from the 2015 CAISO day-ahead markets for the energy and ancillary services [119]. For the investment deferral service, it is assumed that the utility requires the ESS to provide 500 kW (P_{ID}) during hours 18:00 – 20:00, and it pays the ESS at the price of π_{ID} = \$0.5/kW. The utility obtains these values based on their load forecast, the investment amount, the deferral period, and the number of available ESS units that can be dispatched, as well as their impact on mitigating the overload on current assets. The simulation is performed for one year with a daily horizon (T = 24h) and hourly granularity ($\Delta t = 1h$). Since all the binary variables are enforced to equality constraints, the model is linear and convex, and can be efficiently solved with current solvers. Table 7 provides the annual revenue of the modeled ESS for different service combinations denoted by cases 1–15.

Table 6 – Battery ESS Parameters

Parameter	Value	Parameter	Value	Parameter	Value
$P_{ESS}^{-,\min}$	0 kW	$E_{ESS}^{\min}$	400 kW	η_l	100%
$P_{ESS}^{-,\max}$	2000 kW	$E_{ESS}^{\max}$	3600 kW	η_{chg}	90%
$P_{ESS}^{+,\min}$	0 kW	γ_{ru}	0.15 1/h	η_{dis}	90%
$P_{ESS}^{+,\max}$	2000 kW	γ_{rd}	0.15 1/h		

Table 7 – Annual Revenues of Different Services

Case #	Service Annual Revenue ($)				Total Annual Revenue ($)
	Arbitrage	Frequency Regulation	Reserve	Investment Deferral	
1	18,983	-	-	-	18,983
2	-	121,265	-	-	121,265
3	-	-	47,939	-	47,939
4	-	-	-	91,250	91,250
5	-15,360	147,626	-	-	132,266
6	13,533	-	49,062	-	62,595
7	-	118,688	3,723	-	122,411
8	-8,240	139,223	2,026	-	133,009
9	16,390	-	-	91,250	107,640
10	-	173,631	-	91,250	264,881
11	-	-	64,129	91,250	155,380
12	-11,726	141,427	-	91,250	220,951
13	11,977	-	48,302	91,250	151,530
14	-	243,035	0	91,250	334,285
15	-3,631	131,758	2,439	91,250	221,817

Based on the results, the frequency regulation has the highest value among other single services while energy arbitrage has the lowest value. This is reasonable since the impact of the frequency regulation offered capacity on the ESS energy level is less than that of energy bids (proportional to γ_{ru} and γ_{rd}). Thus, frequency regulation bids can be greater for longer periods compared to energy periods. Combining energy arbitrage with frequency regulation increases limits on frequency regulation bids since, for example, if ESS is charging with 2 MW, it can provide up to 4 MW of regulation up service. This increases the revenue of frequency regulation as well as the total revenue by compromising on energy arbitrage revenue. The same reasoning applies to energy arbitrage and reserve services combined. The investment deferral service is effectively stacked with frequency regulation and reserve since their stacked revenue is greater than the sum of their individual service revenues. This shows the superadditivity of revenues from these services.

Higher values of services in cases 10, 11 and 14 than those with the energy arbitrage service (12, 13, and 15, respectively) is because the price of energy dispatch variables is zero in the former cases. Therefore, the frequency regulation and the reserve bids and the revenues are higher in these cases compared to those with energy arbitrage included in the set of services. However, cases 12, 13 and 15 are considered as more realistic cases than cases 10, 11 and 14. In cases 12, 13 and 15, the energy arbitrage is included in the objective function, and energy dispatch variables are associated with costs that limit their dispatch compared to previous cases. Therefore, their total revenue is less than cases 10, 11 and 14, as expected.

Table 7 shows that the highest total revenue among realistic cases (excluding cases 10, 11 and 14) is for the case 15 that combines all services. The total revenue in this case is 79.3%

of the sum of individual revenues. Figure 24 illustrates how individual annual revenues are stacked when all services are co-optimized. While the investment deferral revenue does not change in combined services compared to its individual service, the revenue of the reserve service is decreased significantly in stacked services. This is due to the high price of investment deferral service and low price for reserve market.

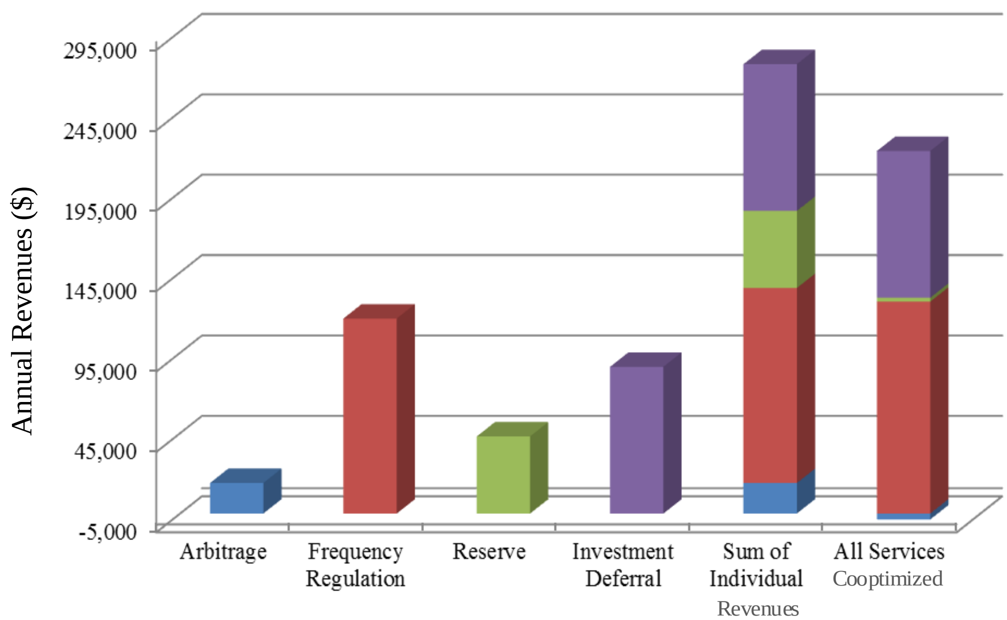

Figure 24 – Single- and stacked-service annual revenues

Using this structured service revenue analysis, the optimal price for the non-market investment deferral service is computed. In these simulations, the investment deferral service is always fully granted, and its revenue does not change when combined with other services. Thus, the price is high enough to incentivize the owner to provide this service under all the scenarios. The utility may choose to offer a lower price for this service while ensuring that the ESS can provide it. In other words, the utility is looking for the marginal cost of providing investment deferral service by the ESS owner. This cost is calculated after the optimization problem is solved. Since the model is strictly convex and strong duality holds, this cost is equal to the Lagrange multiplier (dual variable) associated with the constraint that models the upper bound of the variable lower bound of the ESS minimum discharging power:

$$P_{ESS}^{+,\min} \leq P_{ID} \tag{51}$$

This cost is computed for cases where investment deferral is combined with other service(s) (cases 9–15) and the results are presented in Table 8 under the column "Marginal Cost ($/kW)".

Table 8 – Marginal Cost and Optimal Price for Investment Deferral Service

Case #	Marginal Cost ($/kW)	Optimal Price ($/kW)	Utility Savings ($)
9	0.0783	0.1859	57,323
10	0.0271	0.0813	76,413
11	0.0540	0.1192	69,496
12	0.0318	0.0713	78,238
13	0.0432	0.0628	79,789
14	0.0782	0.1598	62,087
15	0.0340	0.0612	80,081

The results indicate that the current investment deferral service price paid by the utility π_{ID} = $0.5/kW is more than 6 times the marginal cost of providing this service by the ESS owner. This is a considerable amount that the utility can avoid paying by lowering the service price. However, setting this price to the maximum marginal cost does not guarantee service provision by the ESS since it may no longer result in the maximum owner's revenue where P_{ID} may not be fully provided by the ESS and constraint (51) may no longer be active. Meanwhile, this marginal cost gives a lower bound for the service price. The optimal price is found iteratively as the lowest price that guarantees full-amount service provision. Optimal prices as well as the utility savings compared to the base case (π_{ID} = \$0.5/kW) are calculated and provided in Table 8. This analysis shows the significance of setting an optimal price by the utility for procuring such non-market services.

4.6.2 Behind-the-Meter Energy Storage: Economic Assessment and System Impacts in Georgia

This test case presents the application of the proposed optimization approach to maximize the value of behind-the-meter energy storage that is owned and operated by customers. The objective of the optimization problem is to minimize the customer's electricity bill under various utility tariff rates. Each rate structure results in different options for the formulation of the optimization problem if modeled in the conventional way. However, with the proposed generic model, the structure of the problem does not change for each rate and only the input parameters are changed. Publicly available utility tariff rates from Georgia Power are used. The investment cost assumptions are derived from the latest market reports and from available vendor data. The impact of utility tariffs on the energy storage economics and system impacts are quantified. The simulation results show that different categories of behind-the-meter customers can obtain benefits from the installation of energy storage in this region. Moreover, tariffs with demand charges are usually more profitable for customers with energy storage and more desirable for the system operators to achieve a smoother net load curve.

4.6.2.1 Background

The use cases for BTM ESS and their economics vary significantly depending on the ESS technology, regulatory regimes, rate structures, and incentives in various regions. For instance, the Southeast region is generally confronted by market and regulatory conditions, which are substantially different from other states, where explicit state subsidies and/or procurement targets have been enacted, or where explicit market signals incentivize and compensate owners for grid services. Analysis of the benefits of behind-the-meter (BTM) ESS hence requires detailed modeling of the rate structures and specific regulatory aspects of each region.

In this test case, the generic optimization modeling is applied to determine the economic benefits of BTM battery ESS for the customers. The model covers diverse and realistic utility tariff rates, which is an innovative feature in software tools for ESS studies. The economics and system level impacts of BTM ESS are assessed using the optimization approach. The specific contributions of this test case are:

- The application of the proposed generic optimization approach to model various tariff rates including energy charges, time-of-use, demand rates, and real-time pricing,
- Assessment of both BTM use benefits as well as system level impacts,
- Insights on the economic viability of BTM ESS for customers in the Southeast region, yet with generalized models that can be applied in other regions, and

- Mechanism to analyze the interplay between rates and EES impacts. This test case provides insights into the impact of regulatory policies associated with BTM ESS deployment in a region.

The next section describes the methodology including the optimization model as well as system impact and benefit-cost analyses. The development of the datasets needed for the simulation and simulation results are also provided.

4.6.2.2 Proposed Methodology

In this section, the methodologies and assumptions developed for the simulation of BTM ESS are presented. The simulation workflow is illustrated in Figure 25. The analytical modules include:

- Optimization,
- System Impact Analysis, and
- Benefit-Cost Analysis.

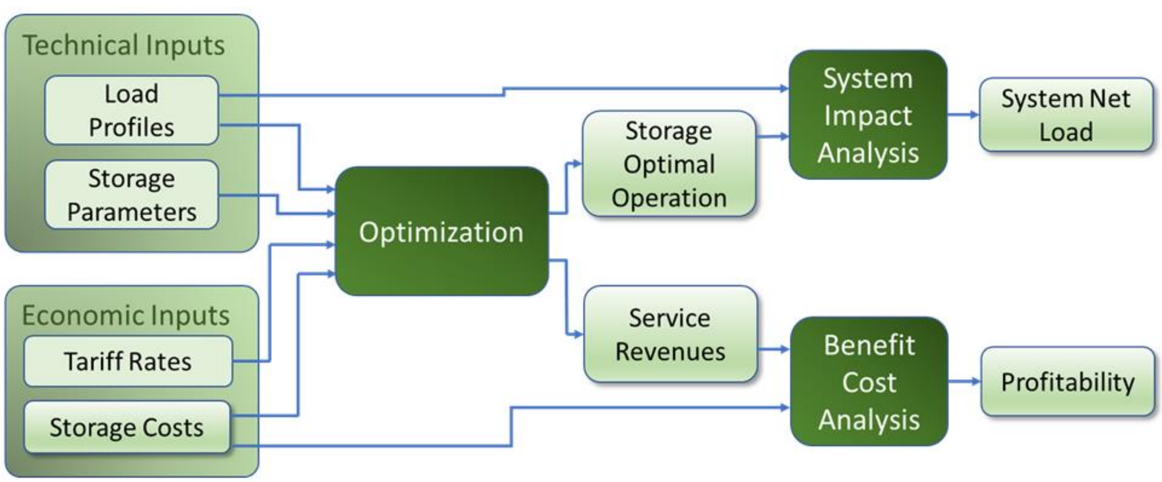

Figure 25 – The simulation workflow for BTM ESS analysis

- Optimization Module:

The core of the methodology developed is the temporal optimization module. Using this module, customers who own and operate ESS can evaluate the minimum monthly charge for their electricity bill. Equivalently, the optimization determines the optimal operation of ESS that minimizes the monthly electricity charge subject to ESS parameters, tariff rates, and customers' load profiles.

Utility tariff rates have different temporal and consumption-dependent structures, e.g. time-of-use, multiple tiers, etc. Modeling each tariff rate requires a specific optimization problem that is designed for that tariff rate. However, this is not a viable option for an ESS analysis tool to be useful and beneficial for customers served by different utilities and tariff rates. Therefore, there are significant needs and benefit in application of the generic optimization framework in BTM ESS analysis. Regardless of the tariff rates and other inputs, the optimization can be generically modeled as in (52)–(69). Although a compact formulation is presented here for the ease of understanding, the formulation can be cast into the proposed generic framework in section 4.4.

$$\min \sum_{t=1}^{T} \pi_t^{ene} P_t^{net} \Delta t + \sum_{b=1}^{B_e} C_b^{ene} E_b^{net} + \sum_{l=1}^{L} \pi_l^{dem} P_l^{dem} + \sum_{b=1}^{B_d} C_b^{dem} P_b^{dem} \tag{52}$$

subject to: $\forall t \in \mathcal{T}$

$$\left\{ P_t^{net} = P_t^{load} + P_t^{chg} - P_t^{dis} \right. \tag{53}$$

$$-sP_{\max}^{dis} \le P_t^{net} \tag{54}$$

$$0 \le u_t^{dis} + u_t^{chg} \le 1 \tag{55}$$

$$0 \le P_t^{dis} \le P_{\max}^{dis} u_t^{dis} \tag{56}$$

$$0 \le P_t^{chg} \le P_{\max}^{chg} u_t^{chg} \tag{57}$$

$$E_t^s = \eta E_{t-1}^s + \left(\eta_{chg} P_t^{chg} - P_t^{dis} / \eta_{dis}\right) \Delta t \tag{58}$$

$$E_{\min}^s \le E_t^s \le E_{\max}^s \tag{59}$$

$$E_T^s = E_0^s \} \tag{60}$$

$$0 \le E_b^{net} \le E_b^{\max} u_b^{ene} \quad \forall b \in \mathcal{B}_e \tag{61}$$

$$u_b^{ene} \ge u_{b+1}^{ene} \quad \forall b \in \mathcal{B}_e \setminus \{B_e\} \tag{62}$$

$$u_{b+1}^{ene} \le \frac{E_b^{net} - E_b^{\max}}{E_b^{\max}} + \varepsilon \le 1 + u_{b+1}^{ene} \quad \forall b \in \mathcal{B}_e \setminus \{B_e\} \tag{63}$$

$$\sum_{b=1}^{B_e} E_b^{net} = \sum_{t=1}^{T} P_t^{net} \Delta t \tag{64}$$

$$P_t^{net} \le P_l^{dem} \quad \forall t \in \mathcal{T}_l, \forall l \in \mathcal{L} \tag{65}$$

$$0 \le P_b^{dem} \le P_b^{\max} u_b^{dem} \quad \forall b \in \mathcal{B}_d \tag{66}$$

$$u_b^{dem} \ge u_{b+1}^{dem} \quad \forall b \in \mathcal{B}_d \setminus \{B_d\} \tag{67}$$

$$u_{b+1}^{dem} \le \frac{P_b^{dem} - P_b^{\max}}{P_b^{\max}} + \varepsilon \le 1 + u_{b+1}^{dem} \quad \forall b \in \mathcal{B}_d \setminus \{B_d\} \tag{68}$$

$$\sum_{b=1}^{B_d} P_b^{dem} = P_l^{dem} \tag{69}$$

The objective function in (52) is the monthly electricity charge that consists of energy charge (the first two terms) and the DC (the second two terms). The energy charge can be calculated based on either a TOU tariff (with price π_t associated with each time period t)

or an energy-tiered tariff (with energy price C_b associated with block b of a stepwise function). The DC can also be calculated similarly. Constraint (53) defines the net load as the load plus ESS output where charging is considered as a positive load and discharging is a negative load. Constraint (54) limits the lower bound of the net load. If net metering does not apply (s=0), the negative net load is avoided. Conversely (s=1), the net load can be a negative value bound by the negative of the ESS maximum discharging power. Constraints (55)–(60) model ESS technology constraints as in (1)–(7).

Constraints (61)–(64) define a stepwise function for the monthly energy consumption. As an example, a tariff charges customers at C_1 \$/kWh for the first $E_1^{\max}$ kWh of their monthly consumption and at C_2 \$/kWh for their next $E_2^{\max}$ kWh. If TOU tariff is applicable, there is only one C_b that models overhead charges energy charge available in some tariffs, e.g. fuel cost recovery. Constraint (65) defines the demand for each demand level l, i.e. the maximum net load over all the time steps in period $\mathcal{T}_l$. We associate demand levels with the temporal variability of DCs, e.g. a two-level demand rate with level one being 5\$/kW during off-peak and level two being 10\$/kW during on peak hours. Moreover, if demand rates are variable based on the maximum demand, i.e. a stepwise function of demand, only one demand level is assumed and the set $\mathcal{T}_l$ is equal to $\mathcal{T}$. In this case, constraints (66)–(69) define the stepwise function for the monthly demand. Note that in both energy and DCs if C_b's are nondecreasing with b, the objective function is convex and integer variables u_b^{ene} and u_b^{dem} are relaxed as well as constraints (62), (63), (67), and (68). Otherwise, these constraints enforce the order of blocks in the optimization, i.e. the block b_1 is used first to include the energy/demand and only if b_1 has reached its maximum of $E_1^{\max}/P_1^{\max}$ then $u_2^{ene}/\, u_2^{dem}$ can become 1 and b_2 is used to include the rest of the energy/demand and so on.

- System Impact Analysis Module:

The system impact of BTM ESS shows how the system's total net load (*NL*) profile changes under various tariff rates and ESS penetration levels (*PL*: the proportion of total customers with BTM ESS). It is expected that customers seeking to minimize their bill operate their ESS as determined by the proposed optimization problem. Therefore, the system impact is calculated using the optimal ESS operation of the customers. If there are *N* customers under study, the system's net load at time *t* is found using (70). This calculation is useful for planning studies as well as rate design.

$$NL_t(PL) = \sum_{n=1}^{N} P_{t,n}^{load} + PL\left(P_{t,n}^{chg*} - P_{t,n}^{dis*}\right) \tag{70}$$

- Economic Analysis Module:

The profitability of BTM ESS is calculated using economic metrics such as net present value (*NPV*) and payback period (*PP*). The optimal revenues found by the optimization module are passed into the Benefit-Cost Analysis module where they are first subtracted by the storage costs. The metrics are then calculated using (71) and (72).

$$NPV(Y) = \sum_{y=1}^{Y} \frac{Revenue_y - Cost_y}{\left(1+r\right)^y} \tag{71}$$

$$PP = \min y \quad ; \quad NPV(y) \geq 0 \tag{72}$$

where *Y* is the expected storage life and *r* is the discount rate. As in (72), payback period is the first year whose *NPV* is nonnegative (if exists). The profitability results are helpful information for customers' investment decisions in managing their electricity bill.

4.6.2.3 Data Collection

In order to simulate the impact of rate structures on optimal operation and payback period in realistic cases, the required input data was collected strategically to represent actual load data sets and battery parameters. Thus, the results better match real-life scenarios, which is critical for decision making.

- Load Profiles:

For residential customer load profiles, the Pecan Street Database [120] is used, which contains high resolution (1-minute) load data for many residential customers. Although none of these customers are in the Southeast region, the customers located in Austin, Texas are chosen due to climate similarity. The average load size (annual demand or maximum load in a year) of these customers is 9.5 kW, and their average monthly energy consumption is about 900 kWh. The sum of daily load profiles for summer (June through September) and winter months (October through May) are plotted with the system impact results in the next section.

For commercial and industrial (C&I) load profiles, a publicly available data source supported by Department of Energy (DOE) is used [121]. This database provides 1-year long hourly simulated load profiles for various locations and a set of commercial buildings, such as restaurants, offices, hospitals, etc. The data simulated for Atlanta location is used to represent the Southeast region. Figure 26 shows the demands (maximum hourly load) and average hourly consumption of the diverse set of load profiles used which represent a realistic spread of actual commercial load variability to better visualize ESS impact. The average daily load profiles for summer and winter months summed up over all these customers are also plotted in the simulation results section.

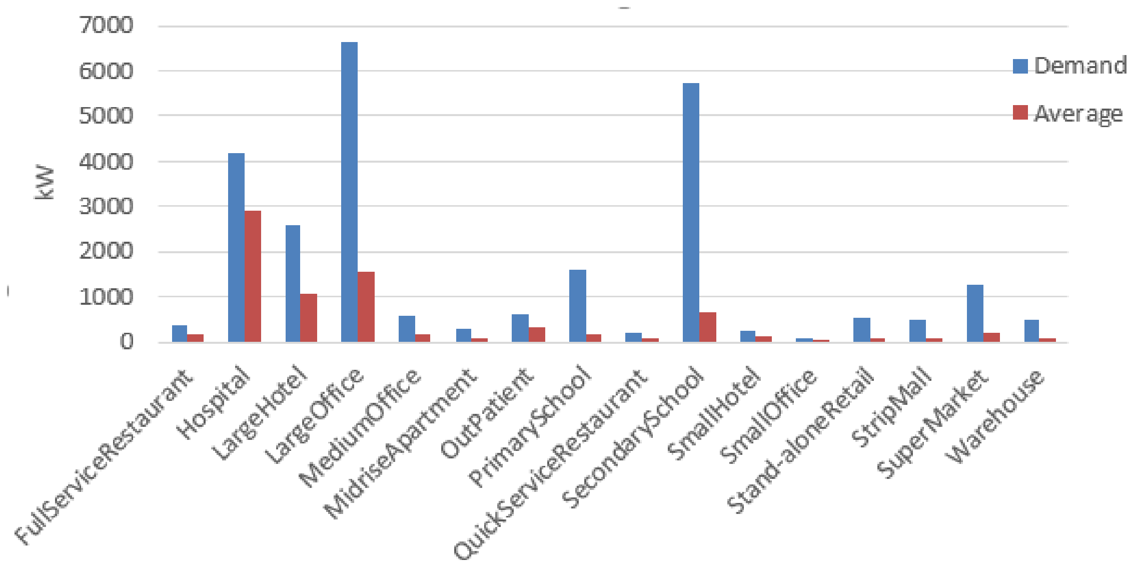

Figure 26 – Maximum and average of C&I loads per each building type

- ESS Parameters:

For residential customers, ESS parameters are selected based on Tesla Powerwall [122]: 7 kW maximum charging/discharging rates, 15 kWh total and 13.5 kWh usable capacity (90% depth of discharge), and 90.25% roundtrip efficiency (95% charging efficiency × 95% discharging efficiency). The cost of the Powerwall is \$6700/module (equivalent to about \$500 per usable kWh of storage). We use this number as fixed capital cost and assume no fixed or variable O&M costs. Based on the load profiles, one module is calculated to be enough for each customer.

For C&I customers, ESS power ratings ($P_{\max}^{dis/chg}$) are selected based on their load profiles. These ratings are assumed to be both equal to 20% of the customer's annual maximum load. The capacity rating is selected as 2 hours for all customers which based on the most common duration parameter for BTM application available at DOE, Energy Storage Database [111]. The same ESS technology used for residential customers are also used for C&I but in larger scale. Therefore, the depth of discharge and efficiencies are assumed similar to those of the residential ESS. The total cost (sum of capital and O&M costs) is assumed to be $400/kWh [14] and incurred in the CapEx year.

- Utility Tariffs:

Publicly available Georgia Power tariff schedules and rate structures [91] are used to create the tariff parameters. Strictly energy-tiered (net consumption) tariffs with no demand charges are not considered for the residential simulations since ESS cannot take advantage of this price structure to offset costs. Only residential TOU tariffs provide economic benefits. There are three of such rates: Nights & Weekends (N&W), Plug-In Electric Vehicle (PEV), and Smart Usage (SU). The SU rate includes DC and TOU energy charges. The C&I load profiles in this study are grouped into medium (demand≤500kW) and large (demand>500kW) subtypes based on Georgia Power definition. For each subtype, the most common two rates are used: energy-tiered with DC (Power and Light, PL), and TOU. Regardless of the customer type, the breakdown of a customer's bill is as follows:

$$\begin{gathered}\textit{Total Monthly Bill Charge} = \textit{Base Rate} + \textit{Other Schedules} + \textit{Municipal} \\ \textit{Franchise Fee} + \textit{Sales Taxes}\end{gathered} \tag{73}$$

where

$$\textit{Base Rate} = \textit{Basic Service Charge} + \textit{Energy Charge} + \textit{Demand Charge} \tag{74}$$

$$\textit{Basic Service Charge} = \textit{Fixed} \tag{75}$$

$$\textit{Energy Charge} = \textit{Energy*rate [c/kWh]} \tag{76}$$

$$\textit{Demand Charge} = \textit{Demand*rate [\$/kW]} \tag{77}$$

$$\textit{Other Schedules} = \textit{25\% Base Rate} + \textit{Energy*Fuel rate [c/kWh]} \tag{78}$$

$$\textit{Municipal Franchise Fee} = \textit{2.9989\% (Inside City Limits) of sum of all above} \tag{79}$$

$$\textit{Sales Taxes} = \textit{6\% of sum of all above} \tag{80}$$

As can be compared, the proposed optimization formulation (52)–(69) can model all of the above details. Using these tariff structures creates six test cases for residential: three cases of TOU where customers can sell back to the utility (net metering is applicable, s=1), and three cases where they cannot (s=0). The C&I tariff structures create six cases as well: two TOU rates and two energy-tiered with DC. For the two TOU rates, two cases where the customer can sell and cannot sell are analyzed. For each test case, the ESS annual revenues for each customer under a specific tariff type were calculated by solving the optimization problem. The results are provided in the next section.

4.6.2.4 Simulation Results

The developed simulation determines the profitability and system level impacts of BTM ESS in various test cases for both residential and C&I customers.

- Residential Test Cases:

Each of the three residential TOU tariff rates is simulated twice with either s=0 or s=1 for all residential customers. Table 9 shows economic results namely the customer's savings and payback periods for the six test cases.

Table 9 – Economic Results for Residential Tariffs

Test Case #	Rate	Annual Cust Savings ($)		Payback Period (years)	
		Med	Max	Med	Min
1	N&W (s=0)	248	277	27.0	24.2
2	N&W (s=1)	277	277	24.2	24.2
3	PEV (s=0)	600	643	11.2	10.4
4	PEV (s=1)	643	643	10.4	10.4
5	SU (s=0)	289	635	23.2	10.5
6	SU (s=1)	305	688	21.9	9.7

Due to the variability of customers' load profiles, a distribution of savings and payback periods is obtained. For the first four cases, most of the customer savings are close to the maximum value. Therefore, the reported median (Med) represents the savings for a typical customer. The maximum savings (Max) shows the best case, which is not much greater than the median. Thus, the customers' savings are very close to the maximum possible regardless of their load profiles. For test cases (2) and (4), since the only revenue is from energy time-shifting with no demand charge and the customers can sell energy, the optimization problem and its outputs are no longer dependent on the load profile. Moreover, since the rates are known with certainty in advance, all customers can obtain maximum revenue and minimum payback period in these two cases.

The minimum payback period for the N&W rate is higher than the other rates since the energy rate is flat during winter months and ESS optimal dispatch is nonzero during the weekdays of four summer months where the energy rate is not flat. While test cases (3)-(6) each have a minimum payback period of less than 11 years, it is important to note that the median payback periods for test cases (5) and (6) are more than double their minimum payback periods, while in test cases (3) and (4) there is a minimal increase between the median and minimum payback periods. This demonstrates how the PEV tariff provides reliable revenue for the majority of residential ESS owners, while the potential revenue from the SU tariff is highly dependent on the individual load profile of the customer. This is driven by the DC in the SU rate that makes the optimization dependent on the load profile. In summary, while the SU rate with s=1 provides the lowest payback period, the risk associated with the savings from this rate is higher than that of the PEV rate. The PEV rate, however, can provide less risky savings with 10 to 11 years of payback period.

The system level impact is calculated from the optimal ESS dispatch of all the customers using (70). For brevity, the results for test cases (3) and (5) are presented in Figure 27(a) and (b), respectively. The first letter (S/W) shows the season and the number after that is the percentage of penetration level of ESS in the system ($PL\times100$). Summer and winter months are plotted separately to capture the impact of the seasonal changes in tariffs.

The high peak prices in both cases incentivize the customers to discharge their ESS during the afternoon hours of summer months and lower their bills. Therefore, peak prices in both these tariffs is a proper signal to shave the summer afternoon peak. However, in test case 3, the peak load is shifted to the super-off-peak hours (11pm to 7am). This can become challenging especially with the increasing penetration of BTM ESS resulting in new peak hours and increasing the generation ramping requirement around the hours that tariffs change their rate. Test case 5, on the other hand, results in a more desirable system impact with the peak load shifted almost evenly throughout the nonpeak hours. The above comparison holds for winter months as well. The more desirable system impact of case 5 is due to the DC in SU tariff that incentivizes the smooth total load that minimizes demand.

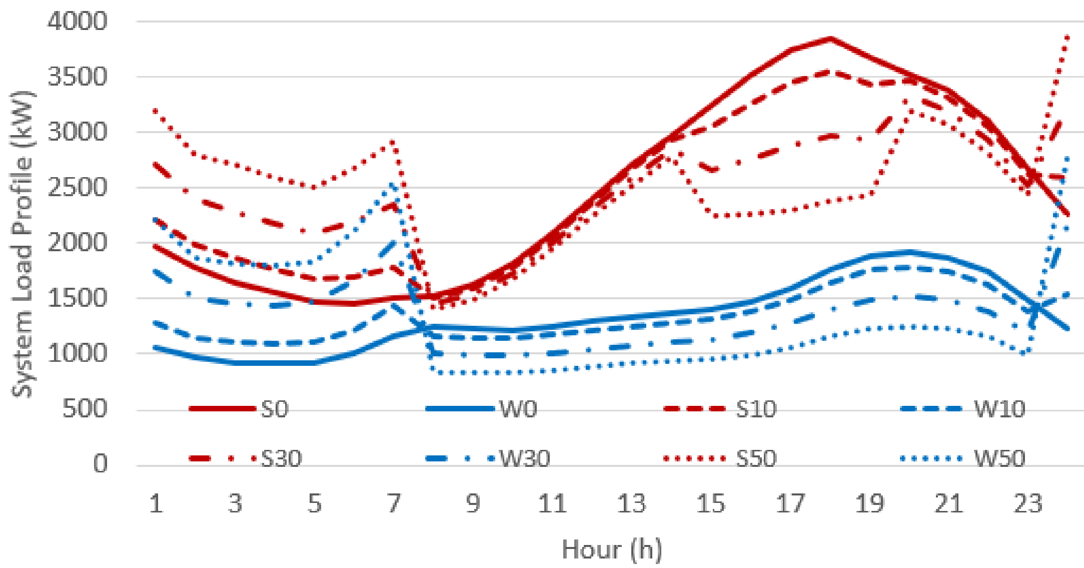

(a)

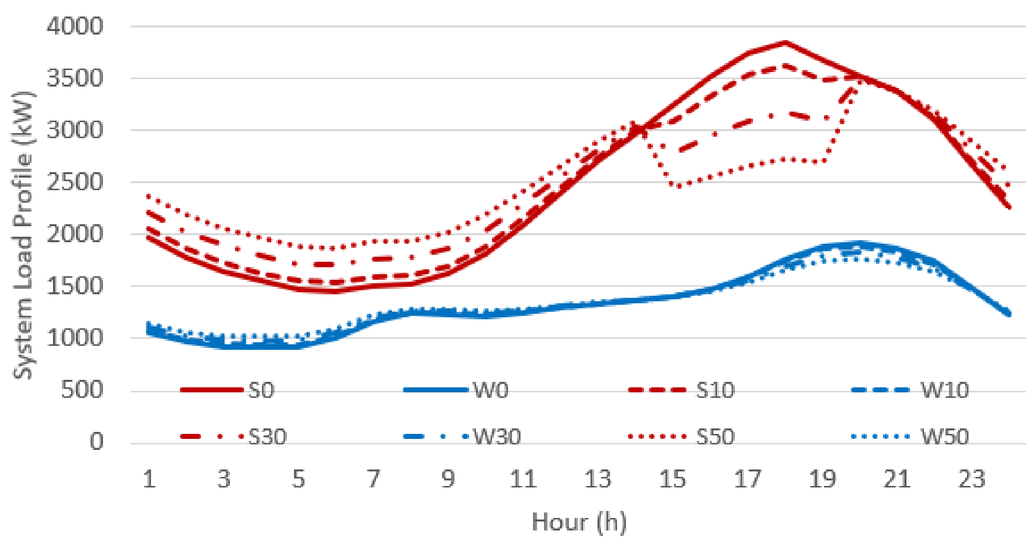

(b)

Figure 27 – System level impact of BTM ESS for test cases a) 3 and b) 5

- C&I Test Cases:

The four C&I test cases (two subtypes and two rates each) are simulated and results are presented here. The parameter *s* is unnecessary here since the net load does not become zero in any case for any of the customers. Table 10 shows the minimum, median and maximum payback periods for these cases. Since the ESS is different for each C&I customer, their total bill and also their savings cannot be compared directly and thus not reported in Table 10.

Table 10 – Economic Results for C&I Tariffs

Test Case #	Rate	Payback Period (years)		
		Min	Med	Max
7	P&L-M	7.7	9.6	12.7
8	TOU-M	5.2	6.8	7.4
9	P&L-L	5.7	8.2	16.9
10	TOU-L	44.6	44.6	44.6

Results for test cases 7, 8, and 9 show promising payback periods. Especially, the TOU tariff for medium-sized loads (case 8) provides the best payback periods in less than 7.4 years regardless of the load profile. This indicates that many of such customers can considerably and reliably benefit from the installation of a BTM ESS at their sites. Also, for the large customers, the TOU tariff results in relatively low payback periods but with more risk compared to the TOU-M. In case 9, the median payback period is higher than that of case 8, which shows that the profitability of installing ESS is more dependent on the customer's peak demand and how much energy is needed to reduce the peak demand. The payback periods in the case 10, TOU tariff for the large customers, are all very large and nonprofitable since the rate is flat for 8 months and the ESS revenue in this case is restricted to the four summer months. The payback periods are also constant since again the optimization problem is independent of the load profile because there is no DC in this tariff.

The system level impact of these test cases is also calculated using (70). In almost all these cases, the system impact is negligible and therefore not reported. The most significant system impact is resulted by case 8 where only during the peak hours of summer months the system total net load is reduced up to 10% with PL = 50% as a result of ESS discharge operations as shown in Figure 28. However, this is change still much less than that in residential test cases.

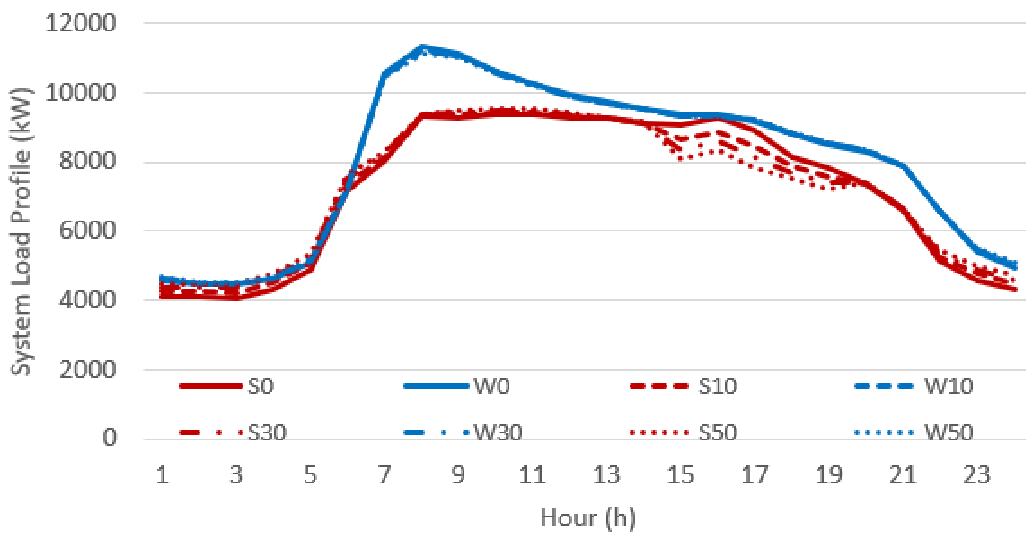

Figure 28 – System level impact of BTM ESS for test case 8

4.7 Summary

This chapter presented a systematic methodology for multiservice analysis of energy storage operation. It also proposed a generic optimization framework that can co-optimize the ESS revenues from multiple services. A software tool is developed based on the designed system architecture. The applications of the generic optimization framework and the software tool in two realistic test cases presented in this chapter and summarized as below:

The first test case analyzed energy arbitrage, frequency regulation, energy reserve, and investment deferral using CAISO historical data. For each service, the generic optimization model is applied with the proper parameters. Service stacking is modeled as co-optimization problems with specific constraints that results in the maximum potential revenue. The modularity of the generic model facilitated the analysis of various service combinations using a systematic build of an optimization problem. With this model ESS owners and investors can estimate the maximum benefits that they can obtain by providing sets of services. The results indicated that frequency regulation has the highest value among the individual services in CAISO while energy arbitrage has the lowest value. Results also showed that different services can be stacked to provide the maximum revenue. Finally, a pricing mechanism for investment deferral as a non-market service was proposed which showed to be beneficial for the ESS owner as well as the utility in the context of procuring this service from privately-owned ESS.

The second test case applied the proposed generic optimization framework in order to analyze the economics and system impacts of behind-the-meter (BTM) energy storage in the state of Georgia. The proposed mixed-integer optimization formulation supports various tariff rates including energy charges, time-of-use, demand rates, and real-time pricing, making the methodology applicable to multiple regions. Georgia Power tariff rates and metered customers' load profiles were used to simulate realistic cases. The results revealed promising payback periods as low as five years for BTM energy storage projects under specific tariff rates. It is shown that the time-of-use rates are usually less profitable for customers but more reliable since they are less dependent on uncertain data. On the other hand, tariffs with demand charges can provide more profit for the customers but with more uncertainty. The system impact assessment of BTM energy storage revealed that demand charge rates can result in smoother system net load profiles with high penetration of BTM energy storage. The results can provide insights for BTM customers to invest in energy storage to reduce their bill, and for utilities to understand the impact of tariff rates on the adoption of BTM storage especially at high penetration levels.

As an extension to the models used in these two applications, the stochasticity of uncertain parameters and storage degradation model can be incorporated. It is also interesting to analyze scenarios where an aggregator can use distributed energy storage devices to participate in ancillary services markets and increase the value of energy storage. A detailed model is proposed and analyzed in the next chapter that includes the above complexities.

CHAPTER 5. THE TEMPORAL COMPLEXITIES OF ENERGY STORAGE OPTIMIZATION MODELS: VALUE AND DECOMPOSITION

5.1 Introduction

In Chapter 4, we proposed a generic multiservice optimization model for energy storage analyses. We showed that the model is scalable to any number of services as well as many other dimensions conditioned on the size and solution tractability. Modeling multiple and/or highly granular dimensions poses numerical challenges and increases the computational time of the optimization model solution. In particular, the time dimension and temporal aspects, i.e. optimization horizon and temporal resolution, are very important in energy storage optimization problems and require in-depth research.

Optimization horizon is important since unlike conventional energy resources, energy storages are considered limited energy resources [7]. This creates a tight temporal dependency of energy storage operation meaning that its operation is dependent on its state of charge and state of charge is determined by its operation at previous time steps. Therefore, to globally optimize the ESS operation, one must solve an optimization problem covering all the periods in the time-horizon. This will increase the value of energy storage but can also increase the computational solution time.

Temporal resolution is another important aspect. Since many new energy storage technologies, such as batteries, have fast response times, they can provide highly granular services with a few seconds resolution, such as in the frequency regulation service where the fast-responding resources are exposed to 2-4 second AGC signal [123]. Optimizing for such a high-resolution and stochastic signal especially for long-time horizons is numerically challenging. However, it is very important to model this real-time operation in scheduling and planning decisions due to energy storage degradation [94] as well as other temporal factors such as ramping.

The current practice is to compromise between the value of the model complexity and the computational capabilities in building and solving that model. A very simple approach used by many researchers and industry actors for long-time horizons in energy storage optimization problems is to break the long-time-horizon into smaller horizons and then optimize for smaller ones [92]. For example, instead of solving the optimal operation for one year, the operation is optimized in 365 days separately with the constraint that ESS state-of-charge at the beginning and end of each day should be equal. This approach is not globally optimal and compromises the accuracy of the calculated ESS benefits. Moreover, several services have temporal resolution of longer than a day. For example, the capacity market in many areas, such as NYISO and ISONE, is a monthly service and capacity bids are unique within each month [93]. Thus, daily optimization does not yield optimal solution. High resolution temporal complexity is usually simplified in the literature where real-time operation models with the high resolution (e.g. in seconds) are decoupled from the lower resolution (e.g. hourly) scheduling problems using a time scale separation principle. Some models use sequential approaches that first solve the scheduling problem and the optimal decisions are passed to the high-resolution operation problem for real-time control purposes [94]. Although the numerical tractability is improved by these simplifications, the value of jointly optimized scheduling and real-time operation is still compromised. Therefore, these complicating temporal aspects is another factor that hinders current optimization models to capture the maximum value of ESS.

5.2 Objective and Contribution

In this Chapter, we analyze the temporal complexities of energy storage optimization problems and answer the following important questions:

- *What is the added value of a temporally complex ESS problem?*
- *How to solve the complex ESS problem in a tractable way?*

For these ends, we first propose a stochastic multi-timescale optimization model for the price-maker participation of aggregated ESS in multiple markets and local services. This complex model has multiple dimensions including:

- Time: high resolution with a long horizon
- Services: wholesale market services as well as local services
- Energy storage technologies: different storage parameters
- Location: different local requirements
- Scenarios: several stochastic realizations of uncertain parameters

While the model can capture several interdependencies between dimensions, we focus on the time dimension where the model jointly optimizes the scheduling variables as well as the real-time operating strategies. Using this optimization model and realistic data, we then explore the added value of a) including high resolution real-time operation in a scheduling problem and b) global solution of a multiday problem with respect to its daily optimization. Results will help to quantify the value that has been blocked due to numerical challenges in solving global and high-resolution optimization problems. Next, we propose two decomposition techniques for solving the numerically challenging optimization problem. These two techniques are based on linear sensitivities and the alternating direction method of multipliers (ADMM) that solve the global problem by breaking it into smaller pieces, each of which are then easier to solve [124] and then iterating between solving the smaller problems to approach the global solution. This way, long-term and high-resolution ESS optimization problems are solved globally without compromising their added value. Thus, we can rely on more profitable ESS projects that attract investors and facilitate their deployment.

The rest of this chapter is organized as follows. The optimization model is presented in section 5.3. The value of the proposed model is simulated with realistic data in section 5.4. The temporal decomposition techniques are proposed in section 5.5 and simulated in section 5.6. Section 5.7. discusses how the proposed methods improve the computational time of large-scale ESS optimization problems. Finally, section 5.8. provides a summary this chapter.

5.3 Stochastic Multi-service Optimization Model for the Jointly Optimal Scheduling and Operation of Aggregated ESS

The formulation of the proposed two-stage stochastic optimization problem is provided in (81)–(103). This problem is solved by the operator/aggregator of multiple ESS sited at different locations, but the same pricing node, participating in month-ahead capacity market, day-ahead energy and ancillary services, i.e. frequency regulation and reserves, markets and providing local services (e.g. limiting the net load of a facility as a non-wire alternative for investment deferral). The first-stage decision variable is the capacity market bid for the next month, while the second-stage variables include energy and ancillary service bids for each hour t in the next month as well as high resolution regulation dispatch, which is modeled as vector $Q_{t,s,\omega}$ for each hour t. The temporal resolution of market bids and prices are hourly, and each index t denotes a one-hour period. However, $Q_{t,s,\omega}$ is a vector of τ decision variables and $1/\tau$ is the resolution of the regulation signal in seconds.

$$\begin{aligned}\max \sum_{\omega=1}^{O} \pi_\omega \Bigg\{ \sum_{s=1}^{S} \mu_\omega^{cap} P_{s,\omega}^{cap} + \Bigg[\sum_{t=1}^{T} \mu_{t,\omega}^{ene} \left(P_{t,s,\omega}^{dis} - P_{t,s,\omega}^{chg} \right) + \mu_{t,\omega}^{reg} P_{t,s,\omega}^{reg} + \mu_{t,\omega}^{mil} P_{t,s,\omega}^{reg} \rho_{t,s,\omega}^{reg} + \mu_{t,\omega}^{res} P_{t,s,\omega}^{res} \\ - C_s^{dev} \left(P_{t,s,\omega}^{dev,lb} + P_{t,s,\omega}^{dev,ub} \right)^2 - C_s^{deg} \left(P_{t,s,\omega}^{dis} + P_{t,s,\omega}^{chg} + \left\| Q_{t,s,\omega} \right\|_1 / \tau \right) \Bigg] \Bigg\}\end{aligned} \tag{81}$$

Subject to $\forall t \in \mathcal{T}, \forall s \in \mathcal{S}, \forall \omega \in \Omega$

$$\Bigg\{ \mu_\omega^{cap} = \mu_\omega^{cap0} - \alpha^{cap} \sum_{s=1}^{S} P_{s,\omega}^{cap} \tag{82}$$

$$\mu_{t,\omega}^{ene} = \mu_{t,\omega}^{ene0} - \alpha^{ene} \sum_{s=1}^{S} \left(P_{t,s,\omega}^{dis} - P_{t,s,\omega}^{chg} \right) \tag{83}$$

$$\mu_{t,\omega}^{reg} = \mu_{t,\omega}^{reg0} - \alpha^{reg} \sum_{s=1}^{S} P_{t,s,\omega}^{reg} \tag{84}$$

$$\mu_{t,\omega}^{res} = \mu_{t,\omega}^{res0} - \alpha^{res} \sum_{s=1}^{S} P_{t,s,\omega}^{res} \tag{85}$$

$$\rho_{t,s,\omega}^{reg} = \left(1 - \frac{\left\| P_{t,s,\omega}^{reg} r_{t,\omega} - Q_{t,s,\omega} \right\|_1}{\left\| P_{t,s,\omega}^{reg} r_{t,\omega} \right\|_1} \right) \tag{86}$$

$$\rho^{reg,\min} \le \rho_{t,s,\omega}^{reg} \tag{87}$$

$$0 \le P_{t,s,\omega}^{dis} \le P_s^{dis,\max} u_{t,s,\omega}^{dis} \tag{88}$$

$$0 \le P_{t,s,\omega}^{chg} \le P_s^{chg,\max} u_{t,s,\omega}^{chg} \tag{89}$$

$$0 \le u_{t,s,\omega}^{dis} + u_{t,s,\omega}^{chg} \le 1 \tag{90}$$

$$0 \le P_{s,\omega}^{cap} \le \left(E_s^{\max} - E_s^{\min} \right) / T^{cap} \tag{91}$$

$$0 \le P_{t,s,\omega}^{reg} \le \min\left(P_s^{dis,\max}, P_s^{chg,\max} \right) \tag{92}$$

$$0 \le P_{t,s,\omega}^{res} \le P_s^{dis,\max} + P_s^{chg,\max} \tag{93}$$

$$P_{t,s,\omega}^{dis} - P_{t,s,\omega}^{chg} + P_{t,s,\omega}^{reg} + P_{t,s,\omega}^{res} + I_t^{cap} P_{s,\omega}^{cap} \le P_s^{dis,\max} \tag{94}$$

$$-P_s^{chg,\max} \le P_{t,s,\omega}^{dis} - P_{t,s,\omega}^{chg} - P_{t,s,\omega}^{reg} + P_{t,s,\omega}^{res} \tag{95}$$

$$P_{t,s,\omega}^{dis} - P_{t,s,\omega}^{chg} + \max(Q_{t,s,\omega}) + \pi_{t,\omega}^{res} P_{t,s,\omega}^{res} + \pi_{t,s,\omega}^{cap} P_{s,\omega}^{cap} \le P_{t,s}^{req,ub} + P_{t,s,\omega}^{dev,ub} \tag{96}$$

$$P_{t,s}^{req,lb} - P_{t,s,\omega}^{dev,lb} \le P_{t,s,\omega}^{dis} - P_{t,s,\omega}^{chg} + \min(Q_{t,s,\omega}) + \pi_{t,s,\omega} P_{s,\omega}^{cap} \tag{97}$$

$$\begin{aligned} E_{t,s,\omega} = \eta_s^l E_{t-1,s,\omega} + \eta_s^{chg} \left(P_{t,s,\omega}^{chg} + \left\| Q_{t,s,\omega} \right\|_1^- / \tau \right) - \\ \left(P_{t,s,\omega}^{dis} + \left\| Q_{t,s,\omega} \right\|_1^+ / \tau + \pi_{t,\omega}^{res} P_{t,s,\omega}^{res} + \pi_{t,\omega}^{cap} P_{t,s,\omega}^{cap} \right) / \eta_s^{dis} \end{aligned} \tag{98}$$

$$E_{t-1,s,\omega} - I_t^{cap} P_{s,\omega}^{cap} / \eta_s^{dis} \ge E_s^{\min} \tag{99}$$

$$E_{0,s,\omega} / E_s^{\max} = SOC_0 \quad ; \quad \lambda_{t=0,s,\omega} \tag{100}$$

$$E_{T,s,\omega} / E_s^{\max} = SOC_T \quad ; \quad \lambda_{t=T,s,\omega} \tag{101}$$

$$\left. E_s^{\min} \le E_{t,s,\omega} \le E_s^{\max} \right\} \tag{102}$$

$$P_{s,\omega}^{cap} = P_{s,\omega+1}^{cap} \quad ; \quad \forall s \in \mathcal{S}, \forall \omega \in \Omega \setminus \{O\} \tag{103}$$

The objective function in (81) maximizes the expected value of the total net profit of an aggregated ESS owner. The first line in (81) models the market revenues from capacity, energy, regulation and reserve services. The regulation market revenue includes capacity payments as well as regulation mileage payments. The second line in (81) models the costs including the penalty cost of the deviation from a requested dispatch a local service as well as the degradation cost modeled as a linear function of ESS exchanged energy. Note that the degradation can be modeled more accurately as a function of the number of cycles with different depth of discharge [62]. Such a detailed modeling is out of the scope of this work and left as future work.

Constraints (82)–(102) hold for all the time periods t, all storage assets s, and all scenarios ω. Constraint (82)–(85) model the impact of ESS bids on market prices, where if the aggregate bid is zero, the price is equal to the simulated price parameter μ^0. We assume the sensitivity coefficients (α) are positive and regulation and reserve participations do not increase prices. This is valid since increasing ancillary service offers will depreciate their prices. Constraint (86) defines the performance score [123] that models how well a regulation resource responds to the regulation signal r. Regulation signal is a high-resolution (2–4seconds) stochastic parameter normalized in the range [-1, 1] and shows the ratio of the regulation bid that should be dispatched in real-time. Figure 29 shows a day-long two-second regulation signal in the PJM market (RegD) [105]. If the regulation dispatch accurately follows the requested regulation ($P^{reg}r$), the performance score is 1 and the mileage payment for a given regulation bid is maximum. Constraint (87) limits the performance score to be no less than a minimum score. The regulation resource must keep its score high enough to be eligible for participation in the regulation market. Although constraint (86) is nonlinear, its application in the objective function using constraint (87) results in linear terms.

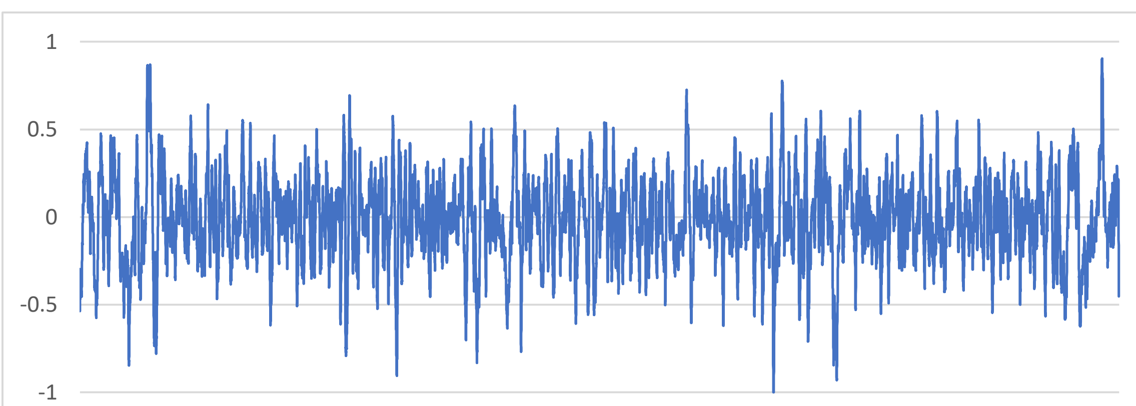

Figure 29 – Two-second regulation signal in the PJM market for a day (1/1/2017)

Constraints (88) and (89) limit the discharging and charging powers, respectively, while constraint (90) ensures that charging and discharging do not happen at the same time. Note that since there is a degradation cost for the sum of charging and discharging powers, constraint (90) is always met and therefore it can be relaxed as well as the binary variables. Constraints (91) – (93) model the constraints on the maximum capacity, regulation and reserve bids, respectively. The capacity market requirement modeled in (91) is defined by the parameter T^{cap} which is the number of consecutive hours that the capacity resource must generate or be discharged during capacity periods $\mathcal{T}^{cap}$. Regulation bid in (92) is assumed to be symmetrical for positive (discharge) and negative (charge) directions. This is the case in markets such as PJM where there is only one regulation product. The reserve bid is assumed to be only for positive direction (discharge). If regulation and reserve products have separate up and down bids, as in CAISO, these constraints can be updated trivially. Constraints (94) and (95) are checked by the market operator and the ESS operator to ensure that energy and ancillary service bids are feasible by the ESS power limits. I^{cap} is an indicator function which is 1 for all the periods in $\mathcal{T}^{cap}$ and zero otherwise. Constraints (96) and (97) model the local services and limit the output power of the ESS based on required dispatch. For example, the output power must be above a threshold to defer an investment of a critical asset such as a transformer. Note that the worst-case scenario for regulation dispatch is also considered. Also, to avoid infeasibility, the auxiliary nonnegative variables $P_{t,s,\omega}^{dev,ub}$ and $P_{t,s,\omega}^{dev,ub}$ are added and penalized with a quadratic cost function in the objective (81).

Constraint (98) models the stored energy at time step t based on the stored energy at t-1 and available at t (η_l models storage leakage over one period) plus the net energy exchange due to the dispatch in all the four markets. It is assumed that the reserve and capacity bids are dispatched with a probability $\pi^{res/cap}$ and therefore their impact on the stored energy is modeled with their expected values. Constraint (99) ensures that the energy required for the capacity market is always available during $\mathcal{T}^{cap}$ even if not dispatched. Constraints (100) and (101) enforce the boundary conditions on the available energy at the beginning and the end of the optimization horizon. The dual variables of these constraints are denoted with λ. These constraints serve as the linking constraints to the adjacent optimization horizons and are key in our proposed decomposition methods. Constraint (102) limits the stored energy at each time step to the ESS maximum and minimum allowable energy levels. Finally, constraint set (103) is the non-anticipativity constraints for first-stage decision variables i.e. capacity market bids.

The proposed ESS optimization problem is a mixed integer quadratic programming. However, as discussed, the binary state variables $u^{dis}_{t,s,\omega}$ and $u^{chg}_{t,s,\omega}$ in constraints (88)–(90) can be relaxed and the problem becomes a convex quadratic program. Thus, since all the constraints are linear, strong duality holds and the optimal dual variables can be used for sensitivity analysis of the optimal solution as constraints are perturbed [124].

Solving for the globally optimal solution of the proposed optimization problem can be challenging due to complicating constraints across each dimension: a) Number of services: the optimal operation of multiple services should be co-optimized and cannot be optimized separately, b) Time horizon (the cardinality of set $\mathcal{T}$): intertemporal dependencies enforced by constraints (100)–(102) and a unique capacity bid do not allow reaching a global solution by merely temporal splitting, c) Temporal resolution: if services have different time scales, the highest resolution is selected as the base resolution for the whole problem and this adds to the complexity of the problem, d) Number of ESS (cardinality of set $\mathcal{S}$): the operation of each ESS *s* impacts the others by changing the market prices. The problem is not trivially separable in this dimension, e) Number of scenarios (cardinality of set Ω): non-anticipativity constraints tie the scenarios together and again the problem cannot be trivially decomposed in this dimension and be solved for each scenario separately. While each of these dimensions require their specific studies, we focus on the temporal ones i.e. the time horizon and the temporal resolution.

5.4 The Value of the Proposed Optimization Model

One of the benefits of the proposed optimization model is that it captures multiple time scales, which complicates the solution but can provide significant added value. In this section, we use realistic market data to quantify the value of the *high temporal resolution* as well as *long time horizon* of the proposed optimization model. We want to maximize the net profit of an ESS owner participating in wholesale market products: monthly capacity, hourly energy, regulation capacity and reserves, as well as the 2-second regulation mileage. Therefore, the horizon is one month, and the temporal resolution is 2 seconds. Since the focus is not on the tractability of the model yet, we assume only one energy storage system ($S=1$) and one scenario ($O=1$) so that the problem is computationally easier to build and solve. The energy storage technical parameters are selected based on a Li-ion battery energy storage system as below:

$$\begin{gathered} P_s^{dis,max} = P_s^{chg,max} = 1MW, \qquad E_s^{min} = 0MWh, \qquad E_s^{max} = 6MWh, \\ \eta_s^{l} = 1, \qquad \eta_s^{chg} = \eta_s^{dis} = 0.95 \end{gathered} \tag{104}$$

The degradation cost parameter is the total capital cost of energy storage prorated by its lifetime energy throughput as in (20). The capital cost of Li-ion batteries are estimated with two linear coefficients C_s^P and C_s^E as below [38], [125]:

$$CapitalCost_s = C_s^P P_s^{dis,\max} + C_s^E E_s^{\max} \tag{105}$$

where C_s^P and C_s^E are assumed to be \$1300/kW and \$75/kWh, respectively [125].

The PJM historical prices and the 2-second regulation signal (RegD) for 2018 are used for simulation [105]. The optimization model is built and solved using Gurobi 8.1 [126] with Python interface on a computer with a core i5 2.6 GHz processor and 32 GB of RAM. Simulation results and discussions are provided in the following two subsections for high temporal resolution and long time horizon, respectively.

5.4.1 The Value of the High Temporal Resolution

Modeling the real-time participation of energy storage in the 2-second granular frequency regulation service is the main source of numerical complexity in the proposed optimization model in (81) – (103). However, it provides three main benefits compared to the hourly models:

- Higher total service revenues,
- Higher net profits i.e. a better trade-off between the revenues and degradation cost,
- More realistic dispatch that can be used for more profitable bidding purposes.

To quantify these benefits, we simulate the proposed model with the storage and market data as described. Four cases are studied, and their parameters are reported in Table 11.

Table 11 – Case Study Parameters

Case #	Resolution	Regulation Mileage Payment	Regulation Performance Score
1	Hourly	No	N/A
2	Hourly	Yes	Minimum (0.7)
3	Hourly	Yes	Maximum (1)
4	2-second	Yes	Optimized

For each case, the proposed model is modified based on the above parameters and ran for each day for all days in 2018. For the hourly models, the performance score (86) is modelled as a parameter. Also, the impact of high-resolution regulation dispatch on the hourly energy level and degradation is captured using a pre-processing of the 2-second regulation signal and the method developed by Sandia National Labs in [50]. For each case, the net profit, objective function (81), of each day and the total service revenue, first line in (81), are calculated. Next, the value of the proposed model (case 4) is calculated as the percentage improvement in net profit and the revenue compared to each of the first three cases. Results for January 2018 are illustrated in Figure 30. Results show that the proposed high-resolution model can capture almost double (90% improvement) the daily net profit compared to the one calculated by an hourly model. Moreover, the proposed model improves the hourly models, on average, 19.4%, 14.7%, and 12.8% in the revenues and 27.2%, 34.6%, and 18.0% in the net profits compared to cases 1, 2 and 3, respectively.

Another benefit of the proposed high-resolution model is in the optimal hourly bid and dispatch decision variables. The optimal dispatch of the hourly and 2-second models for a sample day are shown in Figure 31(a) and (b), respectively. Note that the three hourly models (cases 1,2, and 3) resulted in identical dispatch and thus, only one of them is plotted.

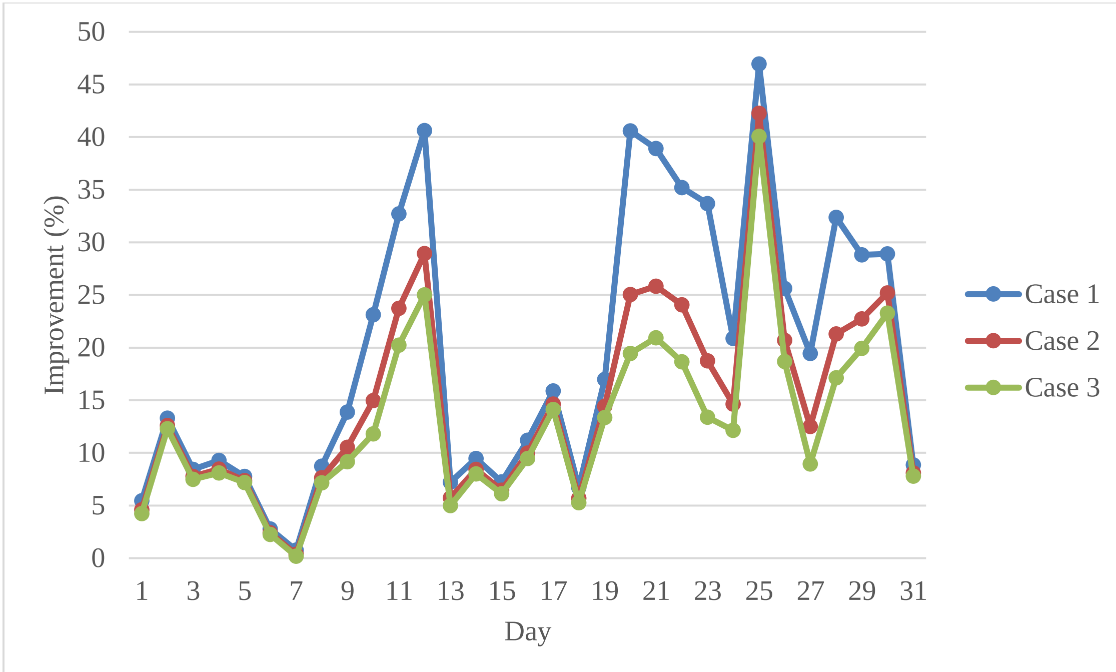

(a)

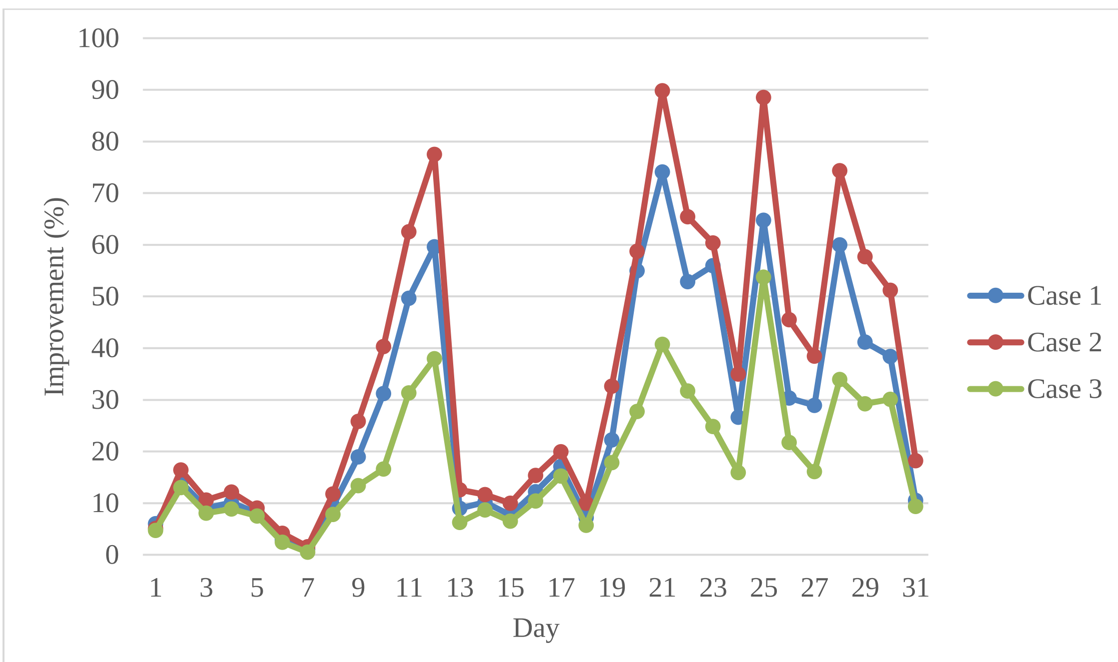

(b)

Figure 30 – The added value of the proposed high-resolution model compared to the hourly models, in terms of improvement in a) revenue and b) net profit

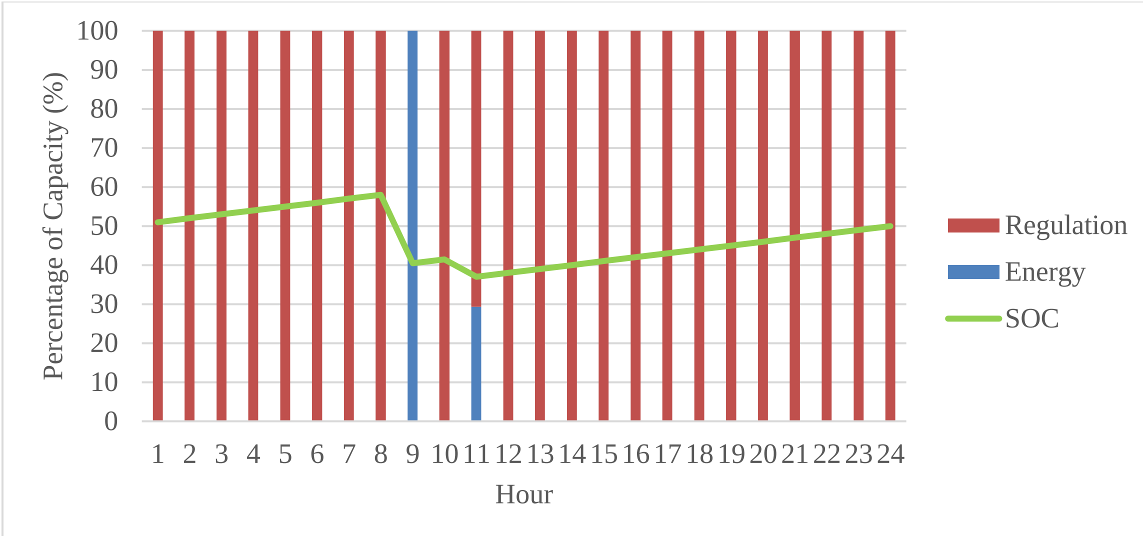

(a)

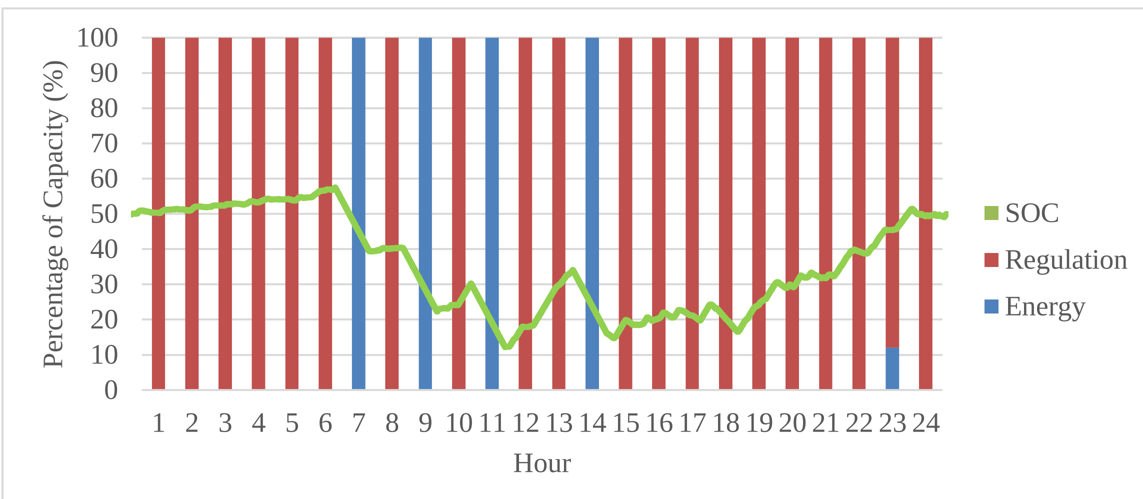

(b)

Figure 31 – ESS optimal dispatch using a) the hourly models and b) 2-second model

Results show how the high-resolution regulation model can impact the optimal participation in energy and regulation markets where in the hourly model, only hour 9 and 11 have non-zero dispatch in the energy market while for the 2-second model hours 7, 9, 11, 14 and 23 are so. For this day, reserve and capacity markets are not profitable enough and therefore not dispatched. Also, while the hourly model just models the aggregate impact of regulation dispatch on the SOC, the 2-second model can accurately model the SOC which is very important in detailed degradation analysis of ESS. Such an analysis is out of scope of this work.

Simulation results provided in this section verify the importance and the added value of the high temporal resolution in ESS optimization problems.

5.4.2 The Value of the Long Time Horizon

Modeling high-resolution dispatch of ESS in optimization horizons longer than a day is not conventional due to the significant added numerical complexity. However, there is value in such a model for two main reasons:

- First, some services have longer time horizons, e.g. monthly capacity auctions, and therefore, optimization models with shorter time horizons, e.g. daily, are not suitable unless they are solved iteratively.
- Shorter time horizons impose additional constraints that serve as links between adjacent time horizons, e.g. initial and final SOC constraints, and therefore, result in sub-optimal solutions i.e. lower net profits.

The objective of this section is to quantify the added value of long time horizons using the proposed model optimization model in (81) – (103) and realistic market data described in section 5.4. Four cases are studied where the first three cases use a daily optimization horizon and the fourth one uses a monthly one. All these cases use a 2-second temporal resolution to capture its high value as shown earlier. Also, the optimal value of the capacity market offer should be equal for all days since it is a monthly offer and thus, cannot be determined using the daily optimized cases without any iterations. Therefore, we assume this value to be a parameter equal to 0%, 50%, and 100% of the maximum discharge power in cases 1, 2 and 3, respectively. For each case, the objective function in (81) is calculated for all the months of 2018. Results are illustrated in Figure 32 as the percentage improvement of the proposed monthly model (case 4) compared to conventional daily models (cases 1, 2 and 3).

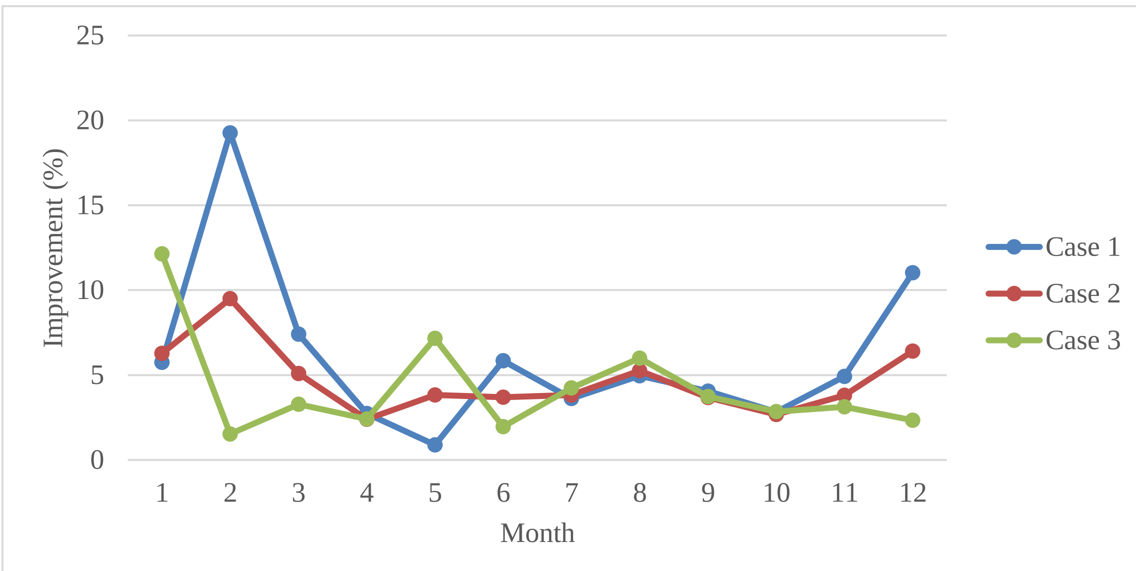

Figure 32 – The added value of the proposed model with monthly horizon compared to the hourly models, in terms of improvement in net profit (objective function (81))

These results show that the proposed optimization model with a monthly time horizon can capture additional value of up to 20% compared to daily optimization models. As mentioned before, this is due to a) the optimal capacity offer which is a decision variable in our proposed model compared, and b) inter-day arbitrage opportunities that are limited by the models with daily time horizon. In these simulations, the proposed monthly model improves the net profit of daily models by an average of 6.1%, 4.7%, and 4.2% compared to cases 1, 2 and 3, respectively. Note that none of the daily three cases provides better results in all the months and based on the model parameters, such as market prices, a more conservative approach (capacity offer = 0) may win or lose against an aggressive approach (capacity offer = maximum discharge power). However, the monthly model always provides a higher net profit as can be easily proven analytically. Simulation results provided in this section quantified the added value of longer time horizons in ESS optimization problems.

Using the proposed optimization model and the realistic market data, we evaluated the benefits captured by temporally complicated ESS problems with high resolution and long time horizon. The computational complexity of all the simulation cases were not a major issue so far; The computational time for an ESS optimization model with 2-second temporal resolution and a monthly time horizon, one ESS, and one scenario was about 35 minutes, almost 78% of that was the solution time and the rest was for building the model. Figure 33 shows the total computational time and its breakdown for each month. While these times show the tractability of the above simulations, the size and computational time of the model can grow significantly for simulations with multiple ESS and stochastic scenarios and result in intractable models. For example, a simulation with only 2 ESS and 10 scenarios was not solved even after a week. The complexity is mainly due to the high resolution of the regulation service. If we want to capture the added benefits of the high-resolution simulations in such intractable problems, we need to use decomposition. In the next section, two decomposition methods are proposed and applied for solving the intractable ESS problems.

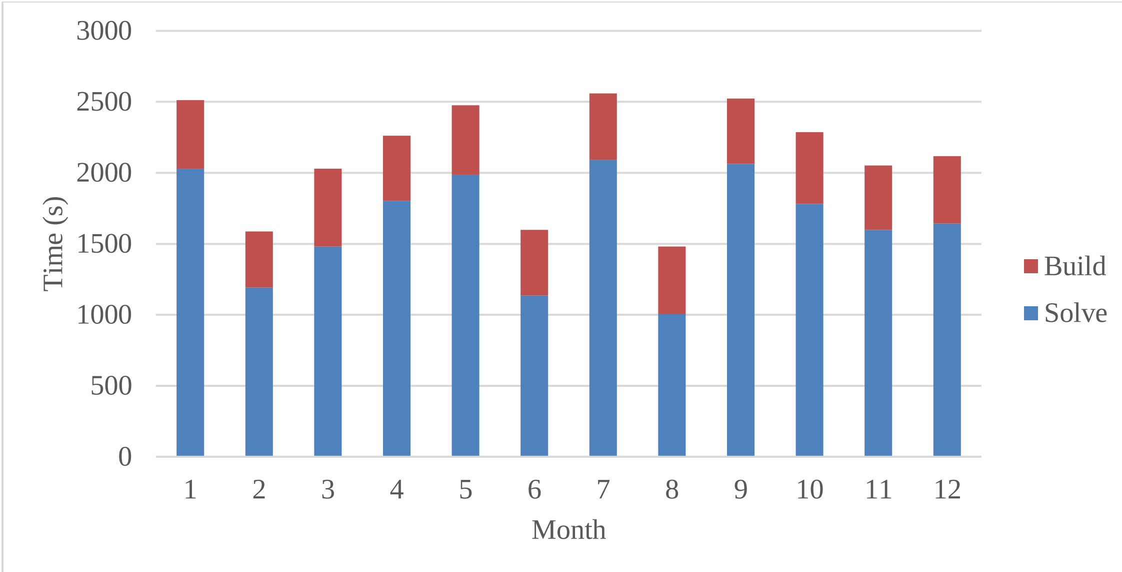

Figure 33 – Computational times of the monthly optimization model

5.5 Temporal Decomposition Methods

The proposed ESS optimization model in (81) – (103) can become intractable for simulations with high temporal resolution, long time horizons, multiple ESS and stochastic scenarios. Thus, proper decomposition methods across the sets of $\mathcal{T}$, $\mathcal{S}$, and Ω can be adopted for efficient solution of the global optimum. Our focus here is on the temporal aspect. We want to iteratively solve tractable subsets of the main intractable problem so that both the total objective function and the computational time improve. The solution process includes the following steps:

- First, split the main big problem into smaller tractable subproblems that can be solved independently. Since we propose to split in the time dimension, we call this step temporal splitting. This step requires assumptions on modifying the temporal links between smaller problems.

- Second, solve the smaller problems independently. Note that this step can be implemented in a parallel processing environment.
- Third, aggregate the solution of smaller problems and check if another iteration is needed (iteration control). If it is, then go to the fourth step. Otherwise, terminate.
- Fourth, update the assumptions on the temporal links and go to the second step.

Two independent temporal decomposition methods are proposed based on linear sensitivities and alternating direction method of multipliers (ADMM). Each method is described in the following subsections. Simulation results are provided in section 5.6 showing the application of the proposed methods to solve an intractable version of the proposed optimization problem.

5.5.1 Method 1: Linear Sensitivities (LS)

This method is based on the perturbation and sensitivity analysis of constraints that model temporal links between subproblems. These constraints model the SOC at the beginning and end of each subproblem, constraints (100) and (101), as well as the identical schedule for the capacity service in all subproblems that can be modeled as

$$P^{cap}_{s,\omega,d} = P^{cap}_{s,\omega} \quad ; \quad \lambda^{cap}_{s,\omega,d} \tag{106}$$

where $P^{cap}_{s,\omega,d}$ is the schedule for the capacity service in subproblem d and $\lambda^{cap}_{s,\omega,d}$ are the dual variables of these constraints.

In the temporal splitting step of this method, the linking constraints are modified to be equal to a parameter instead of decision variables in adjacent subproblems. This way, subproblems become independent of each other and can be solved in parallel.

By solving the subproblems, the optimal dual variables of the linking constraints are also calculated. They show the sensitivity of the optimal objective function with respect to the right-hand-side (RHS) parameter p of the linking constraints i.e. how much the optimal objective function will change if p is perturbed. If the objective function in (81) is denoted by J, then at optimality ($J*$):

$$\frac{\partial J^*}{\partial p} = -\lambda_p^* \tag{107}$$

Based on this important result, the main big optimization problem can be solved globally using the proposed decomposition method. Figure 34 shows the flowchart of the proposed method where subscripts d and i are indices for subproblems and iterations, respectively. Note that the subscripts for time, storage and scenarios used in (81)–(103) are omitted here for brevity. This method starts by splitting the original problem (e.g. one month) into smaller subproblems with shorter time horizons (e.g. daily). Subproblems are then solved in parallel (or sequential) with the RHS of the linking constraints being equal to a parameter identical in all the subproblems. Because the final SOC and capacity service schedule at subproblem d should be equal to the beginning SOC and capacity service schedule at subproblem $d+1$, respectively. So far, this is similar to the simple conventional temporal decomposition method. However, these fixed parameters are not optimal since they prevent arbitrage opportunities between subproblems for the SOC constraints and they do not necessarily result in a unique monthly capacity schedule. Therefore, the proposed decomposition method, iteratively updates these parameters based on the analysis of the optimal dual variables in (107). The updated parameters are fed into the subproblems that are solved again until the stopping criterion is met.

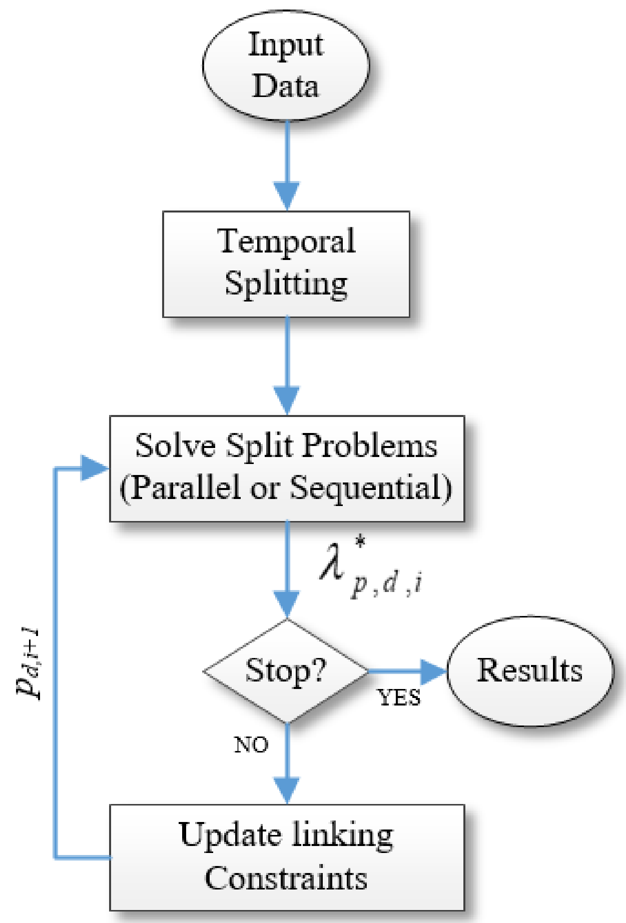

Figure 34 – The flowchart of the proposed decomposition method #1

The updating process for the RHS of the linking constraints, SOC and capacity dispatch parameters, is as follows. For updating SOC parameters, the optimal dual variables found by solving subproblems are compared between each pair of consecutive subproblems. If the optimal dual variable of the final SOC of subproblem d ($\lambda^{*}_{T,d,i}$) is in the ε-neighborhood of the negative of the starting SOC of the next subproblem $d+1$ ($\lambda^{*}_{0,d+1,i}$), it shows that changing their common SOC is not needed since it will increase the objective function for one subproblem and almost equally decrease it for the other one. Therefore, the SOC direction parameter σ for the next iteration is 0. If the sum of those two optimal dual variables with the common SOC is less than a negative threshold it means that the sum of changes in the objective functions of the two subproblems are positive if their common SOC increases. This result is derived from (107):

$$\Delta J = J^{*} - \lambda^{*}_{t=0/T,s,\omega} \Delta SOC_{0/T} \tag{108}$$

Conversely, if the sum of those two optimal dual variables is greater than a positive threshold it means that the sum of changes in the objective functions of the two subproblems are positive if their common SOC decreases. After the direction of the change in the SOC (σ_{SOC}) is determined, the step size Δ_{SOC} is found. It remains unchanged if SOC is changing in the same direction in the last two iterations. Otherwise, Δ_{SOC} shrinks by a factor of $\beta<1$ to improve convergence. The change in the common SOC between two consecutive subproblems ($\sigma_{SOC}\Delta_{SOC}$) is then added to the SOC to update it in the next iteration.

For updating the capacity dispatch parameter, the optimal dual variables found by solving subproblems are summed up altogether to model the impact of changing this parameter on the sum of objective functions of the subproblems. If the result is in the ε-neighborhood of zero, it shows that the capacity parameter is close to optimal and changing it is not needed since its total impact is negligible (less than ε). Therefore, the direction parameter σ_{cap} for the next iteration is 0. If the sum of all the optimal dual variables is less than a negative threshold it means that the sum of changes in the objective functions of sum of subproblems is positive if capacity parameter increases and vice versa. After the direction of the change in the capacity parameter (σ_{cap}) is determined, the step size Δ_{cap} is found. It remains unchanged if capacity parameter is changing in the same direction in the last two iterations.

Otherwise, Δ_{cap} shrinks by a factor of $\beta<1$ to improve convergence. The change in the capacity parameter for all the subproblems ($\sigma_{cap}\Delta_{cap}$) is then added to the capacity parameter at the current iteration to update it in the next iteration.

Updating the linking parameters also includes checking with other constraints so that the new parameters do not to exceed their bounds and also preserve the dependence on other subproblems. For example, the SOC must remain within its range determined by SOC_{max} and SOC_{min}. Also, the SOC at the end of subproblem d should be equal to the SOC at the beginning of subproblem $d+1$.

The process iterates until either the number of iterations reach a maximum threshold, or all the step sizes Δ become less than the minimum step size threshold Δ_{min}. The step sizes are used to calculate the residuals at each iteration as in (109). The residuals are then used to as a measure to analyze the convergence of the LS method.

$$R_i = \sum_{p,d} \left\| \Delta_{p,d,i+1} - \Delta_{p,d,i} \right\|_2^2 \tag{109}$$

The pseudocode of the proposed method is presented in Algorithm 2. This method is simulated with the realistic market data as in the previous sections. Simulation results are provided in section 5.6.

Algorithm 2

Initialize: i, d, $MaxIter$, $\sigma_{SOC,d,i}$, $\Delta_{SOC,d}$, $\sigma_{cap,d,i}$, $\Delta_{cap,d}$, Δ_{min}, ε, β

while $(i \le MaxIter)$ and $(max(\Delta_d) \ge \Delta_{min})$ **do**

  while d <D **do**

    Solve subproblems ($J_{d,i}$) in parallel

    Find $\lambda_{0,d,i}$, $\lambda_{T,d,i}$, $\lambda_{cap,d,i}$

    $d = d + 1$

  while d <D **do**

   if $\left|\lambda^*_{T,d,i} + \lambda^*_{0,d+1,i}\right| \le \varepsilon$ # no change (Optimal)

    $\sigma_{SOC,d,i+1} = 0$

   if $\lambda_{T,d,i} + \lambda_{0,d+1,i} < -\varepsilon$ # increase SOC

    $\sigma_{SOC,d,i+1} = 1$

   if $\lambda_{T,d,i} + \lambda_{0,d+1,i} > \varepsilon$ # decrease SOC

    $\sigma_{SOC,d,i+1} = -1$

   if $\sigma_{SOC,d,i+1}\sigma_{SOC,d,i} < 0$ # same change SOC, decrease step size

    $\Delta_{SOC,d} = \beta\Delta_{SOC,d}$

   $SOC_{T,d,i+1} = SOC_{T,d,i} + \sigma_{SOC,d,i+1}\Delta_{SOC,d}$

   Limit $SOC_{T,d,i+1}$ between SOC_{min} and SOC_{max}

   $SOC_{0,d+1,i+1} = SOC_{T,d,i+1}$

   $d = d + 1$

  if $\left|\sum_d \lambda_{cap,d,i}\right| \le \varepsilon$

   $\sigma_{cap,i+1} = 0$

  if $\sum_d \lambda_{cap,d,i} \le -\varepsilon$

   $\sigma_{cap,i+1} = 1$

  if $\sum_d \lambda_{cap,d,i} \ge \varepsilon$

   $\sigma_{cap,i+1} = -1$

  $P_{cap,i+1} = P_{cap,i+1} + \sigma_{cap,i+1}\Delta_{cap}$

  Limit $P_{cap,i+1}$ between 0 and P_{cap}^{max}

  $i = i + 1$

end while

5.5.2 Method 2: Alternating Direction Method of Multipliers (ADMM)

The second proposed decomposition method is based on the alternating direction method of multipliers (ADMM) which is a well-known method for solving convex optimization problems in a distributed way. The generic formulation of ADMM is provided in [127] and briefly presented here for completeness. Consider the optimization problem in (110) – (113).

$$\min_{x,y} f(x) + g(y) \tag{110}$$

Subject to

$$x \in \mathcal{X} \tag{111}$$

$$y \in \mathcal{Y} \tag{112}$$

$$Ax + By = c \quad ; \quad \lambda \tag{113}$$

where x and y are decision variables in their feasible sets $\mathcal{X}$ and $\mathcal{Y}$, respectively. The equality constraints in (113) is the linking constraint between the two decision variable vectors of x and y. The dual vector of (113) is denoted by λ. For a given dual vector, a positive scalar ρ, the augmented Lagrangian is as follows:

$$\mathcal{L}_\rho(x, y, \lambda) = f(x) + g(y) + \lambda^T (Ax + By - c) + \frac{\rho}{2} \|Ax + By - c\|_2^2 \tag{114}$$

ADMM is an iterative method that updates primal and dual variables in the following three steps at each iteration *i*.

$$x_{i+1} = \min_{x \in \mathcal{X}} \mathcal{L}_\rho(x, y_i, \lambda_i) \tag{115}$$

$$y_{i+1} = \min_{y \in \mathcal{Y}} \mathcal{L}_\rho(x_{i+1}, y, \lambda_i) \tag{116}$$

$$\lambda_{i+1} = \lambda_i + \rho(Ax_{i+1} + By_{i+1} - c) \tag{117}$$

It is proven that ADMM converges to the global optimal value for convex problems [127]. The quadratic term in the augmented Lagrangian provides a superior convergence compared to other decomposable methods, such as method of multipliers [95], [127]. Since the proposed energy storage optimization problem in (81) – (103) is convex, ADMM can be used to solve a decomposed version of the problem with guaranteed convergence to the global optimality.

The process of solving our proposed optimization model using the ADMM method is as follows. First, the main big problem is split into smaller tractable subproblems, indexed by *d*, that can be solved independently. At each iteration *i*, the objective function in in (81) is estimated by J_i defined as the sum of objective functions of the subproblems.

$$J_i := \sum_d J_{d,i} \tag{118}$$

The linking constraints between the subproblems serve as the equality constraint in the generic ADMM method in (113). For these constraints, we assume that their left-hand-side (LHS) is a free variable *z* which is equal to the RHS parameter *p* which is equal between the associated subproblems. ADMM relaxes these constraints and considers them in the augmented objective function. For each subproblem, the augmented Lagrangian is expressed as

$$\mathcal{L}_{\rho,d,i} := J_{d,i} - \sum_p \left[\lambda_{p,d,i} \left(z_{p,d,i} - p_{d,i} \right) + \frac{\rho}{2} \left(z_{p,d,i} - p_{d,i} \right)^2 \right] \tag{119}$$

where $\lambda_{p,d,i}$ is the dual variable for the linking constraint parameter *p* in subproblem *d* at iteration *i*. After the temporal splitting, subproblems are solved independently. This step is similar to the primal updates in the generic ADMM solution steps in (115) and (116). Each subproblem maximizes the augmented Lagrangian in (119) subject to (82) – (103), (102), (103). Note the linking constraints are no longer in the constraint set.

Next, the linking parameters p shared between subproblems are updated by averaging their associated variables z calculated independently in each subproblem. Specifically, for the SOC and capacity linking constraints, we have

$$SOC_{0,d,i+1} = \frac{1}{2}\left(z_{SOC0,d,i} + z_{SOCT,d-1,i}\right) \tag{120}$$

$$P_{cap,d,i+1} = \frac{1}{D}\sum_{d} z_{cap,d,i} \tag{121}$$

The updated linking parameters are used to update the dual variables as below.

$$\lambda_{p,d,i+1} = \lambda_{p,d,i} + \rho\left(p_{d,i+1} - z_{p,d,i}\right) \tag{122}$$

After this step, stopping criteria are checked to decide whether another iteration is required or not. These criteria include the number of iterations, improvement in the total objective function, and primal and dual residuals. The last two criteria are denoted by *PR* and *DR* and are calculated as in (123) and (124), respectively.

$$PR_i = \sum_{p,d} \left\| p_{d,i} - z_{p,d,i} \right\|_2^2 \tag{123}$$

$$DR_i = \sum_{p,d} \left\| p_{d,i+1} - p_{d,i} \right\|_2^2 \tag{124}$$

The primal residual shows the difference between the shared parameter p and its associated decision variable z for all the linking constraints and all the subproblems. A lower *PR* shows a better feasibility of the main problem. The dual residual shows the optimality of the aggregate decomposed solution where a lower *DR* means a better total objective function. This method is simulated with the realistic market data as in the previous sections. Simulation results are provided in section 5.6.

5.6 Simulation and Results

We simulated the two proposed decomposition methods with the realistic market data to study their performance in solving intractable versions of the proposed ESS optimization problem. Specifically, we want to analyze how these methods will improve the solution time and optimality of large-scale ESS optimization problems. Depending on the computational capabilities of the testing machine, the size of an intractable problem may vary between computers. Based on the computational power available for this work (parameters reported in section 5.4.), the proposed optimization model with 2-second temporal resolution and one-month horizon for two ESS and 10 scenarios is considered intractable. Such a model has more than 10 million decision variables and more than 12 million constraints. Note that the intractability is not only because of solution time but also creating that model from the large data sets of input parameters is another key factor in these problems.

Simulation parameters used in this section for market prices and ESS parameters includes similar ones in section 5.4. Additionally, we assume that both ESS are the same type and therefore have the same technical and cost parameters. For scenario generation the proposed random sampling approach is used as described in section 3.4.1.3. For each scenario, all the stochastic parameters, e.g. market prices, are generated independently. Statistical and time series models can be developed to generate scenarios considering dependencies within each scenario or among scenarios [59], [60], [110]. However, since our focus is on the improvements in solution time and optimality of the decomposed methods, more detailed scenario generation is left for future work. As an example of stochastic scenarios, Figure 35 illustrates the 10 stochastic scenarios generated for hourly energy prices of the PJM aggregate node in February 2018. As seen, price differences between scenarios increases with time modeling the higher level of uncertainty for future forecasts.

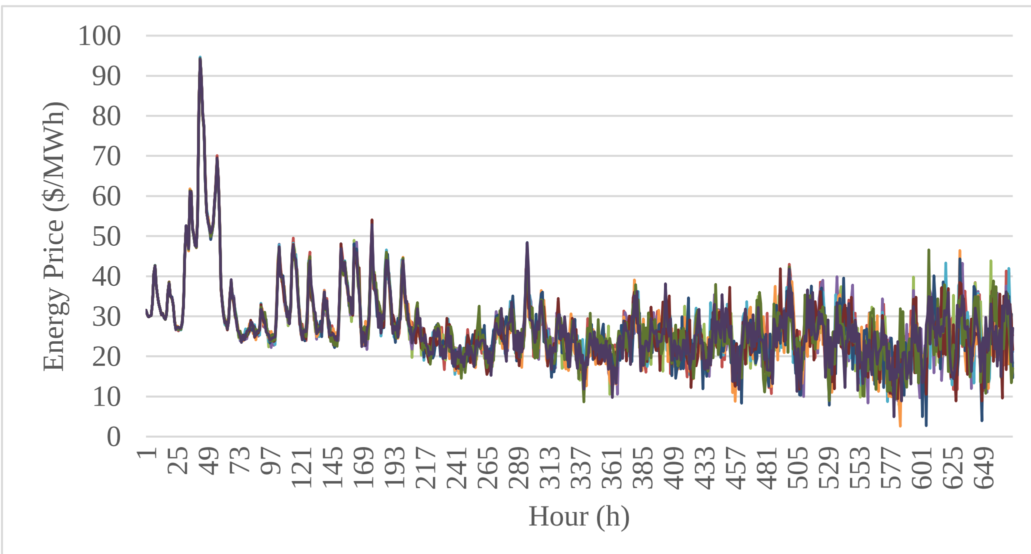

Figure 35 – Stochastic energy price scenarios

After generating stochastic scenarios for the whole optimization horizon (one month), all the input parameters are split into smaller subsets to generate the smaller subproblems. We assume that each subproblem is for one day within that month. Next, we use the proposed decomposition methods to iteratively solve and update the subproblems. As for the initial conditions, we assume that the linking SOCs are all equal to 50% of the total ESS capacity and the capacity market dispatch is zero. At each iteration, the sum of daily objective functions is used to estimate the globally optimal objective function. In the LS method, the objective function is the net profit while in the ADMM method, the augmented Lagrangian is maximized instead of net profit. Therefore, after solving each daily optimization problem using ADMM, the net profit is calculated from the optimal Lagrangian using (119). Since the original problem before decomposition is intractable, the globally optimal objective function (monthly net profit) is unknown so we cannot compare the results from the two methods with that. However, using simulation results, we show how these two methods progress throughout the iterations and compare their solutions against each other. Figure 36 shows the improvement in the total profit calculated by the two proposed decomposition methods at each iteration. This improvement is reported as the percentage of difference in the total net profit compared to a conventional non-iterative approach with initial conditions similar to those used for the LS method. The linear sensitivities method is denoted by LS.

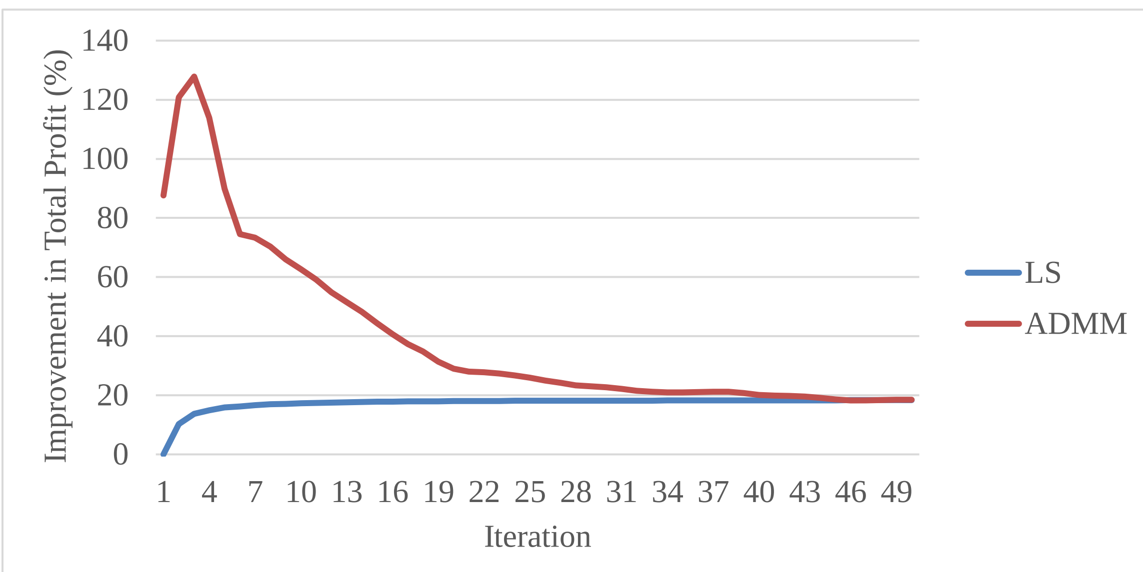

Figure 36 – The evolution of the total net profit by the two proposed decomposition methods

Simulation results show that both methods converge to identical solutions improving the total net profit of a conventional method by almost 20%. The difference between the total net profit of these two methods is less than 1% and 0.02% after 30 and 50 iterations, respectively. Note the difference in the convergence behavior of the two methods where the LS method converges in lower number of iterations compared to the ADMM. Specifically, the LS and ADMM methods stop after 30 and 50 iterations, respectively, when they met their stopping criteria. The LS total net profit at its last iteration is extended to cover the next 50 for a better comparison with the ADMM. Also, the convergence rate for the LS method is decreasing by the number of iterations. However, it is not monotonous for the ADMM. Another difference in the convergence pattern of the methods is that the net profit of the LS method is always less than the optimal value. This can be easily proven due to the convexity of the proposed optimization problem and the fact that all the LS solutions at each iteration are feasible which provides conservative results. However, the ADMM method starts with a better total net profit than the global optimum. This is because the linking constraints are relaxed in ADMM. However, ADMM solution may go below the global optimum at some iterations due to the intrinsic tradeoff between optimality and feasibility imposed by the augmented Lagrangian.

Another measure of convergence is the residuals of the methods at each iteration. Using (109), (123) and (124), we calculated the root mean of these residuals (RMSE) and demonstrate the results in Figure 37. As in the net profit results, LS method provides a better convergence since the RMSE of its residuals are lower than those in the ADMM. Also, comparing the primal dual residuals of ADMM show that it values the optimality of the solution more than its feasibility. This can be changed by modifying the ADMM parameter ρ in (119).

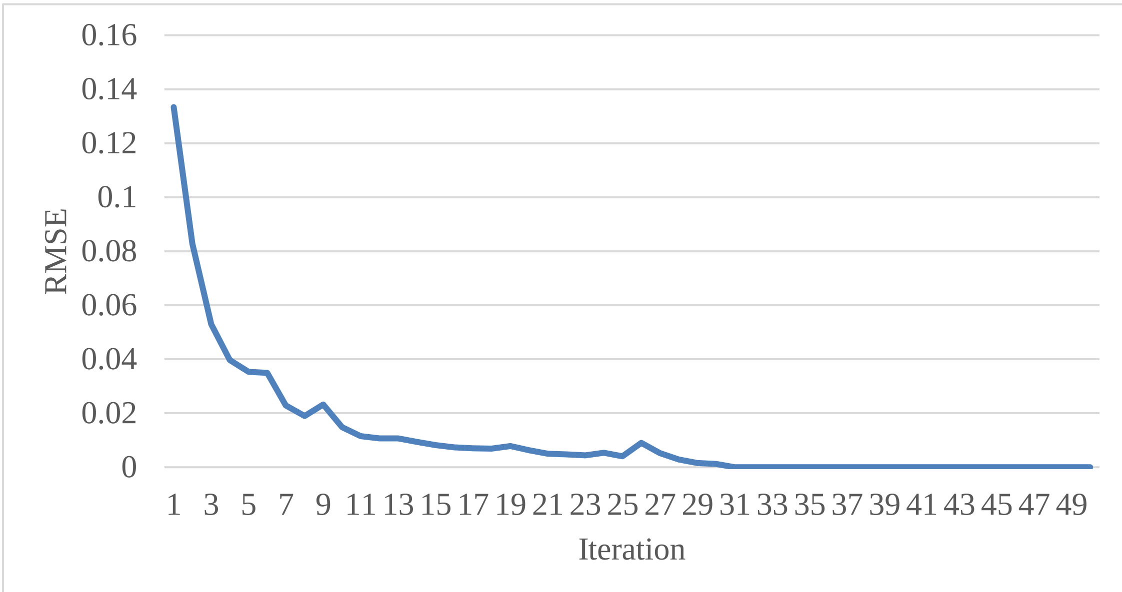

(a) LS residual

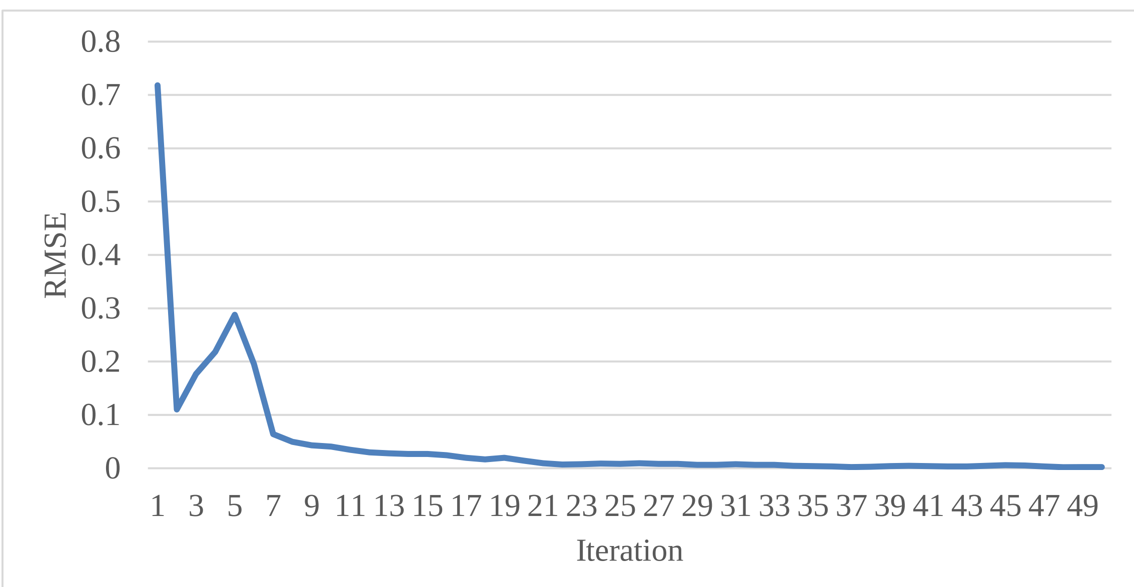

(b) ADMM dual residuals

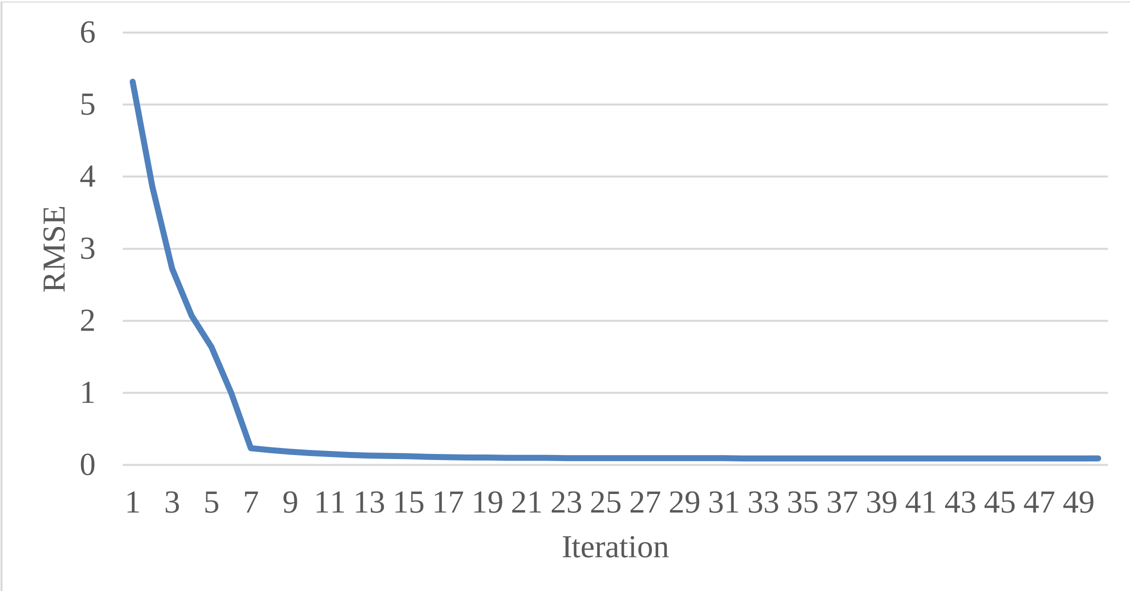

(c) ADMM primal residuals

Figure 37 – RMSE of a) LS residuals, b) ADMM dual residuals, and c) ADMM primal residuals

Besides the quality of the solution i.e. improvement in the net profit and convergence, computational time of the proposed decomposition methods is also important. In each iteration of both methods, subproblems can be solved either sequentially or in parallel due to their independence provided by decomposition. In the case of parallel solution, the total computational time at the end of iteration i (TCT_i) is determined by

$$TCT_i = \sum_{j=1}^{i} \max_s \left(CT_{s,j} \right) \tag{125}$$

where $CT_{s,j}$ is the computational time of subproblem s at iteration j. This shows that the computational time at each iteration is bound by the subproblem with the maximum time. Figure 38 shows TCT_i at each iteration for the two decomposition methods. Note that the ADMM method is faster in each iteration than LS since ADMM has lower number of constraints due to relaxation of temporal linking constraints. However, the LS method converges faster than ADMM. The *TCT* at the final iteration of these methods are 14.9 h and 21.2 h for LS and ADMM, respectively. Comparing the performance of the two methods at equal *TCT*s shows that the LS residuals are lower than those in ADMM. Therefore, the LS method is a better choice for the selected simulation case.

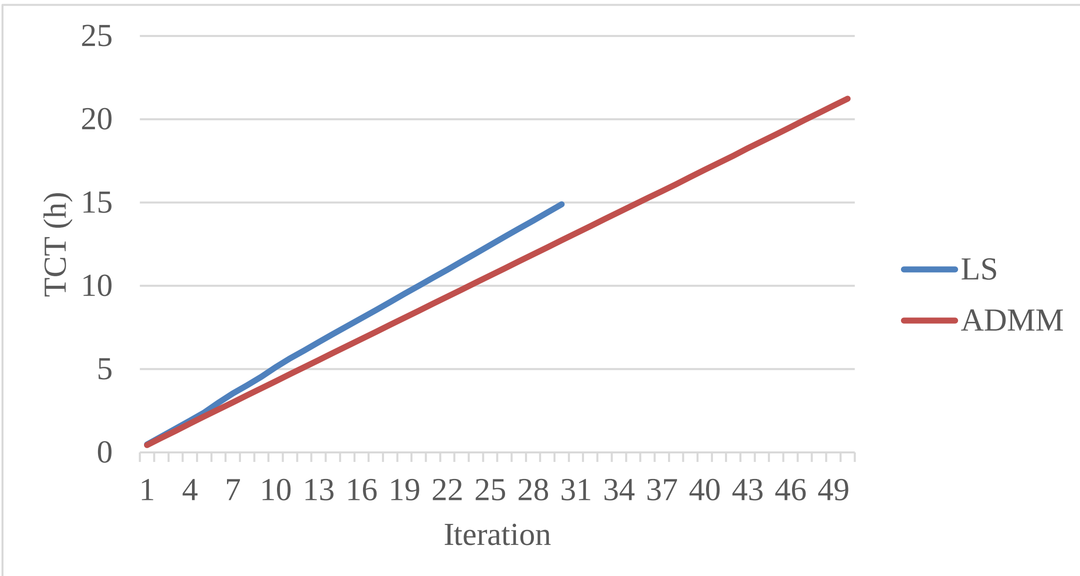

Figure 38 – Computational time of decomposition methods

5.7 Discussion on the Computational Time Improvements

This section analyzes the improvements of the computational time using the proposed methods. Assume the computational time for a given optimization problem is in the order of Z^k ($k \geq 1$) where Z is the complexity of the problem determined based on the structure of the problem, the number of decision variables and constraints. Consider Z is the complexity of the original optimization problem with the monthly time horizon. Using the proposed temporal decomposition methods, it is split into N same size subproblems. Computational time for each subproblem is in the order of $(Z/N)^k$. If the subproblems are solved in parallel, the total computational time is equal to the maximum of solution times for all subproblems.

Otherwise, the N subproblems are solved sequentially with the solution time in the order of $N(Z/N)^k$. We also assume that updating the linking constraints requires a time in the order of $(Z/N)^l$ for each subproblem where $l<<k$ since this process is not computationally intensive. In the worst-case scenario, the main loop of the proposed methods stops after a maximum number of iterations M has been reached. Thus, conditions for proposed methods to outperform the original problem in terms of computational time are

$$M\left(\frac{Z}{N}\right)^k + M\left(\frac{Z}{N}\right)^l < Z^k \tag{126}$$

if subproblems are solved in parallel and

$$MN\left(\frac{Z}{N}\right)^k + MN\left(\frac{Z}{N}\right)^l < Z^k \tag{127}$$

if subproblems are solved sequentially. Since $l<<k$, these conditions can be simplified to

$$M < N^k \tag{128}$$

$$M < N^{k-1} \tag{129}$$

Using (128) and (129), the improvement of the proposed methods can be quantified with respect to the computational capability (k), the number of iterations and the number of subproblems. For example, if both Z and Z/N are in the linear range of the solution time ($k=1$), the total number of iterations m ($m \le M$) must be less than the number of subproblems if parallel solution is applied. Note that the sequential solution of subproblems with the proposed method does not improve the total solution time if $k=1$. However, in most of the cases $k>1$ and the proposed method provides significant improvement in the solution time while providing a better objective function than the conventional decomposition method.

In the test case simulated in section 5.6., the original problem is intractable. However, using decomposition methods, it is solved in less than 15 and 22 hours which is a great improvement.

5.8 Summary

In this Chapter, we analyzed the temporal complexities of energy storage optimization problems. We proposed a stochastic multi-timescale optimization model for the price-maker participation of aggregated ESS in multiple markets and local services. Available ESS optimization problems optimize either the scheduling decisions in longer horizons, or the high-resolution operational and dispatch decisions in shorter horizons. They do not jointly optimize the scheduling and high-resolution dispatch decisions to avoid the numerical challenges from the resulted large-scale optimization problem. However, using the proposed model and realistic market data, we simulated how the temporal complexities can add to the ESS value. Simulation results show that including the high-resolution variables in response to the frequency regulation dispatch signal in the scheduling optimization problem can add up to 90% additional net profit. Also, solving for longer time horizons can provide an additional net profit of up to 20%. Moreover, the numerical complexities of such complicated problems are tackled using two proposed temporal decomposition methods that split the large-scale problem into smaller subproblems independent from each other and then iteratively solve them to reach the optimal global solution. Simulating the decomposition methods show that an intractable problem can be solved efficiently in a parallel processing environment. With the methodologies and results provided in this chapter, the added value of numerical complexities is not compromised for the computational challenges. Thus, this chapter contributes to the evaluation methodologies for maximizing the benefits of energy storage technologies and energy storage investors and developers can rely on more profitable ESS projects that are financially more attractive and can facilitate their deployment.

CHAPTER 6. CONCLUSIONS AND FUTURE WORK

6.1 Conclusions

Several benefits and applications have been identified for energy storage technologies that can contribute to the grid modernization and renewable energy integration objectives. In this dissertation, we developed new optimization methods than can accurately capture the maximum value of energy storage in providing multiple services for a variety of realistic use cases. The tools and methodologies used by industry for evaluation and revenue analysis are not specifically designed for ESS and cannot capture their maximum benefits provided by their flexibility and unique characteristics. Accordingly, they provide overly conservative estimates of storage revenues. Therefore, advanced tools and methodologies are required to maximize the expected revenues of ESS. Developing such methodologies is the focus of this work that was presented in three main chapters and summarized as below:

1. The expected revenues of ESS in the wholesale energy markets were studied and novel solutions were proposed to
    a. maximize the revenues of ESS in the day-ahead (DA) energy market. A straightforward method based on clustering of market prices and regression analysis is proposed that can estimate the maximum ESS revenues. Simulation results with realistic market data show the estimation accuracy of more than 98% compared to optimization problems. The proposed method is easily implementable that is key for optimal placement of ESS among thousands of possible locations.

b. maximize the revenues of ESS in the real-time (RT) energy market. A dynamic optimization with a shrinking horizon is proposed that can update the ESS dispatch decisions dynamically in the RT market. This way, it minimizes the impact of price forecast uncertainty and maximizes the collectible share of RT energy market revenue. Simulation results with realistic market data show that the proposed methodology can capture a significant RT energy market revenue that is almost twice of the revenue from the DA energy market.

c. maximize the total revenues of ESS in both DA and RT energy markets. Two optimization models are proposed for each market that include more details compared to previous methods, such as the load-price sensitivity and a better model for real-time price uncertainty. The high value of the RT market is based on estimations of uncertain data that might not be reliable for a risk-averse ESS operator. Therefore, the RT revenue is modeled as an additional revenue-stream to the DA one. Simulation results show that the RT market participation increases the revenue obtained in the DA market by more than 50% on average. Results also show that multiple services should be modeled as revenue streams to improve the profitability of new ESS technologies. Modeling multiple services is challenging due to service conflicts and synergies.

2. A systematic methodology for multiservice analysis of energy storage operation was proposed that can co-optimize the ESS revenues from multiple services. The proposed method finds the optimal operation of energy storage systems to obtain

the maximum value from providing any combination of services. A sophisticated architecture for the information system and data model was designed with the focus on scalability and modularity of the analysis. A generic optimization formulation is proposed as the center of this design. A software tool was also developed based on the designed system architecture. The tool has been tested on many real-world applications and is already being used by utility industry partners for their energy storage studies and projects. The generic optimization model is applied to two realistic test cases:

a. The first test case analyzed energy arbitrage, frequency regulation, energy reserve, and investment deferral using CAISO historical data. The modularity of the generic model facilitated the analysis of various service combinations using a systematic build of an optimization problem. Simulation results indicated that frequency regulation and energy arbitrage respectively have the highest and lowest value among the individual services in CAISO. Results also showed how different services can be stacked to provide the maximum revenue. Finally, a pricing mechanism for investment deferral as a non-market service was proposed which showed to be beneficial for the ESS owner as well as the utility in the context of procuring this service from privately-owned ESS.

b. The second test case analyzed the economics and system impacts of behind-the-meter (BTM) energy storage in the state of Georgia. The proposed mixed-integer optimization formulation supports various tariff rates and price structures making the methodology applicable to multiple regions.

Simulation results revealed promising payback periods as low as five years for BTM energy storage projects under specific tariff rates. It showed that the time-of-use rates are usually less profitable for customers but more reliable since they are less dependent on uncertain data. On the other hand, tariffs with demand charges can provide more profit for the customers but with more uncertainty. The system impact assessment of BTM energy storage revealed that demand charge rates can result in smoother system net load profiles with high penetration of BTM energy storage. The results can provide insights for BTM customers to invest in energy storage to reduce their bill, and for utilities to understand the impact of tariff rates on the adoption of BTM storage especially at high penetration levels.

3. The temporal complexities of energy storage optimization problems were analyzed. We proposed a stochastic multi-timescale optimization model for the price-maker participation of aggregated ESS in multiple markets and local services which jointly optimizes the scheduling and high-resolution dispatch decisions. The model value and solvability were studied:
    a. The value of the added complexity is quantified by simulating the proposed temporally complex optimization problem with the realistic market data. Results show that including the high-resolution variables in response to the frequency regulation dispatch signal in the scheduling optimization problem can add up to 90% additional net profit. Also, solving for longer time horizons can provide an additional net profit of up to 20%.

b. The numerical complexities of temporally complex ESS optimization problems are also studied. Two temporal decomposition methods were proposed that split the large-scale problem into smaller subproblems independent from each other and then iteratively solve them to reach the optimal global solution. Simulating the decomposition methods show that an intractable problem can be solved efficiently in a parallel processing environment. Therefore, the added value of numerical complexities is not compromised for the computational challenges.

In summary, we conclude that energy storage systems show promising profitability potentials if they are evaluated properly using advanced tools and methodologies.

6.2 Summary of Contributions

The methodologies, optimization models and simulation results provided in this work contributed to the evaluation approaches on maximizing the benefits of energy storage technologies. The specific contributions are listed as follows:

1. Identified the shortcomings and challenges of the methodologies in the literature regarding evaluation of the value of energy storage systems.
2. Developed a straightforward data-driven method for analyzing the energy storage revenue from the day-ahead energy arbitrage service.
3. Discovered the significant value of real-time energy arbitrage service and developed a dynamic optimization methodology to exploit the maximum variability of this market.

4. Developed a risk-averse price-maker methodology to maximize the revenue of energy storage systems that participate in both day-ahead and real-time energy markets.
5. Designed a system architecture and a data model for analysis of energy storage optimal dispatch and maximum service revenues.
6. Implemented a software capable of multiservice benefit cost analysis of energy storage systems. The software is released to and tested by several utilities in the U.S. to make important investment decisions on their energy storage projects.
7. Developed a modular and scalable generic optimization approach for multiservice revenue assessment of energy storage projects.
8. Successfully applied the generic optimization model to realistic test cases:
    a. Market service revenues using CAISO prices,
    b. Behind-the-meter customer benefits using Georgia Power tariff rates.
9. Developed a multidimensional energy storage optimization problem that includes multiple ESSs, services, time scales, and stochastic scenarios.
10. Studied the value and complexity of the energy storage optimization problems with high temporal resolution and long-time horizons and developed methods to address it.
11. Developed two temporal decomposition methods that efficiently solve intractable ESS optimization problem.

6.3 Future Work

Many possible and valuable related research arenas can be addressed as future work that are based on the proposed methodologies. A few of these arenas are briefly discussed as follows:

1. Using the proposed generic optimization model to optimally stack multiple services, research can be done to correlate the maximum revenues with the input parameters and their features. Similar approaches to what we developed only for the day-ahead energy market can be developed to cover multiple services and provide straightforward methodologies that rely less on large amount of forecast input data.
2. The information model proposed for ESS service evaluation can be upgraded to cover all the power grid resources such as conventional generators and renewable energy sources. A structured service evaluation platform and software tool can facilitate the deployment of new technologies, increase energy efficiency and avoid overinvestments for a modernized grid which further provides significant economic and environmental benefits.
3. More detailed modelling of energy storage technologies can be integrated into the proposed optimization methodologies to capture unique technology-specific characteristics of ESS. Such details include the circuitry of the ESS and electrochemistry of batteries. The challenge is to model the details with enough complexity and yet conserve the tractability of the model. Detailed analysis of the added complexities is required to disclose their value in ESS profitability estimation

similar to the one we performed for the added value of high resolution and longer time horizons.

4. Network/grid and volt/var modeling are other valuable arenas for future research. The impact of various grid constraint on the profitability of energy storage multiservice operation is not very well understood. Moreover, the impact of ESS multiservice operation on the grid volt/var requires advanced methodologies. Using the proposed multiservice approach, grid constraints can be added and analyzed. The proposed optimization model can be linked to a powerflow solver to capture and optimize the AC impact of the ESS operation. Due to the complexity of the resulted problem, decomposition methods may be needed. Providing all these capabilities in an automated software is deemed as the challenge but extremely valuable for increased deployment of ESS and renewable energies.

APPENDIX A. ENERGY STORAGE EVALUATION TOOL OVERVIEW

This Appendix presents an overview of the developed software for multiservice revenue analysis of ESS. More information on the tool design, documentation and instructions are reported in [128].

The graphic user-interface of tool is designed in multiple tabs where each tab is for certain steps to run an energy storage revenue optimization problem. The firs tab is for entering energy storage parameters as shown in Figure 39. Users can either manually enter the parameters or select from the default list of energy storage technologies, shown in Figure 40, and change the default parameters. The default parameters are selected from a comprehensive literature review on ESS technologies [128].

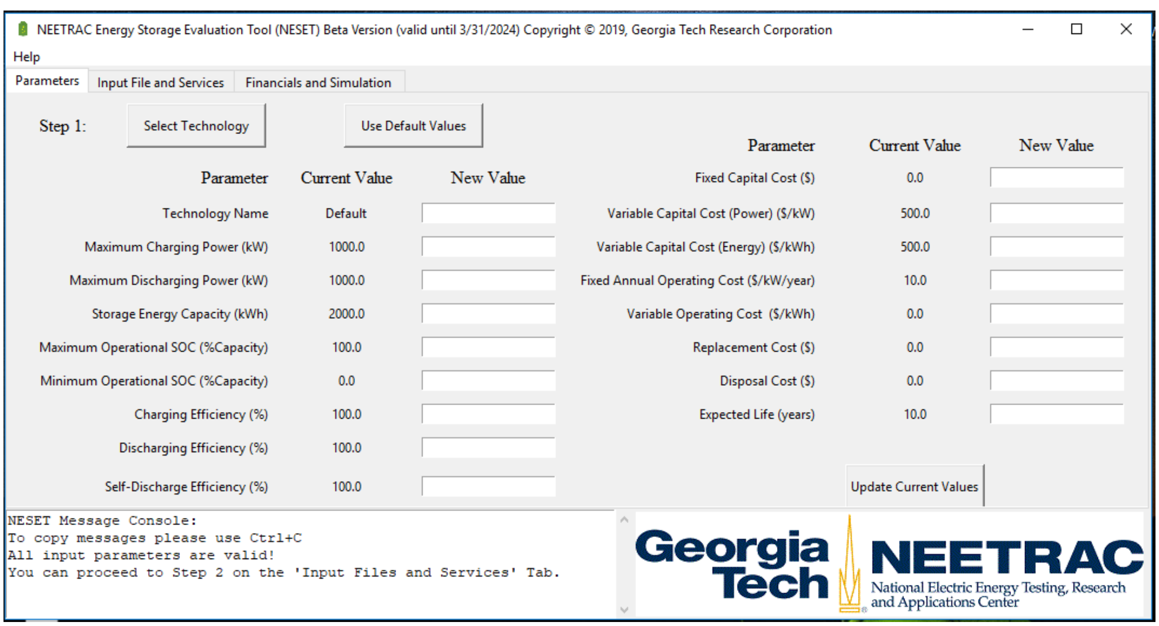

Figure 39 – ESS tool: parameters tab

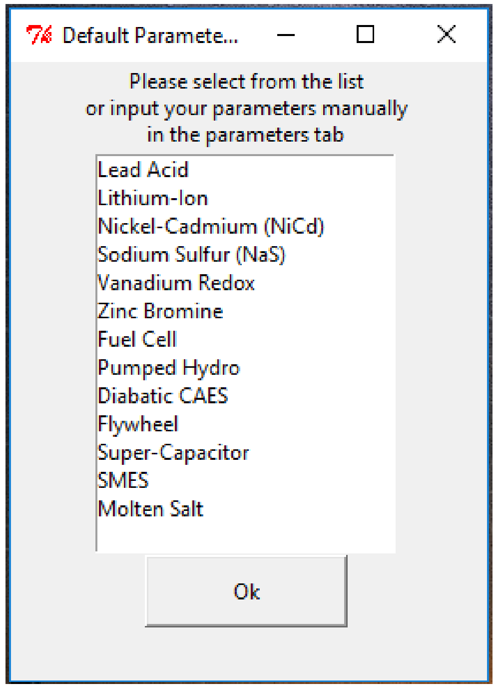

Figure 40 – ESS tool: technology selection

The second tab is shown in Figure 41 where users can import their time-series data and select the desired services based on the imported data file.

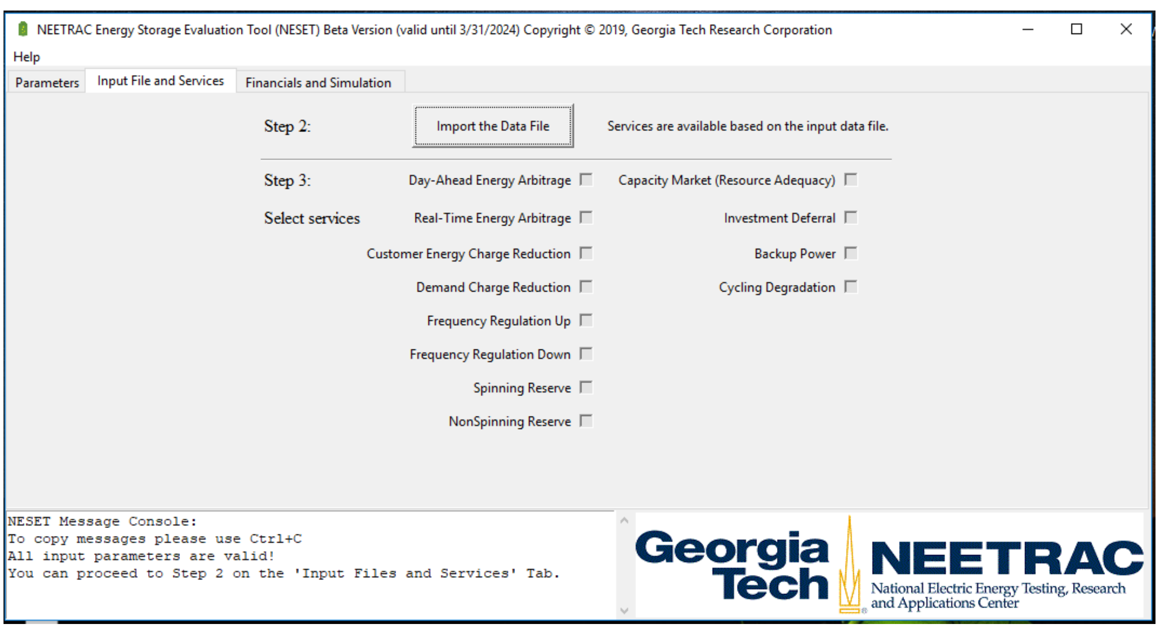

Figure 41 – ESS tool: input file and services tab (before data import)

The imported data file should be in the template format designed for the tool and shown in Figure 42. The input data file includes columns for time-series data including:

- Date and time
- Energy prices (day-ahead and real-time)
- Frequency regulation up/down prices
- Spinning and non-spinning reserve prices
- Renewable output power
- Active load data
- Demand charge rates
- Backup prices
- Capacity payments

	A	B	C	D	E	F	G	H	I	J	K	L
1	Date Time	Day Ahead Energy Price ($/kWh)	Real Time Energy Price ($/kWh)	Regulation Up Price ($/kW)	Regulation Down Price ($/kW)	Spinning Reserve Price ($/kW)	NonSpinning Reserve Price ($/kW)	Renewable Output (kW)	Demand Charge ($/kW/day)	Load (kW)	Backup Price ($/kWh/day)	Capacity Payment ($/kW/day)
2	1/1/2015 0:00	0.03145		0.004	0.004	0.00215	0.001					0
3	1/1/2015 1:00	0.02649		0.004	0.004	0.00215	0.001					0
4	1/1/2015 2:00	0.02454		0.004	0.004	0.00215	0.001					0
5	1/1/2015 3:00	0.02364		0.004	0.004	0.00215	0.001					0
6	1/1/2015 4:00	0.0241		0.004	0.004	0.00215	0.001					0
7	1/1/2015 5:00	0.02632		0.004	0.004	0.00215	0.001					0
8	1/1/2015 6:00	0.03148		0.009	0.009	0.00279	0.00131					0
9	1/1/2015 7:00	0.03057		0.009	0.009	0.005	0.00245					0
10	1/1/2015 8:00	0.03134		0.009	0.009	0.005	0.00245					0
11	1/1/2015 9:00	0.03321		0.009	0.009	0.005	0.00245					0
12	1/1/2015 10:00	0.02985		0.0065	0.0065	0.005	0.00245					0
13	1/1/2015 11:00	0.02978		0.0065	0.0065	0.005	0.00247					0
14	1/1/2015 12:00	0.02896		0.00791	0.00791	0.005	0.00247					0.918
15	1/1/2015 13:00	0.02846		0.0063	0.0063	0.005	0.00247					0.918
16	1/1/2015 14:00	0.02774		0.0065	0.0065	0.005	0.00247					0.918
17	1/1/2015 15:00	0.0289		0.0065	0.0065	0.005	0.00247					0.918
18	1/1/2015 16:00	0.03477		0.009	0.009	0.005	0.00247					0.918
19	1/1/2015 17:00	0.04966		0.009	0.009	0.00999	0.00255					0.918
20	1/1/2015 18:00	0.04415		0.009	0.009	0.00695	0.00255					0
21	1/1/2015 19:00	0.03902		0.009	0.009	0.00621	0.00247					0

Figure 42 – ESS tool: input file template

After importing the input file, users must select their desired services/revenue streams from the "Input Files and Services" tab. From the list of implemented services, the tool displays only those that are available based on the imported data file since each service requires specific input data. For instance, if the imported data file includes the data shown in Figure 42, tab 2 is updated as shown in Figure 43.

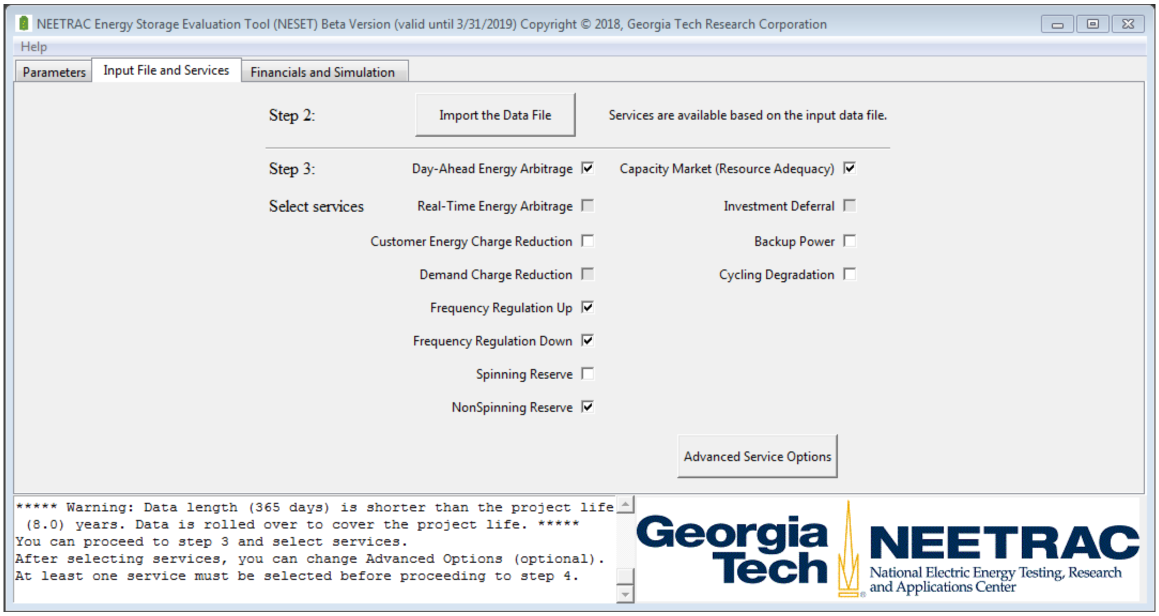

Figure 43 – ESS tool: input file and services tab (after data import)

Users can now select from the available services as shown in Figure 43. For each service to be modeled, certain parameters are considered "advanced service options" and users can change them to customize services based on their assumptions. The "advanced service options" dialog box is shown in Figure 44.

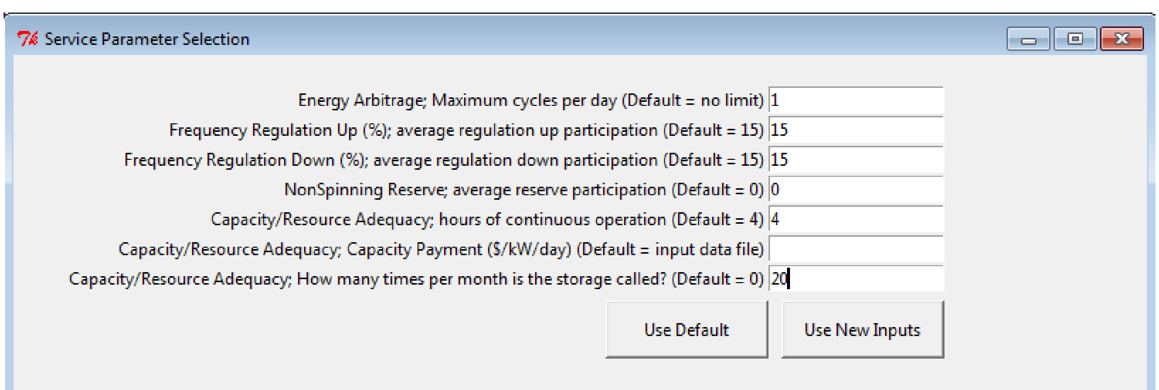

Figure 44 – ESS tool: advanced services options

The last step before running the simulation and obtaining results is to enter the financial rates associated with the energy storage project. These rates are entered in the third tab of the tool as shown in Figure 45.

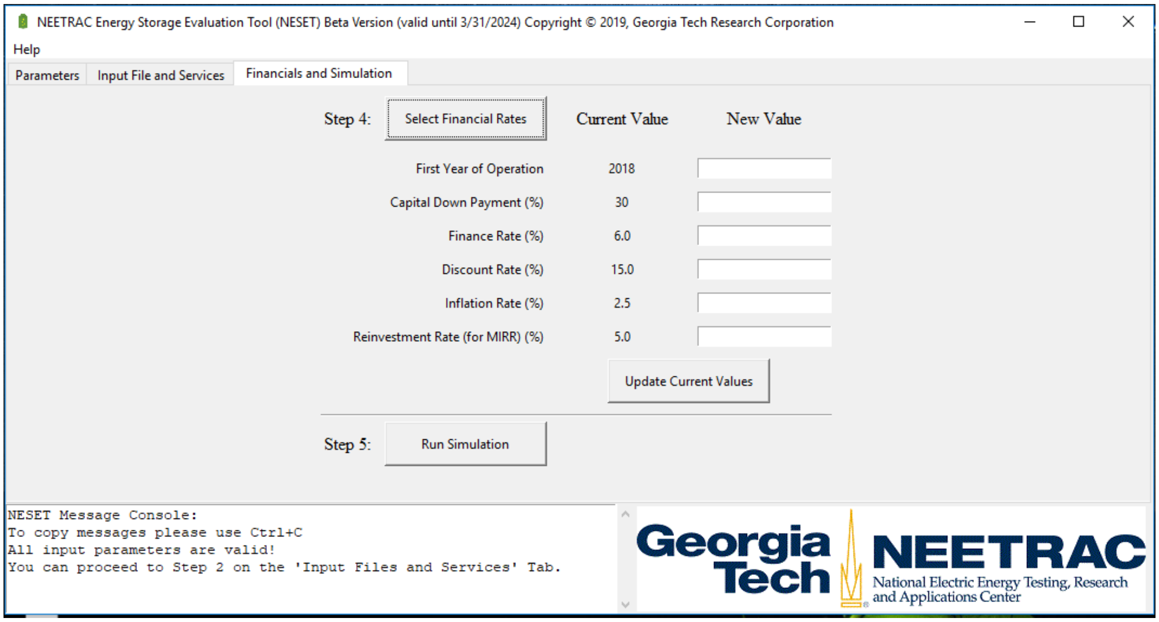

Figure 45 – ESS tool: financials and simulations tab

The financial rates are defined as:

– **Capital Down Payment:** Percentage of the total capital cost that is paid in advance. This cost is shown in the CAPEX year of the project. For example, if the total capital cost is $1,000,000 and the capital down payment is 30%, then $300,000 is paid in CAPEX year and the $700,000 is annuitized through the project life with the finance rate.

– **Finance Rate:** The rate in percentage at which the financed portion of total capital cost is discounted.

– **Discount Rate:** The rate in percentage at which all of the cash flows are discounted to the present value. This rate is determined by the storage/owner and does not include the inflation rate.

– **Inflation Rate:** The rate in percentage indicating a decrease in the purchasing power of energy storage owner/operator.

– **Effective Discount Rate:** This rate is used to calculate the present value of all cash flows (discount all the annual cash flows to the CAPEX year) for Net Present Value analysis. It is calculated based on the Discount and Inflation Rates as:

$$EDR = \frac{\text{Discount Rate}(\%) + \text{Inflation Rate}(\%)}{100 + \text{Inflation Rate}(\%)}$$

  - Note that if the energy storage owner/operator already includes the inflation rate, the tool user can enter the discount rate as it is and enter zero for the inflation rate.

– **Reinvestment Rate (for MIRR):** The reinvestment rate is the amount of interest that can be earned when money is taken out of one fixed-income investment and put into another.

Having all the storage technology parameters with service data as well as financial rates, the optimization-based simulation of the tool can be executed on the third tab by pressing the “Run Simulation” button. If any of the previous steps are incomplete, the tool will inform the user. If all steps are taken successfully, simulation will start. The console displays the status of the simulation in terms of how many days have been solved. Depending on the resolution of the provided data (1 hour, 15 minutes, etc.) and the number of selected services, simulation time may vary from less than a second to a few seconds per day. Simulation will be finished when the last day in the data file is solved. After it is finished, the tool shows a quick dialog box with the most important standard economic metrics for cost benefit analysis, such as the Net Present Value (NPV), Payback Period, Internal Return Rate (IRR), and Modified IRR (MIRR). These metrics are defined as:

- **Net Present Value (NPV):** This is the sum of all years' discounted after-tax cash flows. The NPV method is a valuable indicator because it recognizes the time value of money. Projects whose returns show positive NPVs are attractive. For a discount rate (or in the case of NESET, EDR) *r*, it is calculated as:

$$NPV = \sum_{i=0}^{n} \frac{(Benefit_i - Cost_i)}{(1+r)^i}$$

where *n* is the project life in years and *i* is the year index.

- **Internal Rate of Return (IRR):** It is defined as the discount rate at which the after-tax NPV is zero. The calculated IRR is examined to determine if it exceeds a minimally acceptable return, often called the hurdle rate. The advantage of IRR is that, unlike NPV, its percentage results allow projects of vastly different sizes to be easily compared.

- **Payback Period:** A payback calculation compares revenues with costs and determines the length of time required to recoup the initial investment. A Simple Payback Period is often calculated without regard to the time value of money. This figure of merit is frequently used to analyze retrofit opportunities offering incremental benefits and end-user applications.

- **Modified internal rate of return (MIRR):** It assumes that positive cash flows are reinvested at the firm's cost of capital, and the initial outlays are financed at the firm's financing cost. By contrast, the traditional internal rate of return (IRR) assumes the cash flows from a project are reinvested at the IRR. The MIRR more accurately reflects the cost and profitability of a project. For a project with a life of *n* years, it is calculated by:

$$MIRR = \left(\sqrt[n]{\frac{Future\ Value\ of\ positive\ cash\ flows\ at\ reinvestment\ rate}{|Present\ Value\ of\ negative\ cash\ flows\ at\ EDR|}} \right) - 1$$

The tool will also ask the user to specify a folder and a file name to export and save the results. After this file is exported successfully, a button “Open the Results File” will be shown on the right of the “Run Simulation” button. The user can then view the exported results file by clicking on this button.

An example of the results file is shown in Figure 46. The first sheet, Figure 46(a), shows the “Annual Cash Flow Statement” of the project where the rows are service revenues and project costs and columns are operation years. For each revenue/cost, the NPV is also calculated. Annual cash flows and cumulative cash flows are also calculated in the last two rows of this sheet. This sheet has the capability that the user can change the cell values and all the NPV and cash flow results will be updated automatically. For example, if the project has additional costs, such as upgrade cost, or benefits, such as incentives or tax credits, the user can input these data on this sheet under the name of “Incentives/Credits.” Annual values should be entered and the excel file calculates the NPV for this item and updates all the calculations for the project. The second sheet shown in Figure 46(b) is for daily revenues from selected services as well as the total daily revenue. The third sheet shown in Figure 46(c) displays the optimized operation results for each service.

	A	B	C	D	E	F	G
1	**Cash Flow Item**	**Item PV**	**CAPEX Year**	**Operating Year 1**	**2019**	**2020**	**2021**
2	----------	----------	----------	----------	----------	----------	----------
3	NonSpinning Reserve Revenue	$66,675	$	$12,127	$12,127	$12,127	$12,127
4	Day-Ahead Energy Arbitrage Rever	$245,358	$	$44,628	$44,628	$44,628	$44,628
5	Frequency Regulation Down Rever	$283,326	$	$51,534	$51,534	$51,534	$51,534
6	Frequency Regulation Up Revenue	$909,491	$	$165,426	$165,426	$165,426	$165,426
7	Capacity Market (Resource Adequa	$2,500,482	$	$454,808	$454,808	$454,808	$454,808
8	Incentives/Credits	$	$	$	$	$	$
9	Capital Cost	-$3,748,944	-$1,000,000	-$500,000	-$500,000	-$500,000	-$500,000
10	Fixed O&M Cost	$	$	$	$	$	$
11	Variable O&M Cost	$	$	$	$	$	$
12	Disposal Cost	$	$	$	$	$	$
13	----------	----------	----------	----------	----------	----------	----------
14	**Annual Cash Flow**	$256,388	-$1,000,000	$228,522	$228,522	$228,522	$228,522
15	**Cumulative Cash Flow**	$256,388	-$1,000,000	-$771,478	-$542,956	-$314,434	-$85,912

(a)

	A	B	C	D	E	F	G
1	Date	NonSpinning Reserve	Day-Ahead Energy Arbitrage	Frequency Regulation Down	Frequency Regulation Up	Capacity Market (Resource Adequacy)	Revenue_ Total
2	2018-01-01	$13.52	-$59.78	$104.35	$309.21	$1,836.	$2,203.3
3	2018-01-02	$9.55	-$50.26	$75.1	$336.	$1,836.	$2,206.38
4	2018-01-03	$4.71	-$106.1	$102.64	$379.57	$1,836.	$2,216.82
5	2018-01-04	$.	-$41.28	$136.82	$386.22	$1,836.	$2,317.77
6	2018-01-05	$23.41	$13.94	$279.25	$293.61	$1,836.	$2,446.21
7	2018-01-06	$62.94	$263.83	-$55.42	$85.02	$1,836.	$2,192.37
8	2018-01-07	$68.1	$564.38	-$165.04	$58.15	$1,836.	$2,361.58
9	2018-01-08	$60.28	$529.83	$165.46	$103.56	$1,836.	$2,695.13
10	2018-01-09	$51.7	$184.03	-$201.56	$118.81	$1,836.	$1,988.97
11	2018-01-10	$33.07	$98.17	-$106.68	$173.31	$1,836.	$2,033.88
12	2018-01-11	$31.34	$53.18	-$102.09	$240.92	$1,836.	$2,059.35
13	2018-01-12	$40.3	$191.87	-$132.19	$123.79	$1,836.	$2,059.76
14	2018-01-13	$24.47	$176.1	$396.03	$634.2	$1,836.	$3,066.8
15	2018-01-14	$86.31	$250.11	$331.59	$184.76	$1,836.	$2,688.77
16	2018-01-15	$78.33	$200.21	$54.09	$75.77	$1,836.	$2,244.39
17	2018-01-16	$61.71	$190.02	-$10.51	$104.64	$1,836.	$2,181.87
18	2018-01-17	$29.82	-$11.51	-$61.8	$260.78	$1,836.	$2,053.29
19	2018-01-18	$18.55	-$29.59	$87.22	$393.21	$1,836.	$2,305.39
20	2018-01-19	$16.01	-$23.47	$66.87	$343.81	$1,836.	$2,239.22
21	2018-01-20	$24.85	-$23.92	$102.96	$294.76	$1,836.	$2,234.66

(b)

	A	B	C	D	E	F	G	H	I	J	K	L	M	N
1	Date Time	Day-Ahead Energy Charge(kW)	Day-Ahead Energy Discharge(kW)	Real-Time Energy Charge(kW)	Real-Time Energy Discharge(kW)	Regulation Up Capacity(kW)	Regulation Down Capacity(kW)	Spinning Reserve Capacity(kW)	NonSpinning Reserve Capacity(kW)	Capacity Market (kW)	Investment Deferred? (0/1)	Backup Provided? (0/1)	Output Power(kW)(+:Discharge, -:Charge)	State of Charge(%)
2	2018-01-01 00:00:00	.	.	.	.	2,000.	2,000.	.	.	.	.	.	.	49.76
3	2018-01-01 01:00:00	387.96	.	.	.	2,387.96	1,612.04	.	.	.	.	.	-271.57	51.07
4	2018-01-01 02:00:00	2,000.	.	.	.	4,000.	.	.	.	.	.	.	-1,400.	58.8
5	2018-01-01 03:00:00	2,000.	.	.	.	.	.	.	4,000.	.	.	.	-2,000.	70.53
6	2018-01-01 04:00:00	2,000.	.	.	.	.	.	.	4,000.	.	.	.	-2,000.	82.27
7	2018-01-01 05:00:00	2,000.	.	.	.	4,000.	.	.	.	.	.	.	-1,400.	90.
8	2018-01-01 06:00:00	.	.	.	.	2,000.	2,000.	.	.	.	.	.	.	89.76
9	2018-01-01 07:00:00	.	.	.	.	2,000.	2,000.	.	.	.	.	.	.	89.52
10	2018-01-01 08:00:00	.	.	.	.	2,000.	2,000.	.	.	.	.	.	.	89.28
11	2018-01-01 09:00:00	.	.	.	.	2,000.	2,000.	.	.	.	.	.	.	89.04
12	2018-01-01 10:00:00	.	.	.	.	2,000.	2,000.	.	.	.	.	.	.	88.8
13	2018-01-01 11:00:00	.	.	.	.	2,000.	2,000.	.	.	.	.	.	.	88.56
14	2018-01-01 12:00:00	.	.	.	.	.	2,000.	.	.	2,000.	.	.	588.89	84.39
15	2018-01-01 13:00:00	.	.	.	.	.	2,000.	.	.	2,000.	.	.	588.89	80.23
16	2018-01-01 14:00:00	.	.	.	.	.	2,000.	.	.	2,000.	.	.	588.89	76.06
17	2018-01-01 15:00:00	.	.	.	.	.	2,000.	.	.	2,000.	.	.	588.89	71.9
18	2018-01-01 16:00:00	.	.	.	.	.	2,000.	.	.	2,000.	.	.	588.89	67.73
19	2018-01-01 17:00:00	.	.	.	.	.	2,000.	.	.	2,000.	.	.	588.89	63.56
20	2018-01-01 18:00:00	.	2,000.	.	.	.	4,000.	.	.	.	.	.	1,400.	53.75

(c)

Figure 46 – ESS tool: results file a) annual cash flow statement, b) daily revenues, and c) dispatch

REFERENCES

[1] Department of Energy, "DOE Announces $220 Million in Grid Modernization Funding," 2016. [Online]. Available: https://www.energy.gov/articles/doe-announces-220-million-grid-modernization-funding. [Accessed: 01-Mar-2019].

[2] Department of Energy, "Grid Modernization Mutli-Year Program Plan," 2015.

[3] G. Huff *et al.*, "DOE/EPRI 2013 electricity storage handbook in collaboration with NRECA," *Rep. SAND2013- …*, no. July, p. 340, 2013.

[4] J. Roach, "For Storing Electricity, Utilities Are Turning to Pumped Hydro," 2015. [Online]. Available: http://e360.yale.edu/features/for_storing_electricity_utilities_are_turning_to_pumped_hydro. [Accessed: 01-Oct-2017].

[5] M. Aneke and M. Wang, "Energy storage technologies and real life applications – A state of the art review," *Appl. Energy*, vol. 179, pp. 350–377, 2016.

[6] G. Huff *et al.*, "DOE/EPRI 2013 electricity storage handbook in collaboration with NRECA," *Rep. SAND2013- …*, no. July, p. 340, 2013.

[7] D. D. Rastler *et al.*, "Electric Energy Storage Technology Options: A White Paper Primer on Applications, Costs and Benefits," *Epri*, p. 170, 2010.

[8] I. Gyuk *et al.*, "Grid Energy Storage," *U.S. Dep. Energy*, no. December, p. 67, 2013.

[9] Electropaedia, "Grid Scale Energy Storage Systems." [Online]. Available: https://www.mpoweruk.com/grid_storage.htm. [Accessed: 01-Mar-2019].

[10] J. Eyer and G. Corey, "Energy Storage for the Electricity Grid : Benefits and Market Potential Assessment Guide," 2010.

[11] Energy Storage Association, "A Vision for Energy Storage."

[12] EESI, "Energy Storage Fact Sheet," 2019.

[13] Wood Mackenzie Power and Energy Storage Association, "U. S. energy storage monitor Q3 2019 executive summary Contents (full report)," 2019.

[14] LAZARD, "Lazard's levelized cost of storage—version 2.0."

[15] Bloomberg NEF, "Sustainable Energy in America," 2019.

[16] R. Fu, T. Remo, R. Margolis, R. Fu, T. Remo, and R. Margolis, "2018 U.S. Utility-Scale Photovoltaics- Plus-Energy Storage System Costs Benchmark 2018 U . S . Utility-Scale Photovoltaics- Plus-Energy Storage System Costs Benchmark," no. November, 2018.

[17] U.S. Energy Information Administration, "U. S. Battery Storage Market Trends," no. May, 2018.

[18] R. Sioshansi, P. Denholm, and T. Jenkin, "Market and Policy Barriers to Deployment of Energy Storage," *Econ. Energy Environ. Policy*, vol. 1, no. 2, pp. 1–14, 2012.

[19] A. Shcherbakova, A. Kleit, and J. Cho, “The value of energy storage in South Korea’s electricity market: A Hotelling approach,” *Appl. Energy*, vol. 125, pp. 93–102, 2014.

[20] F. Nieuwenhout, “Feasibility of distributed electricity storage,” *... J. Distrib. ...*, vol. 2, no. 4, pp. 1–21, 2006.

[21] J. Deboever and S. Grijalva, “Energy Storage Dispatch under Different Ownership and Control Models,” *IEEE PES Gen. Meet.*, 2017.

[22] J. Deboever and S. Grijalva, “Optimal scheduling of large-scale price-maker energy storage,” *2016 IEEE Power Energy Conf. Illinois, PECI 2016*, 2016.

[23] P. Mokrian and M. Stephen, *A stochastic programming framework for the valuation of electricity storage*. 2006.

[24] H. Pandzic and I. Kuzle, “Energy storage operation in the day-ahead electricity market,” *2015 12th Int. Conf. Eur. Energy Mark.*, no. 13, pp. 1–6, 2015.

[25] K. Bradbury, L. Pratson, and D. Patiño-Echeverri, “Economic viability of energy storage systems based on price arbitrage potential in real-time U.S. electricity markets,” *Appl. Energy*, vol. 114, pp. 512–519, 2014.

[26] R. Sioshansi, P. Denholm, T. Jenkin, and J. Weiss, “Estimating the value of electricity storage in PJM: Arbitrage and some welfare effects,” *Energy Econ.*, vol. 31, no. 2, pp. 269–277, 2009.

[27] R. H. Byrne, “Estimating Potential Revenue from Electrical Energy Storage in Market Areas,” *Intersolar 2016*, 2016.

[28] R. Moreira, R. Moreno, and G. Strbac, “Synergies and conflicts among energy storage services,” *2016 IEEE Int. Energy Conf. ENERGYCON 2016*, 2016.

[29] H. Khani and M. R. Dadash Zadeh, “Real-time optimal dispatch and economic viability of cryogenic energy storage exploiting arbitrage opportunities in an electricity market,” *IEEE Trans. Smart Grid*, vol. 6, no. 1, pp. 391–401, 2015.

[30] H. Mohsenian-Rad, “Coordinated Price-Maker Operation of Large Energy Storage Units in Nodal Energy Markets,” *IEEE Trans. Power Syst.*, vol. 31, no. 1, pp. 786–797, 2016.

[31] S. van der Kooij, “Optimal charging / discharging strategies for batteries in smart energy grids,” 2016.

[32] H. Khani, “Optimal Scheduling of Energy Storage for Energy Shifting and Ancillary Services to the Grid,” no. August, 2016.

[33] E. Drury, P. Denholm, and R. Sioshansi, “The Value of Compressed Air Energy Storage in Energy and Reserve Markets,” 2011.

[34] R. L. Fares and M. E. Webber, “A flexible model for economic operational management of grid battery energy storage,” *Energy*, vol. 78, no. November, pp. 768–776, 2014.

[35] G. Carpinelli, G. Celli, S. Mocci, F. Mottola, F. Pilo, and D. Proto, “Optimal Integration of Distributed Energy Storage Devices in Smart Grids,” *IEEE Trans. Smart Grid*, vol. 4, no. 2, pp. 985–995, 2013.

[36] J. A. Taylor, D. S. Callaway, and K. Poolla, “Competitive energy storage in the presence of renewables,” *IEEE Trans. Power Syst.*, vol. 28, no. 2, pp. 985–986, 2013.

[37] R. Walawalkar, J. Apt, and R. Mancini, “Economics of electric energy storage for energy arbitrage and regulation in New York,” *Energy Policy*, vol. 35, no. 4, pp. 2558–2568, 2007.

[38] Y. Wang, Y. Dvorkin, R. Fernandez-Blanco, B. Xu, T. Qiu, and D. S. Kirschen, “Look-Ahead Bidding Strategy for Energy Storage,” *IEEE Trans. Sustain. Energy*, vol. 8, no. 3, pp. 1106–1117, 2017.

[39] Q. Huang, Y. Xu, T. Wang, and C. Courcoubetis, “Market Mechanisms for Cooperative Operation of Price- maker Energy Storage in a Power Network IEEE PES Transactions on Power Systems Market Mechanisms for Cooperative Operation of Price-maker Energy Storage in a Power Network,” vol. 8950, no. c, 2017.

[40] P. Zamani-Dehkordi, S. Shafiee, L. Rakai, A. M. Knight, and H. Zareipour, “Price impact assessment for large-scale merchant energy storage facilities,” *Energy*, vol. 125, pp. 27–43, 2017.

[41] S. Shafiee, H. Zareipour, and A. M. Knight, “Developing Bidding and Offering Curves of a Price-maker Energy Storage Facility Based on Robust Optimization,” *IEEE Trans. Smart Grid*, vol. 1, no. c, pp. 1–1, 2017.

[42] E. Nasrolahpour, J. Kazempour, H. Zareipour, and W. D. Rosehart, “A Bilevel Model for Participation of a Storage System in Energy and Reserve Markets,” *IEEE Trans. Sustain. Energy*, vol. 3029, no. c, pp. 1–1, 2017.

[43] S. Shafiee, H. Zareipour, A. M. Knight, N. Amjady, and B. Mohammadi-Ivatloo, “Risk-Constrained Bidding and Offering Strategy for a Merchant Compressed Air Energy Storage Plant,” *IEEE Trans. Power Syst.*, vol. 32, no. 2, pp. 946–957, 2017.

[44] H. Khani, R. K. Varma, M. R. D. Zadeh, and A. H. Hajimiragha, “A Real-Time Multistep Optimization-Based Model for Scheduling of Storage-Based Large-Scale Electricity Consumers in a Wholesale Market,” *IEEE Trans. Sustain. Energy*, vol. 8, no. 2, pp. 836–845, 2017.

[45] J. Liu, N. Zhang, C. Kang, D. S. Kirschen, and Q. Xia, “Decision-Making Models for the Participants in Cloud Energy Storage,” *IEEE Trans. Smart Grid*, vol. 3053, no. c, pp. 1–1, 2017.

[46] H. Chitsaz, P. Zamani-Dehkordi, H. Zareipour, and P. Parikh, “Electricity Price Forecasting for Operational Scheduling of Behind-the-meter Storage Systems,” *IEEE Trans. Smart Grid*, vol. 3053, no. c, pp. 1–11, 2017.

[47] M. Kazemi, H. Zareipour, N. Amjady, W. D. Rosehart, and M. Ehsan, “Operation Scheduling of Battery Storage Systems in Joint Energy and Ancillary Services Markets,” *IEEE Trans. Sustain. Energy*, vol. 8, no. 4, pp. 1–1, 2017.

[48] R. H. Byrne, S. Hamilton, D. R. Borneo, T. Olinsky-Paul, and I. Gyuk, “The Value Proposition for Energy Storage at the Sterling Municipal Light Department,” 2017.

[49] R. H. Byrne, R. J. Concepcion, and C. A. Silva-Monroy, “Estimating potential

revenue from electrical energy storage in PJM," in *IEEE Power and Energy Society General Meeting*, 2016, vol. 2016-November.

[50] R. H. Byrne and C. A. Silva-Monroy, "Estimating the Maximum Potential Revenue for Grid Connected Electricity Storage: Arbitrage and Regulation," *Sand2012-3863*, no. December, p. 64, 2012.

[51] R. Byrne and C. Silva-Monroy, "Potential revenue from electrical energy storage in ERCOT: The impact of location and recent trends," in *in Proceedings of the 2015 IEEE Power and Energy Society (PES) General Meeting*, 2015, pp. 1–5.

[52] T. Zhang, S. X. Chen, H. B. Gooi, and J. M. Maciejowski, "A hierarchical EMS for aggregated BESSs in energy and performance-based regulation markets," *IEEE Trans. Power Syst.*, vol. 32, no. 3, pp. 1751–1760, 2017.

[53] D. S. Kirschen, *Fundamentals of power system economics electronic resource*. 2004.

[54] D. McConnell, T. Forcey, and M. Sandiford, "Estimating the value of electricity storage in an energy-only wholesale market," *Appl. Energy*, vol. 159, pp. 422–432, 2015.

[55] D. Zafirakis, K. J. Chalvatzis, G. Baiocchi, and G. Daskalakis, "The value of arbitrage for energy storage: Evidence from European electricity markets," *Appl. Energy*, vol. 184, pp. 971–986, 2016.

[56] N. Gast, J.-Y. Le Boudec, A. Proutière, and D.-C. Tomozei, "Impact of storage on the efficiency and prices in real-time electricity markets," *Proc. fourth Int. Conf. Futur. energy Syst. - e-Energy '13*, vol. 2, p. 15, 2013.

[57] H. Khani and M. R. D. Zadeh, "Online Adaptive Real-Time Optimal Dispatch of Privately Owned Energy Storage Systems Using Public-Domain Electricity Market Prices," *IEEE Trans. Power Syst.*, vol. 30, no. 2, pp. 930–938, 2015.

[58] S. Vejdan and S. Grijalva, "The Value of Real-Time Energy Arbitrage with Energy Storage Systems," 2018.

[59] D. Krishnamurthy, C. Uckun, Z. Zhou, P. R. Thimmapuram, and A. Botterud, "Energy Storage Arbitrage Under Day-Ahead and Real-Time Price Uncertainty," *IEEE Trans. Power Syst.*, vol. 33, no. 1, pp. 84–93, 2018.

[60] M. Rahimian and L. Baringo, "Strategic Bidding for a Virtual Power Plant in the Day-Ahead and Real-Time Markets: A Price-Taker Robust Optimization Approach," *IEEE Trans. Power Syst.*, vol. 31, no. 4, pp. 2676–2687, 2016.

[61] E. G. Kardakos, C. K. Simoglou, and A. G. Bakirtzis, "Optimal Offering Strategy of a Virtual Power Plant: A Stochastic Bi-Level Approach," *IEEE Trans. Smart Grid2*, vol. 7, no. 2, pp. 794–806, 2016.

[62] B. Xu *et al.*, "Factoring the Cycle Aging Cost of Batteries Participating in Electricity Markets," pp. 1–12.

[63] Y. Dvorkin, R. Fernandez-Blanco, D. S. Kirschen, H. Pandzic, J. P. Watson, and C. A. Silva-Monroy, "Ensuring Profitability of Energy Storage," *IEEE Trans. Power Syst.*, vol. 32, no. 1, pp. 611–623, 2017.

[64] H. Saboori and R. Hemmati, "Maximizing DISCO profit in active distribution networks by optimal planning of energy storage systems and distributed generators," *Renew. Sustain. Energy Rev.*, vol. 71, no. December 2016, pp. 365–372, 2017.

[65] D. Wu, C. Jin, P. Balducci, and M. Kintner-meyer, "An Energy Storage Assessment : Using Optimal Control Strategies to Capture Multiple Services," 2015.

[66] P. Balducci, C. Jin, D. Wu, and M. Kintner-Meyer, "Assessment of Energy Storage Alternatives in the Puget Sound Energy System," 2013.

[67] P. J. Balducci, M. J. E. Alam, T. D. Hardy, and D. Wu, "Assigning value to energy storage systems at multiple points in an electrical grid," *Energy Environ. Sci.*, pp. 1926–1944, 2018.

[68] M. Katsanevakis, R. A. Stewart, and J. Lu, "Aggregated applications and bene fi ts of energy storage systems with application-speci fi c control methods : A review," vol. 75, no. November 2015, pp. 719–741, 2017.

[69] A. Berrada, K. Loudiyi, and I. Zorkani, "Valuation of energy storage in energy and regulation markets," *Energy*, vol. 115, pp. 1109–1118, 2016.

[70] B. Cheng and W. B. Powell, "Co-optimizing battery storage for the frequency regulation and energy arbitrage using multi-scale dynamic programming," *IEEE Trans. Smart Grid*, vol. 9, no. 3, pp. 1997–2005, 2016.

[71] H. Akhavan-Hejazi and H. Mohsenian-Rad, "Optimal operation of independent storage systems in energy and reserve markets with high wind penetration," *IEEE Trans. Smart Grid*, vol. 5, no. 2, 2014.

[72] R. Moreira, L. Ollagnier, D. Papadaskalopoulos, and G. Strbac, "Optimal multi-service business models for electric vehicles," *2017 IEEE Manchester PowerTech*, pp. 1–6, 2017.

[73] A. Perez, R. Moreno, R. Moreira, M. Orchard, and G. Strbac, "Effect of Battery Degradation on Multi-Service Portfolios of Energy Storage," *IEEE Trans. Sustain. Energy*, vol. 7, no. 4, pp. 1718–1729, 2016.

[74] M. R. Narimani, B. Asghari, and R. Sharma, "Energy storage control methods for demand charge reduction and PV utilization improvement," in *2017 IEEE PES Asia-Pacific Power and Energy Engineering Conference (APPEEC)*, 2017, pp. 1–5.

[75] A. Oudalov, R. Cherkaoui, and A. Beguin, "Sizing and optimal operation of battery energy storage system for peak shaving application," in *2007 IEEE Lausanne Power Tech*, 2007, pp. 621–625.

[76] A. Zurfi, G. Albayati, and J. Zhang, "Economic feasibility of residential behind-the-meter battery energy storage under energy time-of-use and demand charge rates," in *2017 IEEE 6th International Conference on Renewable Energy Research and Applications (ICRERA)*, 2017, pp. 842–849.

[77] W. Hu, P. Wang, and H. Gooi, "Assessing the Economics of Customer-Sited Multi-Use Energy Storage."

[78] J. Neubauer, M. Simpson, J. Neubauer, and M. Simpson, "Deployment of Behind-The- Meter Energy Storage for Demand Charge Reduction Deployment of Behind-

The- Meter Energy Storage for Demand Charge Reduction," no. January, 2015.

[79] I. Alsaidan, W. Gao, and A. Khodaei, "Battery energy storage sizing for commercial customers," in *2017 IEEE Power & Energy Society General Meeting*, 2017, pp. 1–5.

[80] M. J. Fisher and J. Apt, "Emissions and Economics of Behind-the-Meter Electricity Storage," *Environ. Sci. Technol.*, vol. 51, no. 3, pp. 1094–1101, 2017.

[81] R. Moslemi, A. Hooshmand, and R. K. Sharma, "A data-driven demand charge management solution for behind-the-meter storage applications," in *2017 IEEE Power & Energy Society Innovative Smart Grid Technologies Conference (ISGT)*, 2017, pp. 1–5.

[82] M. Gitizadeh and H. Fakharzadegan, "Effects of electricity tariffs on optimal battery energy storage sizing in residential PV/storage systems," in *2013 International Conference on Energy Efficient Technologies for Sustainability*, 2013, pp. 1072–1077.

[83] J. Leadbetter and L. Swan, "Battery storage system for residential electricity peak demand shaving," *Energy Build.*, vol. 55, pp. 685–692, 2012.

[84] T. A. Nguyen and R. H. Byrne, "Maximizing the cost-savings for time-of-use and net-metering customers using behind-the-meter energy storage systems," in *2017 North American Power Symposium (NAPS)*, 2017, pp. 1–6.

[85] I. Atzeni, L. G. Ordóñez, G. Scutari, D. P. Palomar, and J. R. Fonollosa, "Noncooperative and Cooperative Optimization of Distributed Energy Generation and Storage in the Demand-Side of the Smart Grid," vol. 61, no. 10, pp. 2454–2472, 2013.

[86] C. O. Adika and L. Wang, "Non-cooperative decentralized charging of homogeneous households' batteries in a smart grid," *IEEE Trans. Smart Grid*, vol. 5, no. 4, pp. 1855–1863, 2014.

[87] R. Carli and M. Dotoli, "Energy scheduling of a smart home under nonlinear pricing," in *53rd IEEE Conference on Decision and Control*, 2014, pp. 5648–5653.

[88] P. Harsha, "Optimal sizing of energy storage for efficient integration of renewable energy."

[89] P. M. Van De Ven, N. Hegde, and L. Massouli, "Optimal control of end-user energy storage."

[90] Y. Ye, D. Papadaskalopoulos, R. Moreira, and G. Strbac, "Strategic capacity withholding by energy storage in electricity markets," *2017 IEEE Manchester PowerTech*, pp. 1–6, 2017.

[91] "Georgia Power Website." [Online]. Available: https://www.georgiapower.com/.

[92] S. Vejdan and S. Grijalva, "The Expected Revenue of Energy Storage from Energy Arbitrage Service Based on the Statistics of Realistic Market Data," *2018 IEEE Texas Power Energy Conf.*, pp. 1–6, 2018.

[93] "ISO New England Manual for the Forward Capacity Market (FCM) ISO New England Manual for the Forward Capacity Market (FCM) Section 3 : Dispatchable

Asset Related Demand Coincident Peak Contribution," 2019.

[94] B. Xu, "Batteries in Electricity Markets : Economic Planning and Operations," 2018.

[95] M. J. Feizollahi, M. Costley, S. Ahmed, and S. Grijalva, "Large-scale decentralized unit commitment," *Int. J. Electr. Power Energy Syst.*, vol. 73, no. September, pp. 97–106, 2015.

[96] J. Guo, S. Member, G. Hug, S. Member, and O. K. Tonguz, "A Case for Nonconvex Distributed Optimization in Large-Scale Power Systems," vol. 32, no. 5, pp. 3842–3851, 2017.

[97] A. K. Marvasti, S. Member, Y. Fu, S. Member, S. Dormohammadi, and N. Omenclature, "Optimal Operation of Active Distribution Grids : A System of Systems Framework," *IEEE Trans. Smart Grid*, vol. 5, no. 3, pp. 1228–1237, 2014.

[98] J. Contreras, A. Losi, M. Russo, and F. F. Wu, "Simulation and Evaluation of Optimization Problem Solutions in Distributed Energy Management Systems," vol. 17, no. 1, pp. 57–62, 2002.

[99] F. Safdarian, S. Member, O. Ciftci, S. Member, and A. Kargarian, "A Time Decomposition and Coordination Strategy for Power System Multi-Interval Operation," pp. 1–5, 2016.

[100] F. Sorourifar, V. M. Zavala, and A. W. Dowling, "Integrated Multiscale Design, Market Participation, and Replacement Strategies for Battery Energy Storage Systems," *IEEE Trans. Sustain. Energy*, 2018.

[101] H. Duran, C. Puech, and J. Diaz, "Optimal operation of multireservoir systems using an aggregation-decomposition approach," *IEEE Trans. Power Appar. Syst.*, no. 8, pp. 2086–2092, 1985.

[102] C. Li, J. Zhou, S. Ouyang, X. Ding, and L. Chen, "Improved decomposition – coordination and discrete differential dynamic programming for optimization of large-scale hydropower system," vol. 84, pp. 363–373, 2014.

[103] S. Samsatli and N. J. Samsatli, "A general spatio-temporal model of energy systems with a detailed account of transport and storage," *Comput. Chem. Eng.*, vol. 80, pp. 155–176, 2015.

[104] S. Vejdan and S. Grijalva, "Analysis of Multiple Revenue Streams for Privately-Owned Energy Storage Systems," 2018.

[105] "PJM Data Miner 2." [Online]. Available: http://dataminer2.pjm.com/list.

[106] T. Hastie, R. Tibdjirani, and J. Friedman, *The Elements of Statistical Learning*, 2nd ed. Springer, 2013.

[107] J. Skaf, S. Boyd, and A. Zeevi, "Shrinking-horizon dynamic programming," *Int. J. Robust Nonlinear Control*, vol. 20, no. 17, pp. 1993–2002, Nov. 2010.

[108] O. Abedinia, N. Amjady, and H. Zareipour, "A New Feature Selection Technique for Load and Price Forecast of Electrical Power Systems," *IEEE Trans. Power Syst.*, pp. 1–11, 2015.

[109] A. Sadeghi-mobarakeh, M. Kohansal, E. E. Papalexakis, and H. Mohsenian-rad,

"Data Mining based on Random Forest Model to Predict the California ISO Day-ahead Market Prices," no. April, 2017.

[110] A. J. Conejo, M. Carrion, and J. M. Morales, *Decision Making Under Uncertainty in Electricity Markets*. Springer, 2010.

[111] Department of Energy, "DOE Global Energy Storage Database." [Online]. Available: https://www.energystorageexchange.org/. [Accessed: 01-Dec-2019].

[112] "MathWorks - Makers of MATLAB and Simulink - MATLAB & Simulink." [Online]. Available: https://www.mathworks.com/. [Accessed: 01-Dec-2019].

[113] M. Aneke and M. Wang, "Energy storage technologies and real life applications – A state of the art review," *Appl. Energy*, vol. 179, pp. 350–377, 2016.

[114] S. Vejdan, A. Kline, M. Totri, R. Simmons, and C. Parameters, "Behind-the-Meter Energy Storage : Economic Assessment and System Impacts in Georgia," 2019.

[115] S. Vejdan, S. Grijalva, and F. Lambert, "Energy Storage in the Future Grid; Final Report," 2019.

[116] Y. Dvorkin, D. S. Kirschen, and M. A. Ortega-vazquez, "Assessing flexibility requirements in power systems," vol. 8, no. April, pp. 1820–1830, 2014.

[117] EPRI, "Cost-Effectiveness of Energy Storage in California."

[118] EPRI, "StorageVET TM V1 . 0 Software User Guide."

[119] "California ISO Open Access Same-time Information System (OASIS)." [Online]. Available: oasis.caiso.com/.

[120] "DataPort, Pecan Street Database." [Online]. Available: https://pecanstreet.org/dataport/.

[121] "Energy Information Datasets." [Online]. Available: https://openei.org/datasets/files/961/pub/.

[122] "Tesla Powerwall." [Online]. Available: https://www.tesla.com/powerwall.

[123] B. Xu, Y. Dvorkin, D. S. Kirschen, C. A. Silva-Monroy, and J. P. Watson, "A comparison of policies on the participation of storage in U.S. frequency regulation markets," *IEEE Power Energy Soc. Gen. Meet.*, vol. 2016-Novem, 2016.

[124] S. Boyd and L. Vandenberghe, *Convex Optimization*, vol. 25, no. 3. 2010.

[125] A. Hassan, "Energy Storage Siting and Sizing in Coordinated Distribution and Transmission Systems," *IEEE Trans. Sustain. Energy*, vol. 9, no. 4, pp. 1692–1701, 2018.

[126] L. L. C. Gurobi Optimization, "Gurobi Optimizer Reference Manual." 2019.

[127] S. Boyd, N. Parikh, E. Chu, B. Peleato, and J. Eckstein, "Distributed Optimization and Statistical Learning via the Alternating Direction Method of Multipliers," vol. 3, no. 1, pp. 1–122, 2011.

[128] S. Vejdan, S. Grijalva, and F. Lambert, "Energy Storage in the Future Grid NEETRAC Baseline Project 17-033 Final Report," 2019.